Multiconfigurational electronic wavefunctions in the Full Optimized Reaction Space: The isomerization of nitrosyl hydride to nitrogen hydroxide in the lowest singlet and triplet states

by

Mary Gilbert Dombek

A Dissertation Submitted to the
Graduate Faculty in Partial Fulfillment of
The Requirements for the Degree of
DOCTOR OF PHILOSOPHY

Department: Chemistry
Major: Physical Chemistry

Approved:

Signature was redacted for privacy.

In Charge of Major Work

Signature was redacted for privacy.

For the Major Department

Signature was redacted for privacy.

For the Graduate College

Iowa State University
Ames, Iowa

1977

TABLE OF CONTENTS

I. INTRODUCTION

A. Chemistry of HNO

Hydrogen, nitrogen and oxygen are among the most abundant elements on earth and there are many compounds involving two or three of these elements. Yet the simple triatomic species HNO (nitrosyl hydride or nitroxyl) is so elusive that it is sometimes referred to as a radical even though it is a molecule with a perfectly normal Lewis structure. Its lifetime has been reported as being up to 40 seconds (Saito and Takagi, 1972a). On the other hand, there are many reactions, atmospheric and otherwise, involving these atoms, for which HNO could well be an intermediate. In order to be able to serve in this role a lifetime of more than a second is certainly very adequate. The isomeric form, HON, has also been postulated as a reaction intermediate, even though it has not yet been observed. The role of both isomers as reaction intermediates is discussed in some detail by Hughes (1968).

Interest in HNO as a possible reaction intermediate goes back to 1929, when Smallwood reported the nitric oxide catalysis of the recombination of H atoms to form H_2. He proposed that the catalysis occurs via a reaction of atomic hydrogen with nitroxyl (HNO). During the 1930's HNO was also postulated as a primary product in the photochemical decomposition reactions of nitromethane and nitroethane (Hirschlaff and Norrish, 1936), and of various nitrites (Purkis and Thompson, 1936). Taylor and Tanford (1944) proposed a mechanism based on HNO for the mercury-sensitized reaction of hydrogen and nitric oxide.

In more recent times, the speculations regarding reactions involving HNO and HON have been pursued in a somewhat more quantitative manner with the help of semirigorous theoretical approaches. Kroto and Santry (1967), in order to develop a semiempirical theory of transition energies and molecular excited-state geometries, made CNDO calculations for several small molecules, including HNO. They calculated the $^1A''$ and $^1A'$ state energies for HNO as a function of bond angle, which ranged from 90° to 180°. Ground state geometries of many small molecules, including HNO, were calculated with the INDO method by Gordon and Pople (1968). Extended Huckel calculations were used by Hoffman, Gleiter, and Mallory (1970) to explore the nonleast-motion approach of two HNO molecules to form the HNO dimer,

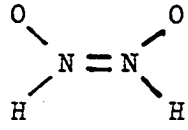

a reaction which is of interest as a model for the dimerization of nitroso compounds (R - N = O), a well-known and facile process. In the same year, Shanshal (1970) reported MINDO calculations of the inversion barrier for RNO compounds, for R = H, CH_3, and C_2H_5, and Haeflinger (1970) calculated the empirical resonance integral parameters for HNO and other small molecules in order to further develop Huckel theory for π-systems with NO bonds. Bespalov and coworkers (1971) determined electron densities for HON and other small molecules in order to elucidate the chemical properties of hydroxynitrenes.

INDO calculations on the HON molecule were also carried out by Hayes, Billingsley and Trindle (1972) as a basis for a discussion of the chemistry of oxynitrenes (R - O - $\bar{N}|$), which are of considerable interest to organic chemists. In a study of nitroxide formation, Ellinger and Serre (1973) discussed the use of nonrigid molecule group theory to explain a mechanism for the reaction

$$HNO + HNO \rightarrow H_2\dot{N}O + \dot{N}O$$

Here HNO provided a model for the reaction of two C-nitroso derivatives (R_1NO), which can combine to form nitroxides ($R_1 - \underset{\underset{\dot{O}}{|}}{N} - R_2$), either thermally or photochemically. Nitroxides are of interest as stable free radicals, and are presently in wide use as spin labels for biological systems.

The experimental and theoretical investigations cited above give some indication of the range of chemical questions which might be illuminated by a better understanding of the behavior of HNO and the isomer. HNO is of current practical interest. It is expected to be an intermediate species in atmospheric pollution (Leighton, 1961), and in combustion processes (Husain and Norrish, 1963). Since the hydrogen, oxygen and nitrogen atoms all have high cosmic abundances (Allen, 1963), searches for interstellar nitroxyl are currently under way (Vardya, 1966; Anders, 1973; Saito and Takagi, 1972b; Fourikis et al., 1974).

B. Experimental Information on HNO

Although Harteck (1933) was the first to obtain a solid compound with the empirical formula HNO, presumably the dimer, the first one

to make exact measurements on HNO (and DNO) was Dalby (1958), who determined the molecular geometry by gas phase absorption spectra. He correctly interpreted the observed electronic spectrum as the $^1A'' \leftarrow {}^1A'$ transition, and commented on the probable existence of a $^3A''$ state lying between these two.

Dalby produced HNO by these methods:

(1) Flash photolysis of nitromethane

(2) Flash photolysis of mixtures of NO and NH_3

(3) Flash photolysis of nitroethane or of isoamyl nitrite.

A fourth preparation was used in several subsequent investigations:

(4) Flash photolysis of a mixture of H_2 and NO to produce the reaction of H atoms and NO.

Less frequent have been the following preparations:

(5) HgH + NO

(6) by reactions of O_2 and NO with atomic hydrogen or organic molecules.

The first solid phase absorption spectrum of HNO isolated in a matrix was reported by Robinson and McCarty (1958). Similar solid phase absorption spectra were obtained by Brown and Pimentel (1958), who used method (1) and trapped the products in a solid Ar matrix at 20° K, and by Harvey and Brown (1959).

Reaction (4) produces a red chemiluminescence. Cashion and Polanyi (1959) attributed this to fluorescence of electrically excited HNO molecules, and set a lower limit for the (H-NO) bond dissociation energy. This emission was also investigated by Clement and Ramsay (1961), who set upper limits for the bond dissociation energy and studied the

predissociation of HNO in the excited ($^1A''$) state.

The kinetics of the formation reaction (4) have been the subject of many investigations. Clyne and Thrush (1961, 1962) followed the reaction by measuring the intensity of the red chemiluminescence produced by ($^1A''$) HNO. They proposed a termolecular mechanism,

$$H + NO + M \rightarrow HNO + M$$

where M is inert. They also proposed a mechanism for the decomposition of HNO and determined the dissociation energy of the ground state HNO molecule. The rate of reaction (4) has also been studied by Simonaitis (1963), Lambert (1966), in a mass-spectrometric study, Hartley and Thrush (1967), Hikida and coworkers (1971), Callear and Wood (1971), who studied the ultraviolet spectrum, Ahumada et al. (1972), and most recently by Oka, Singleton and Cvetanovic', (1977). A crossed molecular beam study of the chemiluminescence produced by reaction (4) (Ibaraki, Kusunoki, and Kodera, 1973), suggests that, under certain conditions, HNO is formed by two-body collisions between NO dimers and H atoms, rather than by the termolecular mechanism proposed by Clyne and Thrush (1961).

Other reactions of HNO have been investigated as well. A discussion of some of the possible reactions is given by Baldwin, et al. (1975). Various mixtures of type (2), some of which reacted explosively, were tried by Bancroft, Hollas, and Ramsay (1962) who studied the HNO and DNO absorption spectra at higher resolution and greater intensities than Dalby had. They confirmed the predissociation limit found by Clement and Ramsay. Zaslonko et al. (1970) studied the kinetics of the

decomposition of methyl nitrite in shock waves by following the chemiluminescence of the electronically-excited HNO which was produced. Reaction (5) has been investigated by Callear and Wood (1971, 1972), and its rate has been determined by Oka et al. (1977), who reported its chemiluminescence. HNO has also been formed by the decomposition of sodium benzenesulfohydroxamate (Seel and Bliefert, 1974).

Studies of decomposition reactions of HNO have been carried out by Kohout and Lampe (1965, 1967), who established the rate of the reaction

$$HNO + HNO \rightarrow N_2O + H_2O$$

by mass-spectrometric methods, and by Callear and Carr (1975), who suggested a mechanism for the thermal decomposition of HNO, in a study that monitored the ultraviolet spectrum.

Additional determinations of the IR spectra have been published by Ogilvie (1967), Shurvell (1971), and Ramaswamy and Ganesan (1974). Recently, some of the vibrational frequency assignments of the early experiments have been disputed. The frequencies ν_1 for the N-H stretching, and ν_3 for the bending, that were determined or used by Harvey and Brown (1959), Cashion and Polanyi (1959), Clement and Ramsay (1961), and Milligan, Jacox, Charles and Pimentel (1962), and compiled in Herzberg's book (1966), were reassigned by Ogilvie (1973), and by Clough, Thrush, Ramsay and Stamper (1973). The new results agree with those of Jacox and Milligan (1973), who performed a very thorough study of the IR spectrum of HNO isolated in an argon or neon matrix at 4° K or 14° K using six different isotopic species.

Microwave spectra of HNO and DNO were reported by Saito and Takagi (1972a, 1972b, 1973). They determined rotational constants in good agreement with those of Dalby, determined the quadropole coupling constants and dipole moments for the two isotopic species, and reported a DNO half-lifetime varying from 1 to 40 sec, depending on the condition of the surfaces of the absorption cell.

Most recently, Johns and McKellar (1977) have published a study of the infrared absorption spectra of HNO and DNO by laser Stark spectroscopy. Their vibrational frequencies agree with the 1973 re-assignments mentioned above; their dipole moments differed somewhat from those of Saito and Takagi (1972a, 1972b, 1973).

The triplet state of HNO, (^{3}A"), has never been directly observed, although many of the cited authors have commented upon its probable existence, and its possible involvement in the predissociation of HNO as well as its possible perturbing effect upon the singlet state spectra. Clyne and Thrush (1962), in a study of the reaction of H + NO, concluded that the ^{1}A" state of HNO should be populated by the ^{3}A" state, and proposed the processes:

$$H(^2S) + NO(^2\pi) + M \rightarrow HNO(^3A'') + M$$

$$HNO(^3A'') \rightleftharpoons HNO(^1A'')$$

Recently the triplet state has been proposed as part of the mechanism of another reaction. Emission spectra of HNO produced in reaction (6) have been reported by Ishiwata, Akimoto, and Tanaka (1973, 1974). They observed the same chemiluminescent HNO spectrum from each of these reactions:

$$O(^3P) + C_3H_6 + NO + O_2\ (^1\Delta g)/O_2$$

$$H + NO + O_2\ (^1\Delta g)/O_2$$

and

$$O(^3P)/O_2 + NO + \text{one of} \begin{cases} \text{acteylene} \\ \text{ethylene} \\ \text{formaldehyde, or} \\ \text{acetaldehyde} \end{cases}$$

The vibrational and rotational distributions of these HNO spectra were different from those observed (by Clyne and Thrush, Clement and Ramsay, and others) in the reactions of H(D) + NO + M. Ishiwata *et al.* propose a mechanism for the first reaction which involves the triplet state:

$$HNO(^1A') + O_2\ (^1\Delta g) \rightarrow HNO(^3A'') + O_2(^3\Sigma_g^-)$$

$$HNO(^3A'') + O_2\ (^1\Delta g) \rightarrow HNO(^1A'') + O_2(^3\Sigma_g^-)$$

They deduce the energy of the $^3A''$ state to lie 18.0 to 19.0 kcal above the ground state.

No experimental observations of the HON isomer have been reported.

C. Theoretical Approach to HNO

From a theoretical point of view, HNO has a number of interesting features. In the stable bent conformation HNO, it has a normal Lewis structure and is expected to have a singlet ground state. The linear conformations HNO and HON, on the other hand, are isoelectronic with O_2 and, hence, can be presumed to have triplet ground states. A crossing of the two potential surfaces can therefore be expected when the

hydrogen swings around the NO core. Furthermore a bent isomeric equilibrium conformation HON also has a Lewis structure, although with a considerable charge transfer towards nitrogen. One would therefore expect this to be a metastable isomer. The properties of this isomer as well as the barrier height between the two forms, are experimentally unknown to date. The elucidation of these questions requires ab-initio calculations. Below are summarized some of the more recent ab-initio calculations on HNO and its isomer.

In an SCF study of simple molecules with an NO bond, Millie and Berthier (1970) calculated the dipole moments, bond energies of the localized orbitals, and the electronic distribution and equilibrium conformation of HNO. Calculations for both isomers were carried out by Peslak, Klett, and David (1971) in a study of the hydrogen, lithium, and fluorine derivatives of nitric oxide. They determined equilibrium geometries, molecular energies, Mulliken population analyses and electron density maps. SCF-MO calculations were also published by J. E. Williams and Murrell (1971) as part of a study of the nitric oxide dimer. As part of a study of $\pi \rightarrow \pi^*$ transitions for small molecules, an SCF-CI calculation for HNO was undertaken by Ditchfield, Del Bene, and Pople (1972a). Their method involved a CI wavefunction of less than 10 configurations. The same authors (1972b) used this type of wavefunction to calculate equilibrium geometries for the three lowest states of HNO. Hariharan and Pople (1973) used single-determinant MO theory to determine the influence of polarization functions on

hydrogenation energies. This included the reaction $HNO + 2H_2 \rightarrow NH_3 + H_2O$.

SCF calculations on the isomerization of HNO to HON were done by Gallup (1975) at seven nonlinear geometries for both the singlet and triplet states. He predicted a triplet ground state for HON. At all geometries the distance from H to the NO bond was varied, but the NO bond length was not. The vertical ionization potential of HNO was calculated by Chong et al. (1975), using Rayleigh-Schroedinger Perturbation theory to obtain corrections to Koopman's Theorem.

More sophisticated calculations on HNO were done by the next group of authors. The unrestricted Hartree-Fock (UHF) method was used by R. D. Brown and G. R. Williams (1974) to calculate several properties of HNO in the ground state, including the dipole moment. Salotto and Burnelle (1969, 1970) also used the UHF method to calculate a potential energy surface for four states of HNO.

The excited states, of HNO were further studied via the equations of motion method by G. R. Williams (1975). This study confirms the presence of the low-lying triplet state. A CI study of the electronic spectrum of HNO undertaken by Wu, Peyerimhoff, and Buenker (1975), further supports the existence of this triplet state. Their calculated energy for the triplet agrees fairly well with that of Williams. They also explore the geometry of 6 states using SCF calculations.

D. Present Investigation

The main thrust of the present investigation is a reliable ab-initio study of the isomerization process for the lowest singlet and triplet state of the HNO molecule. We obtain the equilibrium conformations, the energy difference between the metastable and stable conformations, the energy barriers for the isomerization, and the relative positions of the singlet and triplet curves. With the exception of the energy difference between the singlet and triplet at the equilibrium distance (Wu, et al., 1975; G. R. Williams, 1975), none of these quantities has been calculated previously with a high quality ab-initio wavefunction. Another major objective is the interpretation of the observed results in terms of orbitals and their changes in the course of the reaction.

The calculation is based on a special configuration interaction process of a novel type called a Full Optimized Reaction Space. The aim of this approach is to include those configurations which contribute essentially to the energy changes occurring during the reaction under study and to avoid the calculation of correlations which remain constant. The method involves substantial multiconfigurational self-consistent field calculations as an integral part. For the interpretation of the results a new type of orbital is developed, the Directed Localized Reaction Orbitals, which also form an essential

part of the approach of the Full Optimized Reaction Space. These orbitals turn out to be in gratifying harmony with chemical intuition and furnish interesting insights into the changing bonding patterns that occur during the isomerization of nitrosyl hydride to nitrogen hydroxide.

II. THE METHOD OF THE FULL OPTIMIZED REACTION SPACE

A. Configuration Interaction and Orbital Optimization

In order to obtain chemical accuracy using molecular orbitals, electronic wavefunctions must be expressed as a superposition of many, often thousands, of configurations. Moreover the orbitals from which these configurations are formed must be adapted to the molecule. Ideally then these orbitals should be optimal for the required multiconfigurational wavefunction, but orbital optimization is altogether impossible for a wavefunction involving thousands of configurations. Fortunately it turns out that the shapes of the optimal orbitals are entirely determined by a relatively small number (usually less than thirty), of leading configurations. This number is small enough that the orbitals can be optimized by a multiconfigurational self-consistent-field (MCSCF) procedure such as the one developed by Cheung, Ruedenberg and Sundberg (Cheung 1975; Sundberg 1975). While the energy is markedly improved by <u>including</u> the much larger number of remaining configurations in the CI calculation, such energy improvement does not occur when the orbitals are further refined by including configurations other than the leading ones in the orbital optimization.

A crucial question is therefore: which are the leading configurations that determine the optimal orbitals? A common procedure is to build configurations from the occupied and virtual orbitals obtained from a preliminary self-consistent-field (SCF) calculation, and this

procedure is usually meant by a "straight" configuration interaction (CI) calculation. Previous work in this group has shown however that a single configuration, as assumed in the SCF approach, is inadequate for describing the molecular system along the entire path of many chemical reactions. In such cases optimal orbitals must therefore be obtained from multiconfigurational wavefunctions. One major objective of the present investigation is the development of a systematic process for determining those configurations which are essential for orbital optimization.

The choice of the number and types of configurations which are to be included in the CI calculation is the second important problem and it depends upon the objective to be achieved. We do not aim at the complete recovery of all correlation effects but merely wish to correctly account for that part of the wavefunction which causes chemically significant energy changes in the reaction to be described. Assuming that these reactions principally involve the valence shell we derive a selection of configurations which we call the full configurational reaction space. In this space we optimize the orbitals as mentioned in the preceding paragraph. The resulting set of configurations we call the full optimized reaction space (FORS).

B. The Full Configurational Reaction Space

Let us call the set of orthonormal MO's from which the configurations are generated the configuration-generating orbitals (CGO's). To

determine these orbitals means to find their expansion coefficients in terms of certain quantitative basis orbitals (QBO's) which are given as predetermined contractions of primitive atomic orbitals.

The essential supposition of the present approach is that the expansions of the CGO's in terms of the QBO's can, in principle, be formulated via certain "formal minimal atomic basis orbitals." The H and He atoms would have one s-type formal minimal basis orbital; the atoms from Li to Ne would have four additional formal minimal basis set orbitals: a 2s-type, a 2px-type, a 2py-type and a 2pz-type; etc. In a specific molecule the formal minimal atomic basis set orbitals can be imagined as linear combinations of the QBO's on all atoms in the molecule. The CGO's are then conceived as being linear combinations of these formal minimal basis orbitals. This postulate implies that the number of CGO's is equal to the total number of formal minimal basis set orbitals on all atoms in the molecule and this inference is in fact the only assumption used in the sequel.

Since the number of CGO's deduced by this reasoning is not too large we make only one further simplification: each inner shell is represented by one doubly-occupied CGO and no assumptions are made as to which configurations involving the valence CGO's should be included in the wavefunction, particularly since dependence on chemical intuition does not prove reliable for this purpose. Instead we take into account all configurations formed from the valence CGO's, with the inner shell CGO's doubly-occupied, and it is for this reason that we call the space of

all these configurations a full configurational reaction space. This full configuration space has an important and useful property: it is invariant with respect to nonsingular transformations among the CGO's. That is to say, this same configuration space is also spanned by all configurations made from any alternate set of CGO's provided that they span the same orbital space as the previously considered CGO's. In particular then, this full configuration space can also be imagined to be spanned by all configurations constructed from the formal minimal basis set orbitals, and optimization of the CGO's, therefore implies the optimal determination of molecule-adapted formal minimal basis set orbitals as well. We shall return below to the question of how they can be deduced from the CGO's. Since it is apparent that orbitals of such type will necessarily be the most populated contributing orbitals, no matter how the molecular wavefunction is constructed, our approach amounts to taking into account all configurations made from the most populated contributing orbitals.

C. The Full Optimal Reaction Space and the Natural Reaction Orbitals

Thus, the present approach consists of: (i) assuming as many CGO's as there are formal minimal basis set atomic orbitals in the molecule; (ii) formally expressing the wavefunction in terms of all orbital configurations that can be made from the CGO's; (iii) finding optimal expansions of the CGO's in terms of the QBO's for this type of wavefunction; (iv) finding the CI expansion coefficients. Unless the number

of CGO's is very small the dimension of the full configuration space will normally be too large for the MCSCF procedure to be carried out on and, in accordance with what was said earlier, it is then necessary to identify the leading configurations for the orbital optimization. This task is considerably simplified by the fact that we work in a full configuration space. Because of the invariance of the space against orbital transformations it is namely possible to choose as CGO's the natural orbitals of the wavefunction itself. The CI expansion in terms of the configurations based on the natural orbitals can be expected to show fastest convergence (or nearly so) and determines uniquely the set of leading configurations.

In view of what has been said a straightforward procedure for determining the optimal orbitals in the full configuration space is based on the following steps:

1) Determine a set of initial CGO's:
   a) Carry out an SCF calculation; use the occupied orbitals as some of the starting CGO's.
   b) In general this will not yield a sufficient number of starting CGO's. In order to determine the remaining ones, carry out an MCSCF calculation based on a very small number of obvious correlating configurations in addition to the SCF term, the additional configurations containing the required number of additional CGO's. Furthermore the occupied SCF orbitals can be left frozen during this MCSCF calculation.

2) Determine the CI wavefunction in the full configuration space made from all configurations constructed from these starting orbitals and express it in terms of configurations based on the natural orbitals.

   a) Carry out a CI calculation in the full configuration space based on the starting CGO's.

   b) Determine the natural orbitals for the resulting wavefunction.

   c) Express the wavefunction in terms of configurations made from these natural orbitals. One way to accomplish this is to repeat the CI calculation in terms of these configurations.

3) Improve the CGO's through an MCSCF calculation:

   a) Select a suitable number of leading configurations from the CI expansion obtained in step 2)c). This number will depend upon the convergence of the expansion but, at this stage, should not be significantly larger than 10.

   b) Carry out an MCSCF calculation based on these configurations to optimize the orbitals.

4) Repeat the calculations described in step 2) using now the configurations based on the improved orbitals obtained in step 3).

   a) Carry out the CI calculation.

   b) Determine the natural orbitals.

   c) Express the wavefunction in terms of configurations constructed from natural orbitals.

5) Repeat if necessary the calculations of step 3), but using now a

greater number of leading configurations, which are now obtained from step 4)c).

6) If step 5) was necessary, repeat the calculations described in step 2) using now the orbitals obtained in step 5).

7) This process (steps 5-6) is continued until convergence is achieved. This means that three criteria are satisfied which pertain to the natural-orbital-based expansions obtained in steps 2)c), 4)c), 6)c), etc. Namely, (a) the total energy, (b) the natural orbitals, and (c) the order of the leading natural-orbital-based configurations all remain unchanged. In the experience gained so far, this convergence was already accomplished after step 4). Supporting data will be given in the next chapter.

The well-defined uniqueness of this procedure, introduced by the use of the natural orbitals, is a major advantage when the energy of a reacting system is calculated along the reaction path. It guarantees that orbitals and energy are calculated with equal accuracy at various points along this path.

The final optimal natural orbitals will be called the natural reaction orbitals and the full configuration space spanned by the configurations made from these orbitals will be called the full optimal reaction space.

D. The Localized Reaction Orbitals

We return to the question of finding explicit orbitals that may correspond to the concept of the formal minimal basis set atomic orbitals

introduced in section IIB. According to what has been said earlier, they must be a set of alternate CGO's which are related to the NRO's by a nonsingular transformation. For the sake of simplicity we postulate this transformation to be orthogonal. If the concept has any validity such orbitals must furthermore be localized in the neighborhood of the various atoms. It seems therefore reasonable to try to generate such orbitals by applying a standard localization procedure such as the Edmiston-Ruedenberg (1963) method to the set of natural reaction orbitals. Although, in the past, localization procedures have been applied only to sets of occupied closed shell SCF orbitals there is no reason why they couldn't be used to localize the natural reaction orbitals of a multiconfigurational wavefunction. Since the number of natural reaction orbitals was assumed to be equal to the total number of minimal basis set orbitals in the molecule, physical intuition suggests that the localization procedure will generate, in the neighborhood of each atom, as many localized CGO's as there are formal minimal basis set orbitals. This has indeed been found to be so in those cases which have been investigated and we have thus established a method for unambiguously deducing molecule-adapted atomic orbitals that can serve as configuration-generating orbitals. We shall call them localized reaction orbitals (LRO's).

In order to satisfy chemical intuition we want to achieve more however. We would like the LRO's either to have lone pair character or to be pointing along the directions of various bonds. Straight

application of the localization procedure as suggested in the preceding paragraph does not yield such orbitals however, and it is therefore necessary to make a further orthogonal transformation among the LRO's on each atom to generate what we shall call directed localized reaction orbitals (DLRO's) with the desired characteristics. In order to single out the lone pairs it is only necessary to diagonalize the bond order matrix between the LRO's belonging to one atom. If the diagonalized bond order matrix has diagonal elements close to 2, then the corresponding orbitals will be lone pairs. In general, the remaining orbitals still do not point into bond directions however. A further orthogonal transformation is therefore required which must be based on maximizing, for a given orbital, the totality of the bond orders in one bond direction while at the same time minimizing that quantity in all other bond directions. A specific procedure to accomplish this for a triatomic molecule will be discussed in chapter III.

It is to be noted that because of the orthonormality of the LRO's as well as the DLRO's, the diagonal elements of the bond order matrix represent directly the populations of these orbitals. Furthermore those terms in the first-order density matrix expansion which are associated with the off-diagonal elements of the bond order matrix represent directly the interference densities between the LRO's or DLRO's.

With the help of the directed localized reaction orbitals theoretical results can be expressed in terms that relate to chemical

intuition. It is apparent that this possibility derives from our basic assumption equating the number of CGO's to the total number of formal minimal basis set atomic orbitals in the molecule.

III. THE FULL OPTIMAL REACTION SPACE FOR THE HNO MOLECULE

A. Orbitals

The method outlined in the preceding section will be applied to calculate the lowest two states of the HNO molecule at various geometries, linear as well as nonlinear. The set of QBO's chosen to expand the CGO's consists of 20 atomic orbitals: three s-type orbitals, two px-type orbitals, two py-type orbitals, two pz-type orbitals on both oxygen and nitrogen, and two s-type orbitals on hydrogen. Of the 20 QBO's, 16 are of a' symmetry (symmetric with respect to the plane of the molecule), and 4 are of a" symmetry (antisymmetric with respect to the plane of the molecule). The details of this basis set are described in the Appendix.

The formal minimal basis set orbitals of this molecule are: 1s, 2s, 2px, 2py, 2pz on oxygen, 1s, 2s, 2px, 2py, 2pz on nitrogen, and 1s on hydrogen. Hence there are two inner shell CGO's and nine valence CGO's. Of these nine, seven are of a' symmetry and two are of a" symmetry. For the nonlinear conformations the former will be called sigma orbitals and the latter will be called pi orbitals, in agreement with chemical convention. We shall use the notation σ_1, σ_2, σ_3, σ_4, σ_5, σ_1^*, σ_2^* for the former and π and π^* for the latter. In this notation we have anticipated that the orbitals σ_1^*, σ_2^* and π^* will turn out to have antibonding character. The orbital space spanned by σ_1 to σ_5

corresponds essentially to that spanned by the NO sigma bond, the NH (or OH) sigma bond and three lone pair orbitals.

For the linear conformation there are five sigma CGO's, two πx CGO's, and two πy CGO's. If we identify the pi CGO's of the nonlinear case with the πy CGO's of the linear case then two of the sigma CGO's of the nonlinear case will become the two πx CGO's of the linear case, one of which will be antibonding. We choose these to be the orbitals (σ_4) and (σ_5). In order to have a uniform notation we also introduce orbital labels (1), (2), ... (9) which are related to the previous symbols as indicated below:

Table 1. Labels for orbitals

General Label	1	2	3	4	5	6	7	8	9
Linear Label	σ_1	σ_2	σ_3	πx	πx^*	σ_1^*	σ_2^*	πy	πy^*
Nonlinear Label	σ_1	σ_2	σ_3	σ_4	σ_5	σ_1^*	σ_2^*	π	π^*

B. The Full Configurational Reaction Space

In order to generate the full configurational reaction space, we construct configurations in the form of spin-adapted antisymmetrized products (SAAP's) introduced by Salmon and Ruedenberg (1972), and Salmon, Ruedenberg, and Cheung (1972). A SAAP involving N electrons is defined in terms of d doubly-occupied orbitals, f_1, f_2, ..., f_d, and N-2d singly-occupied orbitals, f_{d+1}, f_{d+2}, ..., f_{N-d}, as well as an N-electron spin eigenfunction $\theta_\alpha^{SM}(1,2,\ldots,N)$. It is given by the formula

$$|f_1^2 \ldots f_d^2 f_{d+1} \ldots f_{N-d} \; ; \; \alpha\rangle = \qquad (3.1)$$

$$2^{-d/2} \mathcal{A} \{f_1^2 f_2^2 \ldots f_d^2 f_{d+1} \ldots f_{N-d} \theta_\alpha^{SM}\}$$

where $\mathcal{A} = (N!)^{-1/2} \sum_P (-1)^p P$ is the regular N-electron antisymmetrizer (for more detail see Salmon, et al. 1972).

Since we are generating all possible SAAP's resulting from arbitrary occupations of the nine valence CGO's by the twelve valence electrons, it follows that at least three orbitals must be doubly-occupied, and at most six orbitals can be singly-occupied. The possible spin functions are therefore those of a six-electron singlet and triplet, respectively.

For the singlet state there exist five six-electron spin eigenfunctions, $\theta_1 \ldots \theta_5$, corresponding to the branching diagrams (Salmon, 1974)

$\theta_1 =$  $\theta_2 =$  $\theta_3 =$  (3.2)

$\theta_4 =$  $\theta_5 =$ 

In order to have A' symmetry in the nonlinear case an even number of electrons must occupy pi orbitals. This leads to the types and numbers of orthonormal configurations shown in Table 2. The full configuration space is thus of dimension 1316.

In principle, this table remains valid also for the linear conformation although in this case certain configurations will vanish

Table 2. SAAP's of singlet full configuration space

Prototype Space Product	Number of Space Products	Spin Eigenfunction	No. of SAAP's
$\sigma_1^2\ \sigma_2^2\ \sigma_3^2\ \sigma_4^2\ \sigma_5^2\ \sigma_6\ \sigma_7$	21	θ_1	21
$\sigma_1^2\ \sigma_2^2\ \sigma_3^2\ \sigma_4^2\ \sigma_5^2\ \sigma_6^2$	7	θ_1	7
$\sigma_1^2\ \sigma_2^2\ \sigma_3^2\ \sigma_4\ \sigma_5\ \sigma_6\ \sigma_7\ \pi_1\ \pi_2$	35	$\theta_1\ \theta_2\ \theta_3\ \theta_4\ \theta_5$	175
$\sigma_1^2\ \sigma_2^2\ \sigma_3^2\ \sigma_4\ \sigma_5\ \sigma_6\ \sigma_7\ \pi_1^2$	35	$\theta_1\ \theta_2$	70
$\sigma_1^2\ \sigma_2^2\ \sigma_3^2\ \sigma_4\ \sigma_5\ \sigma_6\ \sigma_7\ \pi_2^2$	35	$\theta_1\ \theta_2$	70
$\sigma_1^2\ \sigma_2^2\ \sigma_3^2\ \sigma_4^2\ \sigma_5\ \sigma_6\ \ \pi_1\ \pi_2$	105	$\theta_1\ \theta_2$	210
$\sigma_1^2\ \sigma_2^2\ \sigma_3^2\ \sigma_4^2\ \sigma_5\ \sigma_6\ \ \pi_1^2$	105	θ_1	105
$\sigma_1^2\ \sigma_2^2\ \sigma_3^3\ \sigma_4^2\ \sigma_5\ \sigma_6\ \ \pi_2^2$	105	θ_1	105
$\sigma_1^2\ \sigma_2^2\ \sigma_3^2\ \sigma_4^2\ \sigma_5^2\ \ \pi_1\ \pi_2$	21	θ_1	21
$\sigma_1^2\ \sigma_2^2\ \sigma_3^2\ \sigma_4^2\ \sigma_5^2\ \ \pi_1^2$	21	θ_1	21
$\sigma_1^2\ \sigma_2^2\ \sigma_3^2\ \sigma_4^2\ \sigma_5^2\ \ \pi_2^2$	21	θ_1	21

Table 2. Continued

Prototype Space Product	Number of Space Products	Spin Eigenfunction	No. of SAAP's
$\sigma_1^2\ \sigma_2\ \sigma_3\ \sigma_4\ \sigma_5\ \sigma_6\ \sigma_7\ \pi_1^2\ \pi_2^2$	7	$\theta_1\ \theta_2\ \theta_3\ \theta_4\ \theta_5$	35
$\sigma_1^2\ \sigma_2^2\ \sigma_3\ \sigma_4\ \sigma_5\ \sigma_6\ \ \pi_1^2\ \pi_2^2$	105	$\theta_1\ \theta_2$	210
$\sigma_1^2\ \sigma_2^2\ \sigma_3^2\ \sigma_4\ \sigma_5\ \ \pi_1^2\ \pi_2^2$	210	θ_1	210
$\sigma_1^2\ \sigma_2^2\ \sigma_3^2\ \sigma_4^2\ \ \pi_1^2\ \pi_2^2$	35	θ_1	35
Totals:	868		1316

so that the configuration space actually has a somewhat smaller variational dimension for the linear singlet.

For the triplet state there exist nine possible six-electron spin eigenfunctions, $\theta_1 \ldots \theta_9$, corresponding to the branching diagrams

$\theta_1 =$  $\theta_2 =$  $\theta_3 =$  (3.3)

$\theta_4 =$  $\theta_5 =$  $\theta_6 =$ 

$\theta_7 =$  $\theta_8 =$  $\theta_9 =$ 

In order to have A" symmetry an odd number of electrons must occupy pi orbitals. Taking into account these limitations one obtains the types and numbers of configurations shown in Table 3.

The triplet space is thus of dimension 1722. Again certain simplifications obtain in the linear case.

C. Determination of the Starting CGO's

The lowest singlet state at the equilibrium geometry corresponds to the Lewis structure:

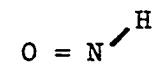

and the simplest approximation to the wavefunction is the self-consistent field wavefunction:

$$\Psi_o \quad (^1A') = \mathcal{A} \left\{ (is)\, \sigma_1^2\, \sigma_2^2\, \sigma_3^2\, \sigma_4^2\, \sigma_5^2\, \pi_1^2\, (\alpha\beta)^6 \right\} \qquad (3.4)$$

Table 3. SAAP's of triplet full configuration space

Prototype Space Product		Number of Space Products	Spin Eigenfunction	No. of SAAP's
$\sigma_1^2 \sigma_2^2 \sigma_3^2 \sigma_4^2 \sigma_5$	$\pi_1^2 \pi_2$	105	θ_1	105
$\sigma_1^2 \sigma_2^2 \sigma_3^2 \sigma_4^2 \sigma_5$	$\pi_2^2 \pi_1$	105	θ_1	105
$\sigma_1^2 \sigma_2^2 \sigma_3^2 \sigma_4 \sigma_5 \sigma_6$	$\pi_1^2 \pi_2$	140	$\theta_1 \theta_2 \theta_3$	420
$\sigma_1^2 \sigma_2^2 \sigma_3^2 \sigma_4 \sigma_5 \sigma_6$	$\pi_2^2 \pi_1$	140	$\theta_1 \theta_2 \theta_3$	420
$\sigma_1^2 \sigma_2^2 \sigma_3 \sigma_4 \sigma_5 \sigma_6 \sigma_7$	$\pi_1^2 \pi_2$	21	$\theta_1 \theta_2 \theta_3 \theta_4 \theta_5 \theta_6 \theta_7 \theta_8 \theta_9$	189
$\sigma_1^2 \sigma_2^2 \sigma_3 \sigma_4 \sigma_5 \sigma_6 \sigma_7$	$\pi_2^2 \pi_1$	21	$\theta_1 \theta_2 \theta_3 \theta_4 \theta_5 \theta_6 \theta_7 \theta_8 \theta_9$	189
$\sigma_1^2 \sigma_2^2 \sigma_3^2 \sigma_4^2 \sigma_5^2 \sigma_6$	π_1	42	θ_1	42
$\sigma_1^2 \sigma_2^2 \sigma_3^2 \sigma_4^2 \sigma_5^2 \sigma_6$	π_2	42	θ_1	42
$\sigma_1^2 \sigma_2^2 \sigma_3^2 \sigma_4^2 \sigma_5 \sigma_6 \sigma_7$	π_1	35	$\theta_1 \theta_2 \theta_3$	105
$\sigma_1^2 \sigma_2^2 \sigma_3^2 \sigma_4^2 \sigma_5 \sigma_6 \sigma_7$	π_2	35	$\theta_1 \theta_2 \theta_3$	105
	Totals:	686		1722

where

$$(is) = (i_o\,\alpha)\ (i_o\,\beta)\ (i_N\,\alpha)\ (i_N\,\beta) \tag{3.5}$$

with (i_o) and (i_N) being the inner shell orbitals on oxygen and nitrogen.

In the linear configuration the lowest singlet state is a doubly-degenerate $^1\Delta$ state whose two components are given by the following open-shell SCF functions:

$$\Psi_o\ (^1\Delta x) = \mathcal{A}\{\ (is)\ \sigma_1^{\,2}\ \sigma_2^{\,2}\ \sigma_3^{\,2}\ \pi x^2\ \pi y^2\ (\pi x^{*2} - \pi y^{*2})(\alpha\beta)^6\ \} \tag{3.6}$$

$$\Psi_o\ (^1\Delta y) = \mathcal{A}\{\ (is)\ \sigma_1^{\,2}\ \sigma_2^{\,2}\ \sigma_3^{\,2}\ \pi x^2\ \pi y^2\ (\pi x^*\ \pi y^* + \pi y^*\ \pi x^*)(\alpha\beta)^6\} \tag{3.7}$$

The component described by equation (3.6) is the one which will remain the lowest singlet upon bending to the nonlinear geometry whereas the component of equation (3.7) will become an excited singlet of symmetry A" in the nonlinear conformation.

In the nonlinear conformations the preliminary SCF calculation yields seven occupied sigma orbitals and one occupied pi orbital, all of which can serve as initial CGO's. Three additional initial CGO's are required (two sigma and one pi), and they must be obtained as linear combinations of the 20 - 8 = 12 virtual SCF orbitals (16 - 7 = 9 sigma and 4 - 1 = 3 pi). As explained in the previous chapter these additional three orbitals are obtained from a preliminary MCSCF calculation whose configurations have to be chosen from intuition. In the present case the three CGO's to be found are the antibonding

orbitals corresponding to the three bonds in the molecule. Reasonable additional configurations are therefore those which would provide for left-right correlation in these three bonds, and they would be obtained by replacing a doubly-occupied bonding orbital by the corresponding doubly-occupied antibonding orbital. The character of the sigma orbitals changes however with the displacement of the H atom. In order to avoid ambiguities it was decided to take into account all configurations obtained by replacing any one of the occupied sigma valence orbitals by the two antibonding orbitals to be determined. Consequently this resulted in the configurations shown in Table 4. Since only the orbitals σ_1^*, σ_2^* and π^* were varied in this MCSCF calculation, no significant savings in computer time would have resulted from choosing less than twelve configurations.

In the linear conformation, HNO is isoelectronic with O_2 and the SCF approximation to the lowest triplet is given by

$$\Psi_o\ (^3\Sigma^-) = \mathcal{A}\left\{ (is)\ \sigma_1^2\ \sigma_2^2\ \sigma_3^2\ \pi y^2\ \pi x^2\ (\pi x^*\ \pi y^* - \pi y^*\ \pi x^*)(\alpha\beta)^5\ \theta+ \right\} \tag{3.8}$$

where $\theta+ = \alpha\alpha,\ \beta\beta,\ (\alpha\beta + \beta\alpha)\ \sqrt{2}$. By analogy with the O_2 molecule, it is apparent that this is the ground state of the linear conformation. When the molecule is bent, this state will be described by the SCF approximation

$$\Psi_o\ (^3A'') = \mathcal{A}\left\{ (is)\ \sigma_1^2\ \sigma_2^2\ \sigma_3^2\ \sigma_4^2\ \pi^2\ (\sigma_5\pi^* - \pi^*\sigma_5)(\alpha\beta)^5\ \theta+ \right\} \tag{3.9}$$

Table 4. SAAP's used to generate initial antibonding CGO's for singlet

$\|\ \sigma_1^2\ \sigma_2^2\ \sigma_3^2\ \sigma_4^2\ \sigma_5^2\ \ \ \ \sigma_8^2\ \ \ \ \theta_1\ \rangle$
$\|\ \ \ \ \sigma_2^2\ \sigma_3^2\ \sigma_4^2\ \sigma_5^2\ \sigma_6^2\ \ \ \sigma_8^2\ \ \ \ \theta_1\ \rangle$
$\|\ \ \ \ \sigma_2^2\ \sigma_3^2\ \sigma_4^2\ \sigma_5^2\ \ \ \sigma_7^2\ \sigma_8^2\ \ \ \ \theta_1\ \rangle$
$\|\ \sigma_1^2\ \ \ \ \sigma_3^2\ \sigma_4^2\ \sigma_5^2\ \sigma_6^2\ \ \ \sigma_8^2\ \ \ \ \theta_1\ \rangle$
$\|\ \sigma_1^2\ \ \ \ \sigma_3^2\ \sigma_4^2\ \sigma_5^2\ \ \ \sigma_7^2\ \sigma_8^2\ \ \ \ \theta_1\ \rangle$
$\|\ \sigma_1^2\ \sigma_2^2\ \ \ \ \sigma_4^2\ \sigma_5^2\ \sigma_6^2\ \ \ \sigma_8^2\ \ \ \ \theta_1\ \rangle$
$\|\ \sigma_1^2\ \sigma_2^2\ \ \ \ \sigma_4^2\ \sigma_5^2\ \ \ \sigma_7^2\ \sigma_8^2\ \ \ \ \theta_1\ \rangle$
$\|\ \sigma_1^2\ \sigma_2^2\ \sigma_3^2\ \ \ \ \sigma_5^2\ \sigma_6^2\ \ \ \sigma_8^2\ \ \ \ \theta_1\ \rangle$
$\|\ \sigma_1^2\ \sigma_2^2\ \sigma_3^2\ \ \ \ \sigma_5^2\ \ \ \sigma_7^2\ \sigma_8^2\ \ \ \ \theta_1\ \rangle$
$\|\ \sigma_1^2\ \sigma_2^2\ \sigma_3^2\ \sigma_4^2\ \ \ \ \sigma_6^2\ \ \ \sigma_8^2\ \ \ \ \theta_1\ \rangle$
$\|\ \sigma_1^2\ \sigma_2^2\ \sigma_3^2\ \sigma_4^2\ \ \ \ \ \ \sigma_7^2\ \sigma_8^2\ \ \ \ \theta_1\ \rangle$
$\|\ \sigma_1^2\ \sigma_2^2\ \sigma_3^2\ \sigma_4^2\ \sigma_5^2\ \ \ \ \ \ \ \ \sigma_9^2\ \ \theta_1\ \rangle$

and it does not necessarily remain the ground state.

In this case the SCF calculation yields nine occupied orbitals, seven sigmas and two pis, and so only the two initial sigma CGO's σ_1^* and σ_2^* have to be determined by the preliminary MCSCF calculation. The configurations for this calculation are again generated by replacing each of the sigma orbitals in equation (3.8) by σ_1^* or σ_2^*, which yields the 11 configurations shown in Table 5. In this MCSCF calculation only σ_1^* and σ_2^* are being varied.

D. Quantitative Aspects

We wish to illustrate the procedure described in the previous chapter by discussing some quantitative results for the singlet state. We shall examine some energetic results at four geometries at which we examined the convergence of the FORS procedure. These geometries are denoted as points B, E, M, and I in the next chapter. For point I which is close to the experimental equilibrium configuration (HNO angle 108.5°, Dalby, 1958) we shall further examine some data relating to the wavefunction. At all four of these points we tested the convergence of the FORS procedure by carrying out the following steps:

1a) Preliminary SCF calculation based on expression (3.4)

1b) Preliminary MCSCF calculation based on configurations of Table 4

2) Full CI calculation and natural orbital determination

3) Orbital optimization through MCSCF calculation based on 9

Table 5. SAAP's used to generate initial antibonding CGO's for triplet

$\|$	σ_1^2	σ_2^2	σ_3^2	σ_4^2		σ_8^2	σ_5	σ_9 $\rangle$
$\|$		σ_2^2	σ_3^2	σ_4^2	σ_6^2	σ_8^2	σ_5	σ_9 $\rangle$
$\|$		σ_2^2	σ_3^2	σ_4^2	σ_7^2	σ_8^2	σ_5	σ_9 $\rangle$
$\|$	σ_1^2		σ_3^2	σ_4^2	σ_6^2	σ_8^2	σ_5	σ_9 $\rangle$
$\|$	σ_1^2		σ_3^2	σ_4^2	σ_7^2	σ_8^2	σ_5	σ_9 $\rangle$
$\|$	σ_1^2	σ_2^2		σ_4^2	σ_6^2	σ_8^2	σ_5	σ_9 $\rangle$
$\|$	σ_1^2	σ_2^2		σ_4^2	σ_7^2	σ_8^2	σ_5	σ_9 $\rangle$
$\|$	σ_1^2	σ_2^2	σ_3^2		σ_6^2	σ_8^2	σ_5	σ_9 $\rangle$
$\|$	σ_1^2	σ_2^2	σ_3^2		σ_7^2	σ_8^2	σ_5	σ_9 $\rangle$
$\|$	σ_1^2	σ_2^2	σ_3^2	σ_4^2		σ_8^2	σ_6	σ_9 $\rangle$
$\|$	σ_1^2	σ_2^2	σ_3^2	σ_4^2		σ_8^2	σ_7	σ_9 $\rangle$

leading natural - orbital - based configurations

4) Full CI calculation and redetermination of natural orbitals

5) Orbital reoptimization through an MCSCF calculation based on the 16 leading configurations

6) Full CI calculation and redetermination of natural orbitals

Table 6 lists the energies of singlet points B, E, M, and I for each of the seven steps just mentioned. This table confirms what was mentioned earlier, namely (1) the CI energy is considerably below the corresponding MCSCF energy, and (2) while the MCSCF calculation of step 3) substantially improves the CI energy of step 4), the MCSCF optimization of step 5) (16 configurations instead of 9) no longer significantly improves the CI energy of step 6). Thus steps 5) and 6) are unnecessary from the energetic point of view.

From this, one would infer that the orbitals have settled down after the optimization of step 3). This conclusion is supported by comparison of the expansions in terms of QBO's for the natural orbitals obtained in step 2), 4), and 6) respectively for point I. Table 7 lists these three expansions for two sigma natural orbitals at that geometry.

One would further expect that, when the natural orbitals have converged, then the relative importance of the various configurations in the CI expansions should stabilize. This is illustrated by the data presented in Table 8, which contains the lists of the 20 leading

Table 6. Total energies (in atomic units) for the seven steps of the FORS calculation at four singlet geometries

Step	Wavefunction	Point B	Point E	Point M	Point I
1a	SCF	-129.4479	-129.3966	-129.3625	-129.4991
1b	Prelim. MCSCF	-129.4845	-129.4483	-129.4312	-129.5696
2	CI	-129.5457	-129.5233	-129.5180	-129.6367
3	9-conf. MCSCF	-129.5231	-129.5102	-129.4948	-129.6200
4	CI	-129.5519	-129.5330	-129.5251	-129.6390
5	16-conf. MCSCF	-129.5400	-129.5180	-129.5076	-129.6268
6	Final CI	-129.5527	-129.5348	-129.5265	-129.6392

Table 7. Illustration of convergence of the expansions of two NO's in terms of QBO's for the singlet state at point I

ETCGAO		First Sample Natural Orbital		
		Step 2	Step 4	Step 6
N	S	0.2668	-0.2937	-0.2964
	S'	-0.6892	0.6661	0.6838
	S''	0.0025	-0.0020	-0.0020
	X	-0.2994	0.3043	0.3154
	X'	-0.0886	0.0807	0.0831
	Y	0.0	0.0	0.0
	Y'	0.0	0.0	0.0
	Z	0.2660	-0.2929	-0.2945
	Z'	0.0615	-0.0678	-0.0663
O	S	-0.1103	0.1724	0.1569
	S'	0.2562	-0.3528	-0.3252
	S''	-0.0020	0.0020	0.0020
	X	0.4264	-0.2847	-0.2659
	X'	0.0204	-0.0200	-0.0203
	Y	0.0	0.0	0.0
	Y'	0.0	0.0	0.0
	Z	0.1833	-0.1942	-0.1860
	Z'	0.0175	-0.0262	-0.0235
H	S	0.0956	-0.0947	-0.1022
	S'	0.0410	-0.0367	-0.0413

Second Sample Natural Orbital		
Step 2	Step 4	Step 6
-0.0111	0.0089	-0.0092
0.1017	-0.1077	0.1098
-0.0041	0.0057	-0.0058
-0.6843	0.6829	-0.6767
-0.0266	0.0240	-0.0260
0.0	0.0	0.0
0.0	0.0	0.0
0.2851	-0.2763	0.2862
-0.0495	0.0455	-0.0476
0.0435	-0.0399	0.0388
-0.0643	0.0574	-0.0568
-0.0047	0.0051	-0.0052
0.2567	-0.2296	0.2273
0.0344	-0.0342	0.0337
0.0	0.0	0.0
0.0	0.0	0.0
-0.3081	0.2951	-0.3096
0.0230	-0.0233	0.0244
-0.2719	0.2875	-0.2782
0.1444	-0.1430	0.1426

Table 8. The 20 leading configurations in the CI expansions of the 6 steps of the FORS calculation for the singlet state at point I. The configurations for each expansion are in terms of MO's (from the MCSCF optimization) or of NO's (natural orbitals of the CI wavefunction) as indicated

	Step 1 (MO's)	Step 2 (NO's)	Step 3 (MO's)	Step 4 (NO's)	Step 5 (MO's)	Step 6 (NO's)
1	1	1	1	1	1	1
2	106	106	106	106	106	106
3	93	99	99	99	99	99
4	73	84	84	84	84	84
5	98	95	95	95	95	95
6	39	87	67	87	87	87
7	84	67	100	67	67	67
8	80	89	889	89	89	93
9	95	91	89	93	93	89
10	45	93	87	91	100	91
11	55	97	93	100	91	100
12	44	100	94	97	889	97
13	41	854	878	889	97	64
14	64	64	64	64	94	889
15	30	44	88	101	64	94
16	40	101	16	94	101	101
17	15	85	81	82	44	82
18	60	81	61	44	878	44
19	61	94	873	885	82	81
20	12	82	85	81	885	885

configurations in the order of their importance for the CI expansion based on: i) the initial orbitals of step 1), ii) the natural orbitals of step 2), iii) the MCSCF orbitals of step 3), iv) the NO's of step 4), v) the MCSCF orbitals of step 5), vi) the NO's of step 6). The numbers used in the table represent a consistent labeling of the various configurations which will be defined in Chapter IV, but which is of no particular concern in the present context. For the CI calculations of steps 4) and 6) the expansion coefficients in terms of the configurations given in Table 8 are listed in Table 9.

It is apparent that the CI expansions in terms of the natural - orbital - based expansions have stabilized after step 4). This is not true to the same degree for the CI expansion in terms of the configurations based on the orbitals which are the direct outcome of the MCSCF calculations. Indeed these two kinds of orbitals are not identical and this is illustrated by the transformation matrix between the MCSCF MO's and the NO's for steps 3) and 4) which is given in Table 10.

E. Directed Localized Reaction Orbitals

In Chapter II we had specified two steps for obtaining directed localized reaction orbitals: i) regular localization of the natural reaction orbitals, giving to each atom as many LRO's as there would be formal minimal basis set atomic orbitals; ii) diagonalization of the local bond order matrix that is generated by the LRO's belonging

Table 9. Expansion coefficients of the 20 leading configurations in the CI expansions of steps 4 and 6 of the FORS calculation for the singlet state at point I

Step 4		Step 6	
1	-0.9576	1	0.9573
106	0.1982	106	-0.1983
99	-0.1078	99	-0.1067
84	0.0734	84	-0.0716
95	0.0655	95	-0.0650
87	0.0611	87	0.0633
67	0.0508	67	-0.0515
89	0.0448	93	-0.0452
93	0.0420	89	0.0447
91	-0.0401	91	0.0410
100	-0.0330	100	-0.0333
97	0.0307	97	-0.0325
889	-0.0257	64	-0.0265
64	0.0257	889	0.0253
101	0.0246	94	-0.0248
94	0.0241	101	0.0247
82	0.0214	82	-0.0220
44	0.0204	44	-0.0201
885	-0.0186	81	-0.0194
81	-0.0183	885	-0.0194

Table 10. Orthogonal transformation between sigma and pi valence NO's and MO's from steps 3 and 4 of the FORS calculation of the singlet state at geometry I

	NO 1	NO 2	NO 3	NO 4	NO 5	NO 6	NO 7
Sigma Transformation							
MO 1	0.6553	-0.7276	-0.1995	-0.0336	-0.0098	-0.0010	-0.0021
2	-0.7552	-0.6353	-0.1583	-0.0280	-0.0058	-0.0000	0.0002
3	-0.0115	0.2553	-0.9666	-0.0155	0.0019	0.0001	-0.0023
4	0.0000	0.0317	0.0240	-0.9322	0.3595	-0.0008	-0.0022
5	0.0021	-0.0244	-0.0103	0.3587	0.9330	-0.0000	-0.0007
6	0.0000	-0.0005	0.0007	-0.0001	-0.0002	0.9443	-0.3288
7	0.0016	-0.0009	-0.0024	-0.0020	0.0015	0.3288	0.9443
Pi Transformation							
MO 1	-0.9999	0.0011					
2	0.0011	0.9999					

to one atom. In HNO, step i) generates one LRO on H and one π-type LRO and three sigma LRO's on O as well as on N. Step ii) is applied only to the sigma LRO's on O and N, and generates lone pairs. The other orbitals on these two atoms do not point into bond directions.

It proved possible to achieve such bond-directedness by the following procedure. Let P_{ij} be the bond order matrix between all seven localized sigma orbitals resulting after step ii). Let the oxygen orbitals be denoted by the indices 1, 2, 3; the nitrogen orbitals by the indices 4, 5, 6; and the hydrogen by 7. Then bond-directed orbitals on the O atom are obtained if one diagonalizes the following matrix

$$D^{\circ}_{ik} = W_i^{-2} \; P_{ii}^2 \; \delta_{ik} + W_i W_k \; (\sum_{j=4}^{6} P_{ij} \; P_{kj} - P_{i7} \; P_{k7}) \qquad (3.10)$$

where

$$W_i = \begin{cases} 3 & \text{if } P_{ii} \leq 1 \\ 3-2P_{ii} & \text{if } P_{ii} \geq 1 \end{cases} \qquad (3.11)$$

The indices i and k run from 1 to 3 only.

Diagonalization of this matrix extremizes the diagonal elements

$$D^{\circ}_{ii} = W_i^{-2} \; P_{ii}^{\;2} + W_i^{\;2} \; (\sum_{j=4}^{6} P_{ij}^{\;2} - P_{i7}^{\;2}). \qquad (3.12)$$

It is apparent that, because of the weighting factors, W_i, the diagonal elements for lone pairs ($P_{ii} \cong 2$) will remain essentially unchanged. For bonding orbitals ($P_{ii} \cong 1$) the diagonalization will make the quantity $(\sum_{j=4}^{6} P_{ij}^2 - P_{i7}^2)$ either maximum or minimum. This results in orbitals which have large bond orders with N and small bond orders with H, or vice-versa. For the orbitals with intermediate character ($P_{ii} \cong 1.5$), such as occur when the H is about equidistant from O and N, compromise orbitals will result. An analogous matrix D_{ik}^{N} is obtained for the directionalization on N if one interchanges the orbitals 1, 2, 3 with the orbitals 4, 5, 6. The quantitative directed localized reaction orbitals which result from this criterion will be discussed in detail in Chapters IV and V.

IV. THE ISOMERIZATION OF HNO: QUANTITATIVE RESULTS

A. The Quantitative Basis Orbitals

Since a major objective of this investigation is to test the power of the FORS procedure, it was decided to deemphasize the power of the basis and so a relatively modest basis was chosen, namely a (6s, 4p) Gaussian primitive set contracted to a (3s, 2p) QBO set on N and O, and a (4s) Gaussian primitive set contracted to a (2s) QBO set on H, resulting in a total of 20 QBO's.

In order to make up for this relative simplicity the orbital exponent parameters were optimized by SCF calculations with the uncontracted basis sets at various conformations. This was possible because even-tempered Gaussian sets were used for the primitives (Ruedenberg, Raffenetti, and Bardo 1973; Bardo and Ruedenberg, 1973; Raffenetti and Ruedenberg, 1973) and, for these, orbital exponent optimization is quite feasible, even in molecules.

Concretely, two sets of two parameters have to be independently determined for O and N, one set (αs, βs) for the s functions and another set (αp, βp) for the p functions; for H only one set, (αs, βs), is required. From these optimized uncontracted bases, contractions were then derived which optimally simulate the uncontracted bases for each conformation, using the method developed by Bardo and Ruedenberg (1974) and modified by Cheung (1975).

This entire optimization procedure was carried out at five points which were chosen as follows. Elliptic coordinates ξ, η ($1 \leq \xi \leq \infty$; $-1 \leq \eta \leq +1$) were defined with the N and O atom at the experimental bond distance (2.289 bohr radii) as foci. In this coordinate system the H atom at its experimental position (ONH angle = 108.5° ; NH bond distance = 2.007 bohr) corresponds to $\xi = (R_{OH} + R_{NH})/R_{NO} = 2.37$ and $\eta = (R_{OH} - R_{NH})/R_{NO} = 0.65$. The five points mentioned were chosen to lie on the ellipse $\xi = 2.37$ and having the η values -1.0, -0.7, 0.0, +0.7, +1.0, the first and the last values being the linear conformations. From the values of all the (α, β) parameters at these five points, values of the same parameters were deduced by a rough interpolation for eight additional points corresponding to the η values $\pm.1$, $\pm.3$, $\pm.5$, $\pm.9$. At these points the same contraction process was then carried out. Figure 1 shows the hyperbolae corresponding to the 10 η values $\pm.9$, $\pm.7$, $\pm.5$, $\pm.3$, $\pm.1$ and their intersection with the ellipse $\xi = 2.37$.

Minimizations of the various parameter pairs (α_i, β_i) were carried out using a novel two-dimensional nonlinear minimization program called MINPOP which is described in Appendix B.

The explicit expansions of the resulting QBO's in terms of the primitives and the orbital exponents of the primitives are given in Table 95 to 107 in Appendix A for the 13 η values considered.

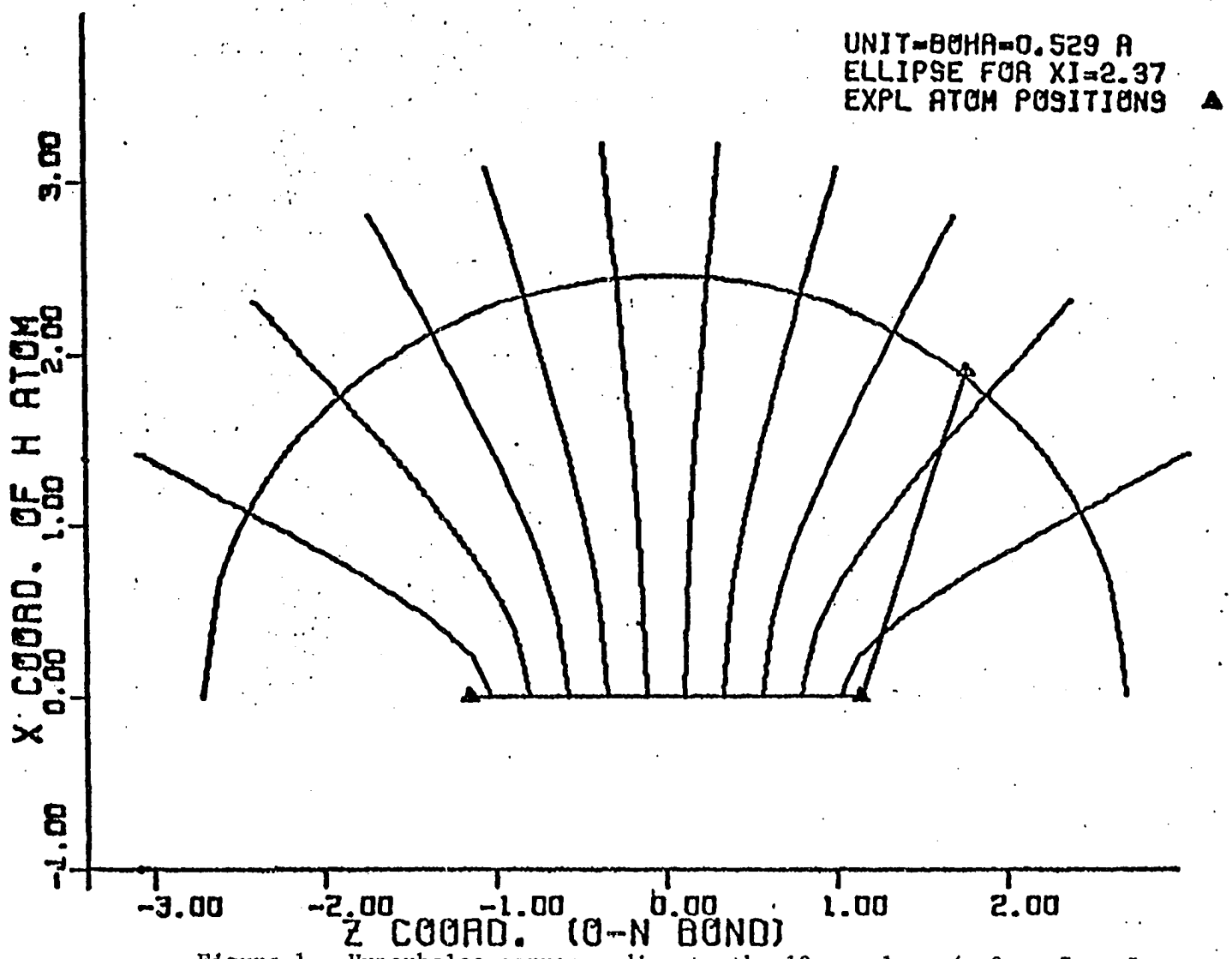

Figure 1. Hyperbolae corresponding to the 10 η values (-.9, -.7, -.5, -.3, -.1, .1, .3, .5, .7, .9) and the ellipse passing through the experimental points

B. Geometry Optimization

The HNO molecule has three independent geometric parameters. We choose these to be the NO distance, R_{NO}, and the elliptic coordinates ξ and η. For example the three internuclear distances can be expressed in terms of these independent parameters as follows: $R_{NO} = R_{NO}$, $R_{OH} = \frac{1}{2}R_{NO} \cdot (\xi + \eta)$, and $R_{NH} = \frac{1}{2}R_{NO} \cdot (\xi - \eta)$. We choose η as <u>independent reaction coordinate for the isomerization displacement of the H</u>. Accordingly, we optimize the geometry, for each of the 13 fixed η values -1, -.9, -.7, -.5, -.3, -.1, 0.0, .1, .3, .5, .7, .9, 1, with respect to the other two variables ξ and R_{NO}. If the resulting reaction path would correspond to an ellipse ξ = constant, then it would be a path of steepest descent or gentlest ascent, because the curves η = constant are orthogonal trajectories of the curve ξ = constant. In fact, this is not the case but the calculated reaction path is still meaningful since the angles it forms with the curves η = constant do not deviate too much from $\pi/2$. In any event the minima and maxima on the reaction path calculated in this manner will be the points at which all three derivatives will vanish. Hence they are the true minima and maxima of the energy surface, and correspond, to the stable and metastable equilibrium points and to the reaction barrier.

The geometry optimizations were based on the molecular energies calculated with the open and closed shell SCF wavefunction formulated in equations 3.4, 3.6, 3.8 and 3.9. They were carried out separately

for the singlet and triplet state. Minimizations in the (R_{NO}, ξ) space for each given η were carried out using again the MINPOP procedure of Appendix B.

The Cartesian coordinates for the resulting conformations are given in Table 11a. The corresponding bond angles and bond distances are given in Table 11b. In the sequel these 13 points will be referred to as points A to L, as indicated in the Table. This data is graphically displayed in Figure 2, vs. arc length as abscissa. The lower part shows the path of the H atom for the singlet and triplet states, and the ranges of the O and N positions. The upper part gives the plots of the three bond lengths. The lengths of the reaction paths along the curve traveled by the H atom shown in the lower part, calculated from the center point = 0.0 to each of the 13 points mentioned, are listed in Table 11b.

Figure 3 shows a drawing, to the same scale as Figure 1, of the bonds in HNO for various nonlinear conformations of the singlet state with the H atom always connected to the nearer one of the heavy atoms. Figure 4 is the result of superimposing Figure 3 on Figure 1, and shows how the reaction path traced out by the optimized geometries differs from that of the ellipse which passes through the experimental conformation.

C. Energies Along the Reaction Path

As mentioned in Section IIID, a six-step FORS calculation was carried out for the singlet at four of the 13 optimized points listed in Table 11.

Table 11a. Optimal geometries in bohrs for all points. Coordinates of all atoms in the (X,Z) plane. All Y-coordinates are zero.

Name	Eta	State	Xn	Zn	Xo	Zo	Xh	Zh
A	-1.0	S	0.0	1.215	0.0	-1.215	0.0	-2.950
		T	0.0	1.225	0.0	-1.225	0.0	-2.958
B	-0.9	S	0.0	1.210	0.0	-1.210	1.120	-2.556
		T	0.0	1.250	0.0	-1.250	1.131	-2.592
C	-0.7	S	0.0	1.229	0.0	-1.229	1.675	-1.853
		T	0.0	1.276	0.0	-1.276	1.681	-1.874
D	-0.5	S	0.0	1.243	0.0	-1.243	1.847	-1.234
		T	0.0	1.293	0.0	-1.293	1.847	-1.247
E	-0.3	S	0.0	1.262	0.0	-1.262	1.844	-0.692
		T	0.0	1.303	0.0	-1.303	1.865	-0.705
F	-0.1	S	0.0	1.262	0.0	-1.262	1.822	-0.222
		T	0.0	1.291	0.0	-1.291	1.839	-0.225
M	0.0	S	0.0	1.237	0.0	-1.237	1.863	0.0
		T	0.0	1.268	0.0	-1.268	1.875	0.0
G	0.1	S	0.0	1.215	0.0	-1.215	1.961	0.232
		T	0.0	1.259	0.0	-1.259	1.978	0.235
H	0.3	S	0.0	1.179	0.0	-1.179	2.067	0.740
		T	0.0	1.255	0.0	-1.255	2.006	0.735
I	0.5	S	0.0	1.160	0.0	-1.160	1.953	1.268
		T	0.0	1.243	0.0	-1.243	1.943	1.283
J	0.7	S	0.0	1.145	0.0	-1.145	1.721	1.868
		T	0.0	1.205	0.0	-1.205	1.732	1.896
K	0.9	S	0.0	1.139	0.0	-1.139	1.283	2.545
		T	0.0	1.148	0.0	-1.148	1.137	2.565
L	1.0	S	0.0	1.143	0.0	-1.143	0.0	2.953
		T	0.0	1.145	0.0	-1.145	0.0	2.955

Table 11b. Bond lengths, bond angles, and arc lengths along curve for all points. Distances are in bohrs, angles in degrees. A = atom (N or O) closer to H. B = atom (N or O) further from H.

Name	Eta	State	R(N-O)	R(H-A)	< HAB	Arc
A	-1.0	S	2.431	1.735	180.0	-4.019
		T	2.451	1.733	180.0	-4.227
B	-0.9	S	2.420	1.751	140.2	-2.829
		T	2.500	1.755	139.9	-3.024
C	-0.7	S	2.459	1.787	110.4	-1.893
		T	2.553	1.784	109.6	-1.962
D	-0.5	S	2.487	1.847	89.7	-1.241
		T	2.586	1.847	88.6	-1.254
E	-0.3	S	2.524	1.930	72.8	-0.698
		T	2.606	1.959	72.2	-0.710
F	-0.1	S	2.525	2.098	60.3	-0.226
		T	2.583	2.126	59.9	-0.228
M	0.0	S	2.474	2.236	56.4	0.0
		T	2.536	2.263	55.9	0.0
G	0.1	S	2.429	2.214	62.4	0.252
		T	2.518	2.227	62.6	0.258
H	0.3	S	2.359	2.130	76.0	0.773
		T	2.509	2.072	75.5	0.768
I	0.5	S	2.320	1.953	90.7	1.319
		T	2.486	1.944	91.2	1.323
J	0.7	S	2.289	1.844	111.1	1.985
		T	2.409	1.865	111.8	1.979
K	0.9	S	2.278	1.897	137.4	2.967
		T	2.296	1.817	141.3	2.907
L	1.0	S	2.286	1.808	180.0	4.176
		T	2.290	1.811	180.0	4.112

Figure 2. Optimized geometries for the isomerization HON → NOH in the singlet and triplet state

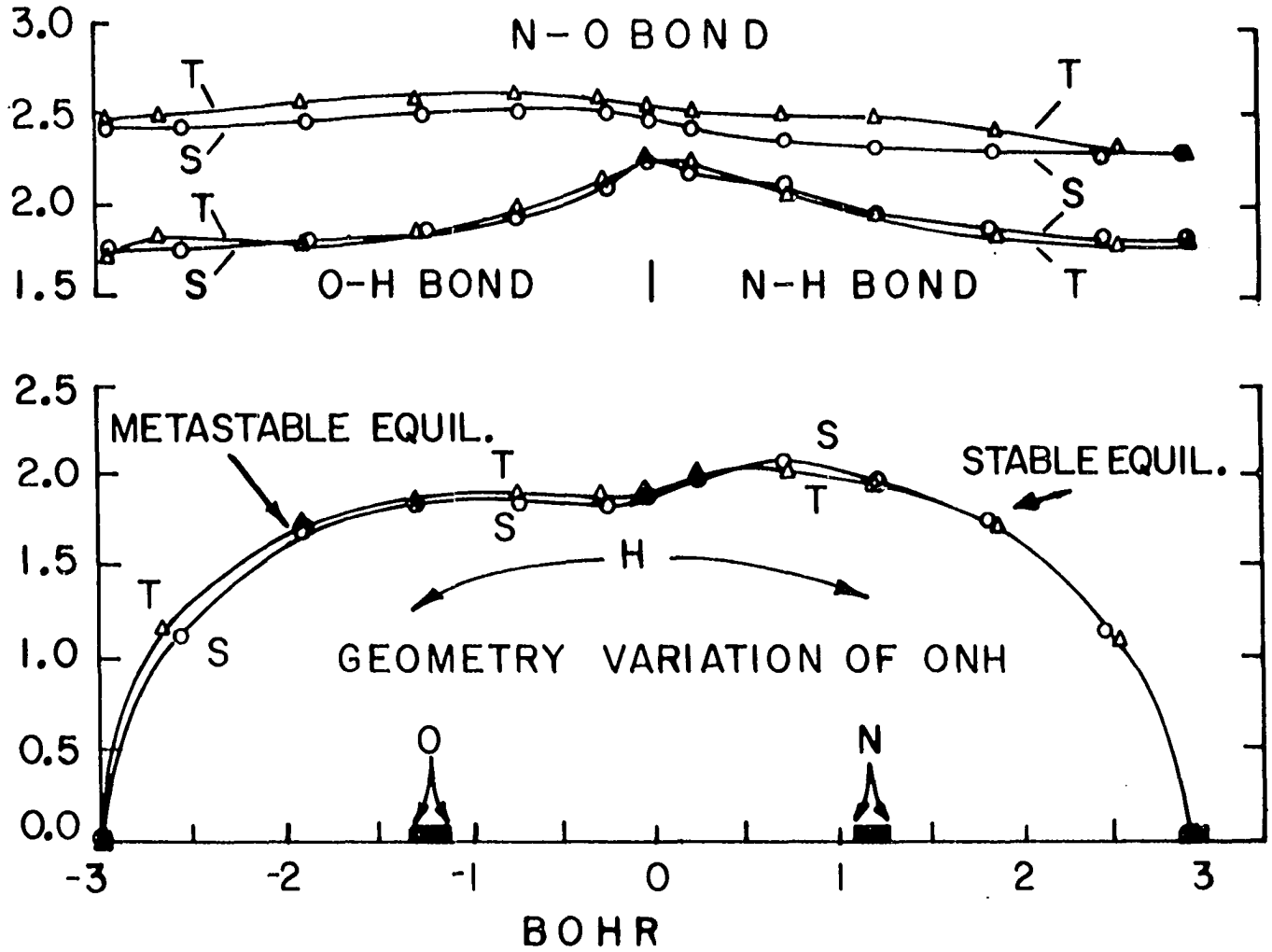
3.0
2.5
2.0
1.5
N-O BOND
T
S
T
S
T
S
O-H BOND
N-H BOND
T
2.5
2.0
1.5
1.0
0.5
0.0
METASTABLE EQUIL.
STABLE EQUIL.
T
S
S
T
H
T
S
GEOMETRY VARIATION OF ONH
O
N
-3
-2
-1
0
1
2
3
BOHR

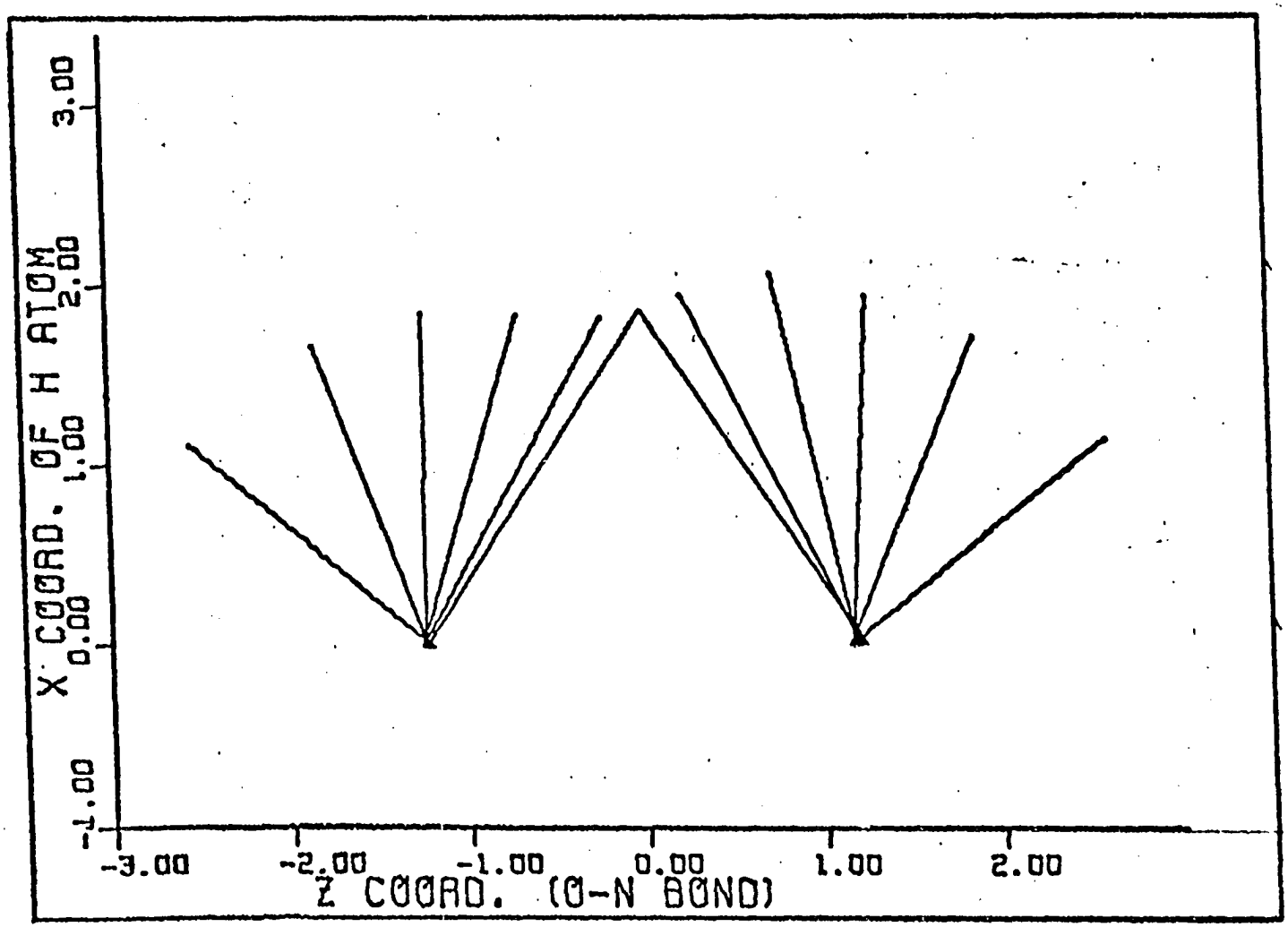

Figure 3. Positions of bonds to H for the optimized geometries of the nonlinear singlet points

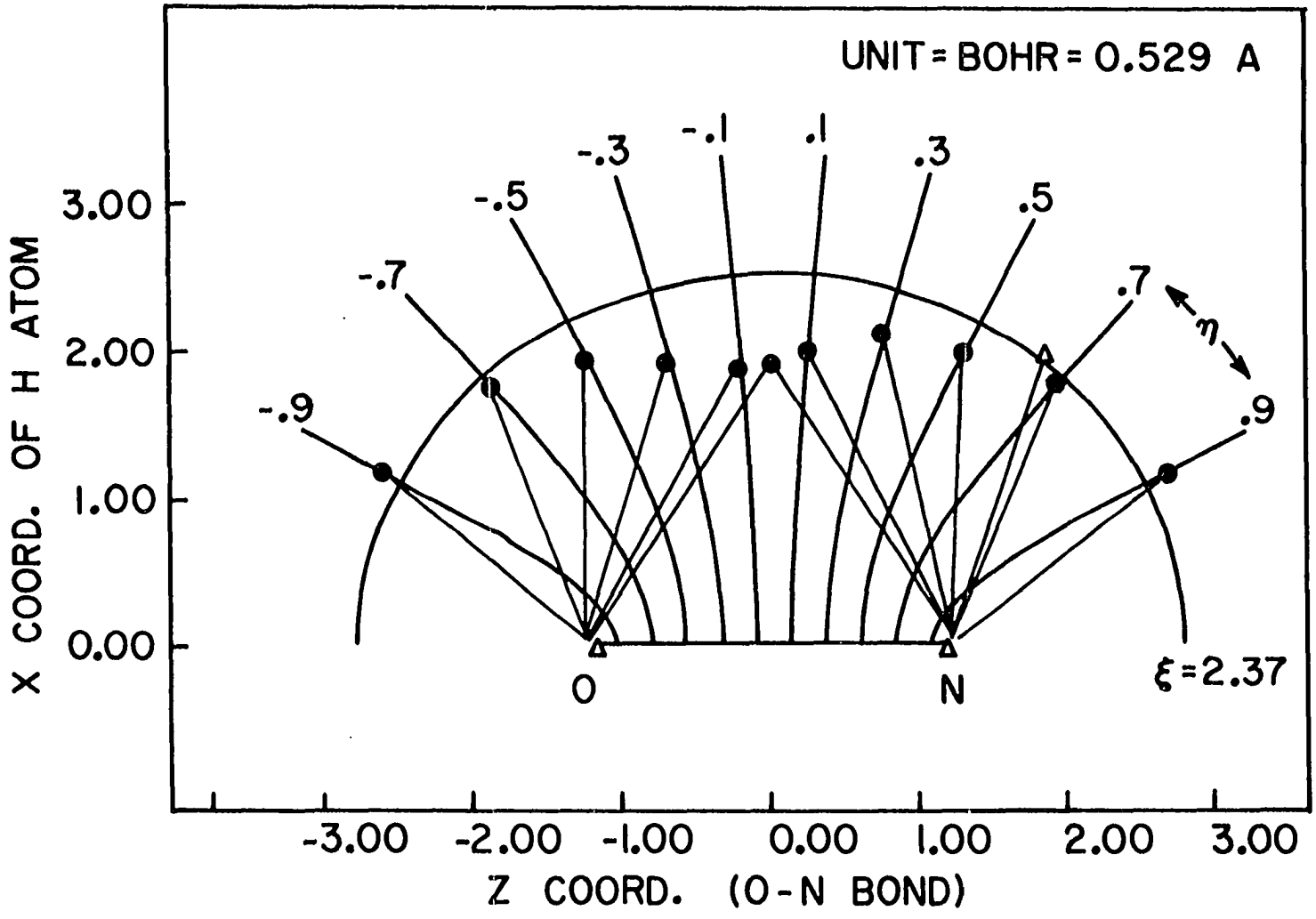

Figure 4. Optimized geometries and elliptic coordinates for the nonlinear singlet points

In each of these cases millihartree accuracy was already reached after the fourth step. Consequently, the four-step FORS procedure was deemed adequate for the remaining points of the singlet state and for all points of the triplet state. These four-step FORS energies as well as the appropriate SCF are listed, for all 13 points, in Table 12. They give rise to the two energy curves plotted in Figures 5 and 6. The figures show that HNO has two equilibrium conformations corresponding to the formulas HNO and HON. The FORS curves show that HNO is the more stable one for the singlet, in agreement with the Lewis structure, by 46.6 kcal/mole. For the triplet it is more stable by only 10.5 kcal/mole. The FORS calculation yields a barrier height of 84.4 kcal/mole for the singlet and 58.2 kcal/mole for the triplet, both counted from the stable HNO equilibrium. In the SCF approximation all these values are reduced and, more notably, the relative stabilities of the two triplet equilibrium positions is reversed.

It is to be expected that the pair of single-occupied SCF orbitals in the triplet are less affected by the correlation correction than the doubly-occupied SCF orbitals, and, indeed, the triplet and singlet curves lie closer to each other in the FORS calculation than in the SCF calculation. It is seen that in the SCF approximation the triplet curve is everywhere lower than the singlet curve. But in the FORS calculation the singlet surface crosses the triplet surface in the neighborhood of the stable equilibrium. Hence, in that conformation, the molecule has a singlet ground state, the triplet lying about

Table 12. Total energies (in atomic units) of the HNO-NOH isomerization

	Singlet		Triplet	
	SCF	FORS	SCF	FORS
A	-129.4656	-129.5381	-129.5261	-129.5906
B	.4479	.5527	.5245	.5963
C	.4685	.5799	.5360	.6160
D	.4438	.5643	.5159	.6013
E	.3966	.5348	.4748	.5762
F	.3603	.5196	.4289	.5453
M	.3625	.5265	.4181	.5412
G	.3819	.5452	.4301	.5545
H	.4459	.5978	.4751	.5800
I	.4991	.6392	.5110	.6092
J	.5188	.6541	.5275	.6327
K	.4884	.6193	.5234	.6270
L	.4760	.5849	.5186	.6209

Figure 5. SCF energy curves for the HON → NOH isomerization

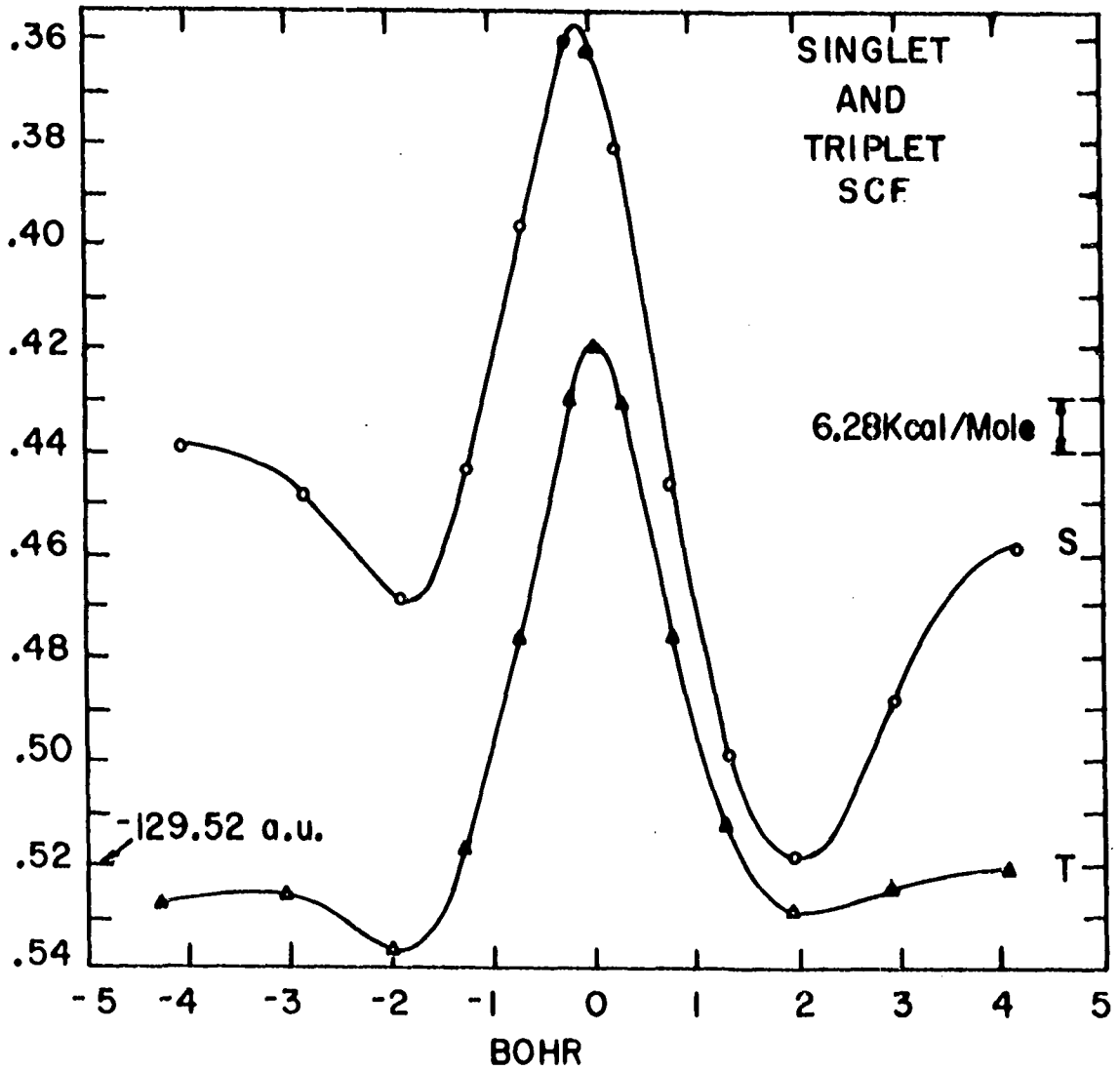
SINGLET
AND
TRIPLET
SCF
6.28Kcal/Mole
S
T
-129.52 a.u.
.36
.38
.40
.42
.44
.46
.48
.50
.52
.54
-5
-4
-3
-2
-1
0
1
2
3
4
5
BOHR

Figure 6. FORS energy curves for the HON → NOH isomerization

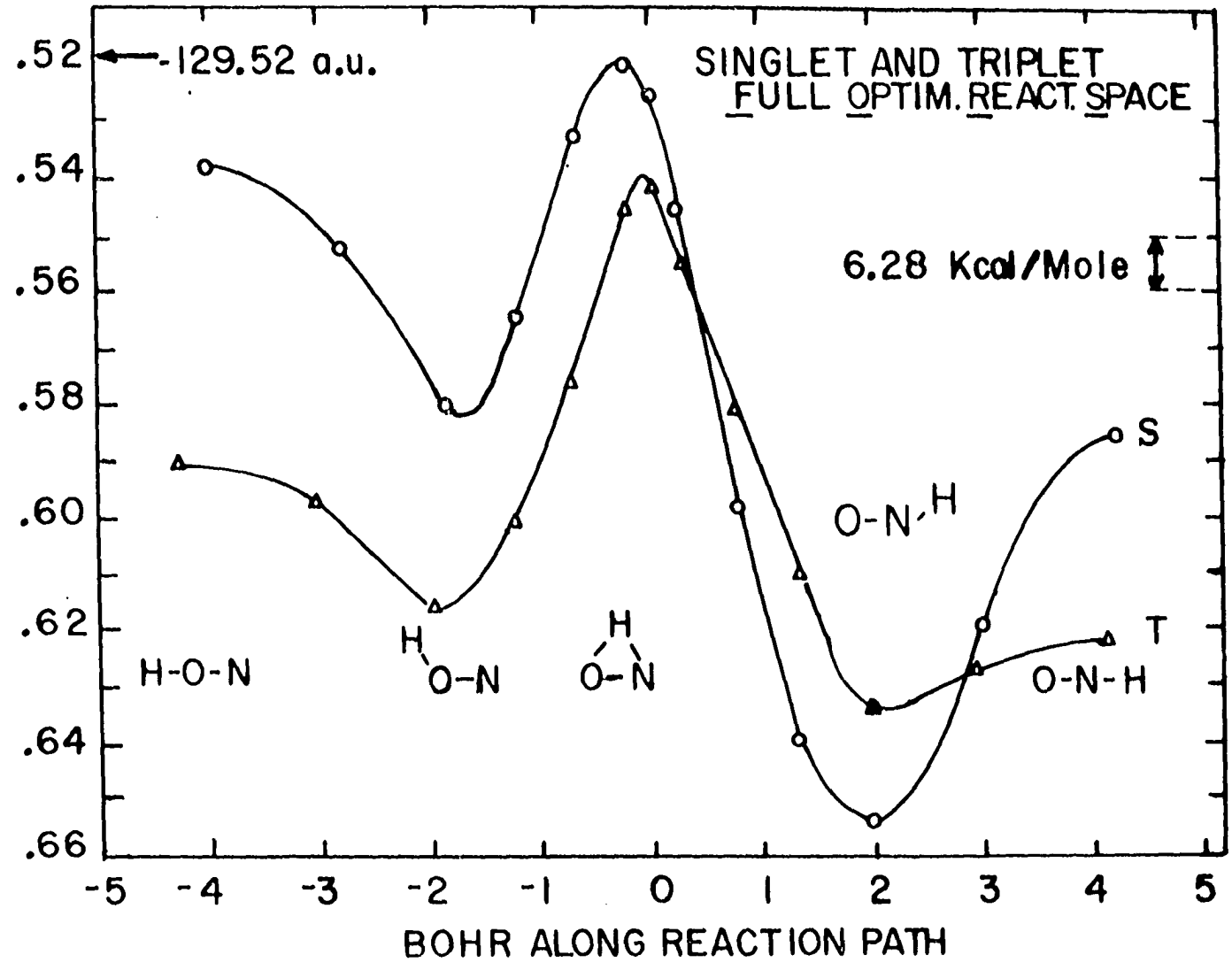
.52
.54
.56
.58
.60
.62
.64
.66
-129.52 a.u.
SINGLET AND TRIPLET
FULL OPTIM. REACT. SPACE
6.28 Kcal/Mole
S
T
O-N-H
H-O-N
H
O-N
H
O-N
O-N-H
-5
-4
-3
-2
-1
0
1
2
3
4
5
BOHR ALONG REACTION PATH

0.58 eV above the ground state. This compares to a singlet-triplet separation of .71 eV calculated by Wu, et al. (1975), .68 eV calculated by G. R. Williams (1975), and an estimate of .78 to .83 eV by Ishiwata, et al. (1974).

Because of the very high barrier the metastable conformation would not automatically convert into the stable conformation. The metastable ground state is however a triplet and hence is expected to be quite reactive. It is probably for this reason that, so far, it has been observed only in the dimer form, hyponitrous acid HON-NOH (Cotton and Wilkinson 1967; Hughes 1968).

D. FORS CI Expansions

In both calculated states, the open and closed shell SCF terms mentioned in Section IIIC are the leading terms in the CI expansion. The remaining terms, 1315 for the singlet and 1721 for the triplet converge quite slowly. Tables 13 to 16 contain information about these CI expansions. Table 13 lists the 17 leading configurations and their expansion coefficients at all points for the singlet. The configurations are characterized by a numerical label which is explained by Table 14. Table 15 and 16 do the same for the triplet state.

While the configurations obtained upon replacement of the bonding orbitals by the corresponding antibonding orbitals are among the leading configurations, as one would expect, it is apparent that it would be difficult to predict intuitively all the important configurations. The left-right correlation in the pi bond seems to be the most effective correlating term. Noteworthy also is the similarity between

Table 13. The 17 leading configurations and their coefficients in the FORS wavefunction based on the NRO's for the singlet state of HNO-NOH

A		B		C		D		E		F		M	
1	0.9748	1	0.9714	1	0.9712	1	0.9688	1	0.9638	1	0.9542	1	0.9505
106	-0.1198	106	-0.1158	99	0.1176	99	0.1200	99	0.1234	106	-0.1469	106	-0.1666
99	-0.1056	99	0.1119	106	-0.1100	106	-0.1109	106	-0.1192	99	0.1249	99	0.1234
95	-0.0712	95	-0.0754	84	-0.0832	95	-0.0851	95	-0.0881	93	0.1094	93	-0.1091
93	-0.0467	84	-0.0678	95	-0.0827	84	-0.0830	93	0.0329	95	-0.0864	95	-0.0848
84	-0.0408	67	-0.0519	93	0.0529	93	-0.0638	84	-0.0755	88	-0.0642	88	0.0598
89	-0.0399	93	-0.0443	67	-0.0469	87	-0.0535	87	0.0600	87	0.0640	87	-0.0566
44	-0.0346	44	-0.0368	87	0.0366	67	-0.0475	67	-0.0469	66	-0.0612	84	-0.0554
88	-0.0336	83	-0.0359	89	0.0315	89	-0.0311	88	-0.0465	84	-0.0511	44	-0.0489
41	-0.0303	89	0.0354	64	-0.0258	88	0.0310	53	0.0290	44	-0.0501	85	-0.0476
67	-0.0282	395	0.0256	44	-0.0253	64	-0.0265	100	0.0288	85	-0.0459	66	-0.0452
94	-0.0267	64	-0.0242	88	-0.0244	100	0.0258	94	0.0280	94	0.0371	100	0.0399
97	-0.0253	77	-0.0232	100	0.0238	94	-0.0240	64	-0.0264	100	0.0333	65	0.0350
64	-0.0244	88	0.0232	395	0.0232	395	-0.0229	44	-0.0226	886	0.0273	94	-0.0345
100	-0.0232	100	0.0226	94	0.0227	44	-0.0215	395	-0.0224	41	-0.0264	889	0.0295
395	-0.0217	101	-0.0223	77	0.0188	889	0.0177	54	-0.0211	889	0.0261	90	0.0287

Table 13. Continued

G		H		I		J		K		L	
1	0.9486	1	0.9521	1	0.9573	1	0.9594	1	0.9593	1	0.9547
106	-0.1838	106	-0.1958	106	-0.1983	106	-0.1949	106	-0.1966	106	-0.2014
93	-0.1036	95	-0.0984	99	-0.1067	99	0.1150	99	0.1107	98	-0.1181
99	0.1026	93	-0.0982	84	-0.0716	84	-0.0783	95	-0.0649	91	-0.1124
95	-0.0924	87	-0.0737	95	-0.0650	95	-0.0652	67	-0.0582	82	-0.0649
87	-0.0730	99	0.0709	87	0.0633	67	-0.0553	84	-0.0548	66	-0.0466
84	-0.0627	84	-0.0572	67	-0.0515	89	-0.0411	83	-0.0449	92	-0.0339
67	-0.0523	67	-0.0508	93	-0.0452	100	0.0287	72	-0.0365	79	-0.0326
100	0.0439	91	-0.0471	89	0.0447	889	0.0272	85	-0.0330	71	-0.0320
88	0.0437	96	0.0427	91	0.0410	80	0.0269	82	-0.0316	65	0.0311
56	0.0327	100	0.0363	100	-0.0333	83	0.0250	101	-0.0313	95	-0.0296
98	-0.0322	97	-0.0349	97	-0.0325	44	-0.0249	100	0.0310	876	0.0274
94	-0.0300	101	0.0296	64	-0.0265	91	0.0208	80	0.0265	81	0.0255
889	0.0290	94	-0.0273	889	0.0253	86	0.0201	889	0.0265	70	0.0249
91	0.0289	889	0.0256	94	-0.0248	94	-0.0198	44	-0.0244	94	-0.0234
60	-0.0271	64	-0.0253	101	0.0247	81	0.0190	89	-0.0239	67	-0.0233
85	-0.0263	82	-0.0252	82	-0.0220	85	-0.0189	96	0.0227	80	0.0226

Table 14. Identification of singlet configurations appearing in Table 13

1	$\lvert \sigma_1^2 \sigma_2^2 \sigma_3^2 \sigma_4^2 \sigma_5^2 \pi^2 \theta_1 \rangle$
41	$\lvert \sigma_1^2 \sigma_3^2 \sigma_4^2 \sigma_5^2 \sigma_1^{*2} \pi^2 \theta_1 \rangle$
44	$\lvert \sigma_1^2 \sigma_3^2 \sigma_4^2 \sigma_5^2 \pi^2 \pi^{*2} \theta_1 \rangle$
53	$\lvert \sigma_1^2 \sigma_3^2 \sigma_5^2 \sigma_2^{*2} \pi^2 \sigma_2 \sigma_4 \theta_1 \rangle$
54	$\lvert \sigma_1^2 \sigma_3^2 \sigma_5^2 \pi^2 \pi^{*2} \sigma_2 \sigma_4 \theta_1 \rangle$
56	$\lvert \sigma_1^2 \sigma_3^2 \sigma_4^2 \pi^2 \sigma_2 \sigma_5 \sigma_1^* \sigma_2^* \theta_1 \rangle$
60	$\lvert \sigma_1^2 \sigma_3^2 \sigma_4^2 \sigma_5^2 \sigma_2 \sigma_1^* \pi \pi^* \theta_1 \rangle$
64	$\lvert \sigma_1^2 \sigma_2^2 \sigma_4^2 \sigma_5^2 \sigma_1^{*2} \pi^2 \theta_1 \rangle$
65	$\lvert \sigma_1^2 \sigma_2^2 \sigma_4^2 \sigma_5^2 \pi^2 \sigma_1^* \sigma_2^* \theta_1 \rangle$
66	$\lvert \sigma_1^2 \sigma_2^2 \sigma_4^2 \sigma_5^2 \sigma_2^{*2} \pi^2 \theta_1 \rangle$
67	$\lvert \sigma_1^2 \sigma_2^2 \sigma_4^2 \sigma_5^2 \pi^2 \pi^{*2} \theta_1 \rangle$
70	$\lvert \sigma_1^2 \sigma_2^2 \sigma_5^2 \pi^2 \sigma_3 \sigma_4 \sigma_1^* \sigma_2^* \theta_2 \rangle$
71	$\lvert \sigma_1^2 \sigma_2^2 \sigma_5^2 \sigma_2^{*2} \pi^2 \sigma_3 \sigma_4 \theta_1 \rangle$
72	$\lvert \sigma_1^2 \sigma_2^2 \sigma_5^2 \pi^2 \pi^{*2} \sigma_3 \sigma_4 \theta_1 \rangle$
77	$\lvert \sigma_1^2 \sigma_2^2 \sigma_4^2 \pi^2 \pi^{*2} \sigma_3 \sigma_5 \theta_1 \rangle$
79	$\lvert \sigma_1^2 \sigma_2^2 \sigma_4^2 \sigma_5^2 \sigma_3 \sigma_1^* \pi \pi^* \theta_2 \rangle$

Table 14. Continued

80	$\vert \sigma_1^2 \sigma_2^2 \sigma_4^2 \sigma_5^2 \sigma_3 \sigma_2^* \pi \pi^* \theta_1 \rangle$
81	$\vert \sigma_1^2 \sigma_2^2 \sigma_4^2 \sigma_5^2 \sigma_3 \sigma_2^* \pi \pi^* \theta_2 \rangle$
82	$\vert \sigma_1^2 \sigma_2^2 \sigma_3^2 \sigma_5^2 \sigma_1^{*2} \pi^{*2} \theta_1 \rangle$
83	$\vert \sigma_1^2 \sigma_2^2 \sigma_3^2 \sigma_5^2 \pi^2 \sigma_1^* \sigma_2^* \theta_1 \rangle$
84	$\vert \sigma_1^2 \sigma_2^2 \sigma_3^2 \sigma_5^2 \sigma_2^{*2} \pi^* \theta_1 \rangle$
85	$\vert \sigma_1^2 \sigma_2^2 \sigma_3^2 \sigma_5^2 \pi^2 \pi^{*2} \theta_1 \rangle$
86	$\vert \sigma_1^2 \sigma_2^2 \sigma_3^2 \sigma_1^{*2} \pi^2 \sigma_4 \sigma_5 \theta_1 \rangle$
87	$\vert \sigma_1^2 \sigma_2^2 \sigma_3^2 \pi^2 \sigma_4 \sigma_5 \sigma_1^* \sigma_2^* \theta_1 \rangle$
88	$\vert \sigma_1^2 \sigma_2^2 \sigma_3^2 \pi^2 \sigma_4 \sigma_5 \sigma_1^* \sigma_2^* \theta_2 \rangle$
89	$\vert \sigma_1^2 \sigma_2^2 \sigma_3^2 \sigma_2^{*2} \pi^2 \sigma_4 \sigma_5 \theta_1 \rangle$
90	$\vert \sigma_1^2 \sigma_2^2 \sigma_3^2 \pi^2 \pi^{*2} \sigma_4 \sigma_5 \theta_1 \rangle$
91	$\vert \sigma_1^2 \sigma_2^2 \sigma_3^2 \sigma_5^2 \sigma_4 \sigma_1^* \pi \pi^* \theta_1 \rangle$
92	$\vert \sigma_1^2 \sigma_2^2 \sigma_3^2 \sigma_5^2 \sigma_4 \sigma_1^* \pi \pi^* \theta_2 \rangle$
93	$\vert \sigma_1^2 \sigma_2^2 \sigma_3^2 \sigma_5^2 \sigma_4 \sigma_2^* \pi \pi^* \theta_1 \rangle$
94	$\vert \sigma_1^2 \sigma_2^2 \sigma_3^2 \sigma_5^2 \sigma_4 \sigma_2^* \pi \pi^* \theta_2 \rangle$

Table 14. Continued

95	$\vert \sigma_1^2 \sigma_2^2 \sigma_3^2 \sigma_4^2 \sigma_1^{*2} \pi^2 \theta_1 \rangle$
96	$\vert \sigma_1^2 \sigma_2^2 \sigma_3^2 \sigma_4^2 \pi^2 \sigma_1^* \sigma_2^* \theta_1 \rangle$
97	$\vert \sigma_1^2 \sigma_2^2 \sigma_3^2 \sigma_4^2 \sigma_2^{*2} \pi^2 \theta_1 \rangle$
98	$\vert \sigma_1^2 \sigma_2^2 \sigma_3^2 \sigma_4^2 \pi^2 \pi^{*2} \theta_1 \rangle$
99	$\vert \sigma_1^2 \sigma_2^2 \sigma_3^2 \sigma_4^2 \sigma_5 \sigma_1^* \pi \pi^* \theta_1 \rangle$
100	$\vert \sigma_1^2 \sigma_2^2 \sigma_3^2 \sigma_4^2 \sigma_5 \sigma_1^* \pi \pi^* \theta_2 \rangle$
101	$\vert \sigma_1^2 \sigma_2^2 \sigma_3^2 \sigma_4^2 \sigma_5 \sigma_2^* \pi \pi^* \theta_1 \rangle$
106	$\vert \sigma_1^2 \sigma_2^2 \sigma_3^2 \sigma_4^2 \sigma_5^2 \pi^{*2} \theta_1 \rangle$
395	$\vert \sigma_1^2 \sigma_2^2 \sigma_3^2 \sigma_4^2 \pi^{*2} \sigma_5 \sigma_1^* \theta_1 \rangle$
876	$\vert \sigma_1^2 \sigma_2^2 \sigma_3^2 \sigma_5^2 \sigma_1^{*2} \pi^{*2} \theta_1 \rangle$
879	$\vert \sigma_1^2 \sigma_2^2 \sigma_3^2 \sigma_1^{*2} \sigma_4 \sigma_2^* \pi \pi^* \theta_1 \rangle$
886	$\vert \sigma_1^2 \sigma_2^2 \sigma_3^2 \pi^{*2} \sigma_4 \sigma_5 \sigma_1^* \sigma_2^* \theta_2 \rangle$
889	$\vert \sigma_1^2 \sigma_2^2 \sigma_3^2 \sigma_4^2 \sigma_1^{*2} \pi^{*2} \theta_1 \rangle$

Table 15. The 17 leading configurations and their coefficients in the FORS wavefunction based on the NRO's for the singlet state of HNO-NOH

A		B		C		D		E		F		M	
5	0.9827	5	0.9805	5	0.9784	5	0.9755	5	0.9704	5	0.9636	5	0.9623
485	-0.0758	485	-0.0900	485	-0.1034	485	-0.1097	485	-0.1092	485	-0.0976	485	-0.0868
507	-0.0584	507	0.0628	426	-0.0789	426	-0.0865	426	-0.0905	426	-0.0806	77	0.0825
85	-0.0553	426	-0.0616	507	-0.0690	507	-0.0734	507	-0.0770	77	0.0795	85	0.0803
70	0.0492	505	0.0452	505	-0.0509	505	-0.0549	505	-0.0575	507	0.0792	507	0.0777
68	-0.0484	448	0.0365	55	-0.0331	506	0.0332	68	-0.0424	85	-0.0623	426	-0.0667
505	-0.0419	68	-0.0329	506	0.0319	70	-0.0326	70	0.0407	519	-0.0609	519	0.0588
380	-0.0357	55	-0.0316	54	-0.0314	441	0.0322	495	0.0380	495	-0.0581	505	0.0566
489	-0.0353	85	0.0308	70	-0.0297	88	-0.0318	85	-0.0378	505	0.0575	68	-0.0561
69	-0.0341	70	0.0308	68	0.0288	54	-0.0317	519	-0.0362	68	0.0552	495	0.0544
506	0.0277	506	-0.0294	307	-0.0286	68	0.0316	77	0.0359	70	-0.0514	70	0.0534
311	-0.0267	54	-0.0277	88	-0.0265	55	-0.0315	506	0.0336	69	0.0377	69	-0.0408
55	-0.0258	307	-0.0237	441	0.0265	307	-0.0299	54	-0.0321	78	0.0362	78	0.0370
54	-0.0256	50	0.0226	448	0.0264	85	0.0280	55	-0.0315	506	-0.0336	79	-0.0332
125	-0.0235	28	0.0209	85	0.0263	467	0.0258	307	-0.0312	79	-0.0326	74	-0.0323
28	-0.0233	69	-0.0209	467	0.0235	440	-0.0240	441	-0.0311	307	-0.0301	506	-0.0322
29	-0.0225	425	0.0199	89	-0.0206	89	-0.0240	88	0.0283	54	0.0292	54	-0.0273

Table 15. Continued

G		H		I		J		K		L	
5	0.9611	5	0.9638	5	0.9650	5	0.9657	5	0.9705	5	0.9706
99	0.0719	85	0.1166	85	-0.0997	99	-0.1369	99	0.1253	85	0.1017
476	0.0664	485	-0.0921	99	-0.0952	85	0.0743	85	0.0730	99	-0.0983
85	0.0631	507	0.0869	507	-0.0760	70	-0.0584	70	0.0538	70	-0.0539
422	-0.0629	426	-0.0686	485	-0.0710	507	-0.0553	507	0.0507	507	-0.0519
91	-0.0610	70	0.0573	70	0.0574	86	0.0540	476	-0.0493	476	0.0500
489	-0.0538	505	0.0571	426	-0.0572	476	-0.0539	86	0.0447	311	-0.0453
70	-0.0538	68	-0.0568	86	0.0525	348	-0.0470	69	-0.0413	485	-0.0425
519	-0.0510	69	-0.0457	505	-0.0474	69	0.0460	311	-0.0410	86	0.0424
485	-0.0482	467	-0.0413	69	-0.0460	485	-0.0442	485	-0.0402	69	0.0422
507	-0.0438	506	-0.0361	348	-0.0422	426	-0.0416	348	0.0386	66	-0.0420
69	0.0422	348	0.0338	436	-0.0410	422	-0.0407	422	-0.0378	422	-0.0406
66	0.0420	1114	-0.0293	476	0.0388	436	0.0402	66	-0.0342	54	0.0400
77	-0.0411	307	-0.0264	506	0.0344	311	-0.0400	436	-0.0339	55	0.0390
474	0.0405	311	-0.0263	467	0.0341	66	-0.0348	474	-0.0335	505	-0.0337
436	-0.0396	65	-0.0263	311	-0.0316	474	-0.0345	505	0.0307	474	-0.0325
505	-0.0396	77	-0.0255	66	-0.0306	505	-0.0338	426	-0.0299	436	0.0318

Table 16. Identification of triplet configurations appearing in Table 15

5	$\vert \sigma_1^2 \sigma_2^2 \sigma_3^2 \sigma_4^2 \pi^2 \sigma_5 \pi^* \theta_1 \rangle$
28	$\vert \sigma_2^2 \sigma_3^2 \sigma_4^2 \pi^2 \sigma_1 \sigma_5 \sigma_1^* \pi^* \theta_1 \rangle$
50	$\vert \sigma_1^2 \sigma_3^2 \sigma_5^2 \pi^2 \sigma_2 \sigma_4 \sigma_1^* \pi^* \theta_3 \rangle$
54	$\vert \sigma_1^2 \sigma_3^2 \sigma_4^2 \pi^2 \sigma_2 \sigma_5 \sigma_1^* \theta_1 \rangle$
55	$\vert \sigma_1^2 \sigma_3^2 \sigma_4^2 \pi^2 \sigma_2 \sigma_5 \sigma_1^* \theta_2 \rangle$
65	$\vert \sigma_1^2 \sigma_3^2 \sigma_4^2 \sigma_5^2 \pi^{*2} \sigma_2 \pi \theta_1 \rangle$
66	$\vert \sigma_1^2 \sigma_2^2 \sigma_4^2 \sigma_5^2 \pi^2 \sigma_1^* \pi^* \theta_1 \rangle$
68	$\vert \sigma_1^2 \sigma_2^2 \sigma_5^2 \pi^2 \sigma_3 \sigma_4 \sigma_1^* \pi^* \theta_1 \rangle$
69	$\vert \sigma_1^2 \sigma_2^2 \sigma_5^2 \pi^2 \sigma_3 \sigma_4 \sigma_1^* \pi^* \theta_2 \rangle$
70	$\vert \sigma_1^2 \sigma_2^2 \sigma_5^2 \pi^2 \sigma_3 \sigma_4 \sigma_1^* \pi^* \theta_3 \rangle$
74	$\vert \sigma_1^2 \sigma_2^2 \sigma_4^2 \pi^2 \sigma_3 \sigma_5 \sigma_1^* \pi^* \theta_1 \rangle$
77	$\vert \sigma_1^2 \sigma_2^2 \sigma_4^2 \pi^2 \sigma_3 \sigma_5 \sigma_2^* \pi^* \theta_1 \rangle$
78	$\vert \sigma_1^2 \sigma_2^2 \sigma_4^2 \pi^2 \sigma_3 \sigma_5 \sigma_2^* \pi^* \theta_2 \rangle$
79	$\vert \sigma_1^2 \sigma_2^2 \sigma_4^2 \pi^2 \sigma_3 \sigma_5 \sigma_2^* \pi^* \theta_3 \rangle$
85	$\vert \sigma_1^2 \sigma_2^2 \sigma_4^2 \sigma_5^2 \pi^{*2} \sigma_3 \pi \theta_1 \rangle$

Table 16. Continued

86	$\vert \sigma_1^2 \sigma_2^2 \sigma_3^2 \sigma_5^2 \pi^2 \sigma_1^* \pi^* \theta_1 \rangle$
88	$\vert \sigma_1^2 \sigma_2^2 \sigma_3^2 \pi^2 \sigma_4 \sigma_5 \sigma_1^* \pi^* \theta_1 \rangle$
89	$\vert \sigma_1^2 \sigma_2^2 \sigma_3^2 \pi^2 \sigma_4 \sigma_5 \sigma_1^* \pi^* \theta_2 \rangle$
91	$\vert \sigma_1^2 \sigma_2^2 \sigma_3^2 \pi^2 \sigma_4 \sigma_5 \sigma_2^* \pi^* \theta_1 \rangle$
99	$\vert \sigma_1^2 \sigma_2^2 \sigma_3^2 \sigma_5^2 \pi^{*2} \sigma_4 \pi \theta_1 \rangle$
307	$\vert \sigma_1^2 \sigma_3^2 \sigma_4^2 \sigma_1^{*2} \pi^2 \sigma_5 \pi^* \theta_1 \rangle$
311	$\vert \sigma_1^2 \sigma_3^2 \sigma_4^2 \sigma_2^{*2} \pi^2 \sigma_5 \pi^* \theta_1 \rangle$
348	$\vert \sigma_1^2 \sigma_4^2 \sigma_2^{*2} \pi^2 \sigma_2 \sigma_3 \sigma_5 \pi^* \theta_1 \rangle$
422	$\vert \sigma_1^2 \sigma_2^2 \sigma_4^2 \sigma_1^{*2} \pi^2 \sigma_5 \pi^* \theta_1 \rangle$
425	$\vert \sigma_1^2 \sigma_2^2 \sigma_4^2 \pi^2 \sigma_5 \sigma_1^* \sigma_2^* \pi^* \theta_3 \rangle$
426	$\vert \sigma_1^2 \sigma_2^2 \sigma_4^2 \sigma_2^{*2} \pi^2 \sigma_5 \pi^* \theta_1 \rangle$
436	$\vert \sigma_1^2 \sigma_2^2 \sigma_1^{*2} \pi^2 \sigma_3 \sigma_4 \sigma_5 \pi^* \theta_1 \rangle$
440	$\vert \sigma_1^2 \sigma_2^2 \pi^2 \sigma_3 \sigma_4 \sigma_5 \sigma_1^* \sigma_2^* \pi^* \theta_2 \rangle$
441	$\vert \sigma_1^2 \sigma_2^2 \pi^2 \sigma_3 \sigma_4 \sigma_5 \sigma_1^* \sigma_2^* \pi^* \theta_3 \rangle$
448	$\vert \sigma_1^2 \sigma_2^2 \sigma_2^{*2} \pi^2 \sigma_3 \sigma_4 \sigma_5 \pi^* \theta_1 \rangle$

Table 16. Continued

467	$\vert \sigma_1^2 \sigma_2^2 \sigma_4^2 \sigma_2^{*2} \pi^2 \sigma_3 \pi^* \theta_1 \rangle$
474	$\vert \sigma_1^2 \sigma_2^2 \sigma_4^2 \pi^{*2} \sigma_3 \sigma_5 \sigma_1^* \pi \theta_1 \rangle$
476	$\vert \sigma_1^2 \sigma_2^2 \sigma_4^2 \pi^{*2} \sigma_3 \sigma_5 \sigma_1^* \pi \theta_3 \rangle$
485	$\vert \sigma_1^2 \sigma_2^2 \sigma_3^2 \sigma_1^{*2} \pi^2 \sigma_5 \pi^* \theta_1 \rangle$
489	$\vert \sigma_1^2 \sigma_2^2 \sigma_3^2 \sigma_2^{*2} \pi^2 \sigma_5 \pi^* \theta_1 \rangle$
495	$\vert \sigma_1^2 \sigma_2^2 \sigma_3^2 \pi^2 \sigma_4 \sigma_1^* \sigma_2^* \pi^* \theta_1 \rangle$
505	$\vert \sigma_1^2 \sigma_2^2 \sigma_3^2 \pi^{*2} \sigma_4 \sigma_5 \sigma_1^* \pi \theta_1 \rangle$
506	$\vert \sigma_1^2 \sigma_2^2 \sigma_3^2 \pi^{*2} \sigma_4 \sigma_5 \sigma_1^* \pi \theta_2 \rangle$
507	$\vert \sigma_1^2 \sigma_2^2 \sigma_3^2 \pi^{*2} \sigma_4 \sigma_5 \sigma_1^* \pi \theta_3 \rangle$
519	$\vert \sigma_1^2 \sigma_2^2 \sigma_3^2 \sigma_4^2 \pi^{*2} \sigma_2^* \pi \theta_1 \rangle$
1114	$\vert \sigma_1^2 \sigma_2^2 \sigma_5^2 \sigma_1^{*2} \pi^{*2} \sigma_3 \pi \theta_1 \rangle$

the CI expansions of neighboring conformations. Some similarity can be seen too in the CI expansions corresponding to the two equilibrium positions.

E. Natural Reaction Orbitals and Directed Localized Reaction Orbitals

The expansions of the optimized molecular orbitals are given in Tables 17 to 42 for the sigmas and Tables 43 to 68 for the pi orbitals. Each table has two parts, designated a and b. The "a" table gives the expansions of the directed localized reaction orbitals in terms of the quantitative basis set and also shows their occupation numbers. The "b" table gives the expansion coefficients of the natural reaction orbitals (NRO's) in terms of the DLRO's. By combining the two tables the expansions of the NRO's in terms of the QBO's may be obtained.

For the DLRO's the following names are introduced in these tables:

O_σ = oxygen bonding orbital pointing to N

N_σ = nitrogen bonding orbital pointing to O

O_H = oxygen orbital which is directed so that it can make a bond with H

N_H = nitrogen orbital which is directed so that it can make a bond with H

O_L and N_L = orbitals on O and N which are always lone pairs

The meaning of these designations will become clearer in the discussion of Chapter V.

Table 17a. Sigma DLROs and occupation numbers for singlet HNO geometry A

		(O 1s)	(N 1s)	(O-hydr)	(O-sigma)	(O-lone)	(N-hydr)	(N-sigma)	(N-lone)	(H)
ETCGAO		2.000000	2.000000	1.119386	1.516530	1.997879	1.996421	0.662223	1.983346	0.717013
N	S	-0.000024	0.996034	0.009950	-0.005569	-0.000000	0.000003	-0.037527	-0.107867	-0.008163
	S'	-0.000360	0.071606	0.100921	-0.078077	0.000001	-0.000016	0.240356	0.651019	-0.083764
	S''	-0.000243	-0.000355	-0.006270	0.009177	0.000000	0.000000	-0.014596	-0.000656	-0.003216
	X	0.000000	0.000000	-0.000003	0.000005	-0.165238	1.041739	0.000004	0.000026	0.000002
	X'	0.000000	0.000000	0.000000	0.000001	-0.057874	-0.010877	0.000000	-0.000000	-0.000000
	Y	0.0	0.0	0.0	0.0	0.0	0.0	0.0	0.0	0.0
	Y'	0.0	0.0	0.0	0.0	0.0	0.0	0.0	0.0	0.0
	Z	-0.003468	-0.000186	-0.114577	0.128619	-0.000004	-0.000008	-1.020131	0.389588	0.038926
	Z'	-0.000883	0.003380	0.035915	-0.064786	0.000001	-0.000003	0.177174	0.105579	-0.001663
O	S	0.997679	0.010383	-0.015566	-0.050491	-0.000001	0.000000	-0.037469	-0.002738	-0.051779
	S'	0.058152	0.003894	0.457283	0.994299	0.000009	0.000001	-0.290587	-0.042886	-0.345542
	S''	-0.000099	-0.000257	0.030553	0.015972	0.000000	0.000000	-0.019858	0.004652	-0.048715
	X	-0.000000	-0.000000	-0.000001	-0.000011	1.043150	-0.112672	-0.000006	-0.000004	-0.000002
	X'	-0.000000	-0.000000	0.000001	0.000001	-0.024560	-0.062264	-0.000001	-0.000001	-0.000002
	Y	0.0	0.0	0.0	0.0	0.0	0.0	0.0	0.0	0.0
	Y'	0.0	0.0	0.0	0.0	0.0	0.0	0.0	0.0	0.0
	Z	0.001649	0.010685	-0.957532	0.338860	0.000003	-0.000011	-0.072974	0.288229	0.220350
	Z'	0.001554	0.006663	0.382465	-0.235985	-0.000000	-0.000008	0.216008	0.371795	-0.000134
H	S	0.004755	0.008020	-0.278797	-0.118274	0.000001	-0.000011	0.066782	0.381451	1.168069
	S'	-0.000028	-0.001538	-0.081981	-0.009955	0.000000	0.000002	-0.002993	0.000002	0.256317

Table 17b. Transformation from sigma NROs to sigma DLROs for singlet HNO geometry A

		(O 1s)	(N 1s)	(O-hydr)	(O-sigma)	(O-lone)	(N-hydr)	(N-sigma)	(N-lone)	(H)
O	1s	1.0								
N	1s		1.0							
NRO	1			-0.45139	0.54854	0.00001	0.00000	0.52865	-0.32774	-0.32933
	2			0.59359	0.50062	0.00000	0.00001	0.02192	-0.41777	0.47119
	3			-0.00000	-0.00001	0.82877	0.55959	-0.00000	0.00001	-0.00000
	4			0.07290	0.45787	-0.00000	-0.00001	0.21154	0.84517	0.16121
	5			0.00000	0.00000	0.55959	-0.82877	-0.00000	-0.00001	0.00000
	6			0.21084	-0.48768	0.00000	-0.00000	0.81960	-0.00002	0.21439
	7			-0.62780	-0.03169	0.0	-0.00000	-0.05957	-0.06123	0.77303

Table 18a. Sigma DLROs and occupation numbers for singlet HNO geometry B

		(O 1s)	(N 1s)	(O-hydr)	(O-sigma)	(O-lone)	(N-hydr)	(N-sigma)	(N-lone)	(H)
ETCGAO		2.000000	2.000000	1.145287	1.291773	1.997347	1.991029	0.753089	1.976204	0.833416
N	S	-0.000509	0.906547	0.025924	-0.095376	-0.003313	0.294396	0.151121	0.217474	-0.013976
	S'	0.002911	0.314013	-0.042521	0.164122	0.001368	-0.659940	-0.339974	-0.496684	0.025062
	S''	0.000576	-0.000087	-0.004192	0.018690	-0.004421	-0.002246	-0.012830	0.000341	-0.002257
	X	0.009219	-0.002652	-0.020132	-0.043874	0.120059	0.623333	-0.011314	-0.819322	-0.091801
	X'	0.000572	-0.000226	0.002776	0.010945	-0.049815	-0.015957	0.011870	-0.001435	0.033211
	Y	0.0	0.0	0.0	0.0	0.0	0.0	0.0	0.0	0.0
	Y'	0.0	0.0	0.0	0.0	0.0	0.0	0.0	0.0	0.0
	Z	0.003028	-0.007011	-0.052578	0.192155	-0.008953	0.276932	-1.049683	0.161257	0.031746
	Z'	-0.000768	-0.001673	-0.006877	0.061444	0.014492	-0.035235	-0.149519	-0.040855	-0.008375
O	S	-0.937670	0.002834	0.197066	0.257959	0.222328	-0.016747	-0.136378	-0.030180	-0.137785
	S'	-0.221627	-0.003901	-0.481089	-0.640337	-0.612718	0.036926	0.227636	0.039692	0.221456
	S''	0.000276	-0.000165	0.022491	0.010418	-0.000343	-0.000142	-0.015520	0.005121	-0.028410
	X	0.002143	-0.002259	0.681936	0.303634	-0.737463	-0.100728	0.078656	0.061655	0.034031
	X'	0.001691	-0.000606	-0.250604	-0.036341	-0.090280	-0.073446	0.121095	-0.012502	0.266614
	Y	0.0	0.0	0.0	0.0	0.0	0.0	0.0	0.0	0.0
	Y'	0.0	0.0	0.0	0.0	0.0	0.0	0.0	0.0	0.0
	Z	-0.001448	0.000675	-0.611443	0.784316	-0.227166	0.054568	-0.181496	0.024661	0.107653
	Z'	-0.000636	0.001430	0.206412	-0.247201	0.035991	0.108788	0.095247	0.089635	-0.045271
H	S	-0.004725	0.000991	-0.268479	-0.021356	0.120698	0.118559	-0.110690	0.078888	0.994527
	S'	0.000708	-0.000426	-0.068396	0.001516	-0.055958	-0.063839	0.052595	-0.063839	0.175164

Table 18b. Transformation from sigma NROs to sigma DLROs for singlet HNO geometry B

		(O 1s)	(N 1s)	(O-hydr)	(O-sigma)	(O-lone)	(N-hydr)	(N-sigma)	(N-lone)	(H)
O	1s	1.0								
N	1s		1.0							
NBO	1			-0.17834	0.69703	-0.05116	-0.28368	0.57114	-0.17756	-0.20378
	2			0.72148	0.25658	-0.12283	-0.18212	0.02126	-0.01572	0.60388
	3			0.13266	0.20606	0.21438	0.85556	0.13117	-0.37829	0.04112
	4			0.03726	0.09957	0.91122	-0.10674	0.06051	0.37131	0.07387
	5			-0.05097	0.21132	-0.32560	0.37781	0.15334	0.82417	0.03488
	6			-0.00031	-0.57947	-0.00203	0.00491	0.78472	-0.00980	0.21977
	7			-0.65274	0.12450	-0.00078	0.01449	-0.11478	-0.08890	0.73290

Table 19a. Sigma DLROs and occupation numbers for singlet HNO geometry C

		(O 1s)	(N 1s)	(O-hydr)	(O-sigma)	(O-lone)	(N-hydr)	(N-sigma)	(N-lone)	(H)
ETCGAO		2.000000	2.000000	1.133119	1.193202	1.997040	1.993945	0.820941	1.986614	0.867423
N	S	-0.003017	0.897789	0.015371	-0.098047	0.014962	0.253008	0.130988	0.299080	-0.026907
	S'	0.000143	0.350050	-0.020441	0.163653	-0.021204	-0.492587	-0.297769	-0.675981	0.043687
	S''	0.000599	0.000219	-0.000580	0.021643	-0.008804	-0.001393	-0.010545	0.001312	-0.001134
	X	-0.029445	-0.026294	-0.031788	-0.014242	0.076592	0.832148	-0.038605	-0.599816	-0.102707
	X'	-0.000121	-0.000375	-0.008915	-0.002551	0.030594	0.016141	-0.007745	-0.006011	-0.032527
	Y	0.0	0.0	0.0	0.0	0.0	0.0	0.0	0.0	0.0
	Y'	0.0	0.0	0.0	0.0	0.0	0.0	0.0	0.0	0.0
	Z	0.002434	-0.005581	-0.005413	0.187104	-0.006527	0.177688	-1.027495	0.262906	0.021578
	Z'	0.000761	0.001473	0.010688	-0.060921	-0.020116	0.027003	0.149046	0.051956	-0.006295
O	S	-0.916509	-0.000078	0.190339	0.210788	0.313278	-0.031069	-0.117778	-0.004094	-0.123264
	S'	-0.289824	-0.003239	-0.430772	-0.481714	-0.720653	0.007250	0.189465	0.043768	0.189066
	S''	0.000316	-0.000150	0.020805	0.017240	0.001023	-0.002005	-0.022147	0.001708	-0.026302
	X	-0.009462	-0.000770	0.892998	0.131388	-0.522812	-0.099312	0.079206	0.022010	-0.005947
	X'	0.001234	0.000837	-0.294007	-0.021469	-0.085361	-0.058037	0.112804	-0.032695	0.287074
	Y	0.0	0.0	0.0	0.0	0.0	0.0	0.0	0.0	0.0
	Y'	0.0	0.0	0.0	0.0	0.0	0.0	0.0	0.0	0.0
	Z	-0.006722	0.000312	-0.311777	0.917408	-0.324021	0.003112	-0.127769	0.015070	0.067136
	Z'	0.000574	0.000580	0.080270	-0.260920	-0.018101	0.045197	0.151615	0.070336	0.002510
H	S	0.002309	0.001334	-0.262352	-0.032345	0.105921	0.045021	-0.135046	0.113201	0.935456
	S'	-0.000787	0.000374	-0.066942	0.019032	-0.065267	-0.058002	0.065221	-0.058002	0.202029

Table 19b. Transformation from sigma NROs to sigma DLROs for singlet HNO geometry C

		(O 1s)	(N 1s)	(O-hydr)	(O-sigma)	(O-lone)	(N-hydr)	(N-sigma)	(N-lone)	(H)
O 1s		1.0								
N 1s			1.0							
NRO	1			-0.16172	0.70449	-0.06166	-0.17080	0.60439	-0.20432	-0.19375
	2			0.72484	0.20939	-0.12489	-0.13868	0.08014	-0.05088	0.62203
	3			0.12394	0.12948	0.44545	0.83294	0.09515	-0.25232	0.05422
	4			0.02377	0.08709	0.82059	-0.33195	0.06582	0.44736	0.06185
	5			-0.01554	0.18423	-0.32985	0.38337	0.14423	0.82984	0.02464
	6			0.08570	-0.63368	-0.00191	0.00025	0.76865	0.00738	0.01469
	7			-0.65188	-0.00185	-0.00134	0.02533	0.05729	-0.05637	0.75363

Table 20a. Sigma DLROs and occupation numbers for singlet HNO geometry D

		(O 1s)	(N 1s)	(O-hydr)	(O-sigma)	(O-lone)	(N-hydr)	(N-sigma)	(N-lone)	(H)
ETCGAO		2.000000	2.000000	1.158329	1.171408	1.996757	1.996726	0.836538	1.988281	0.844347
N	S	-0.001505	0.892602	0.009117	-0.095101	0.021671	-0.021353	0.122844	0.403225	-0.031175
	S'	-0.002096	0.368586	-0.010301	0.156140	-0.024222	0.143094	-0.280060	-0.822712	0.058275
	S''	0.000533	0.000404	0.001643	0.019621	-0.009049	-0.002159	-0.008316	0.001905	-0.000107
	X	-0.029565	-0.045235	-0.028739	0.006363	0.046258	1.020416	-0.036876	0.178281	-0.120176
	X'	-0.000435	-0.000911	-0.015262	0.005102	0.010630	0.023994	0.007224	-0.003796	-0.031975
	Y	0.0	0.0	0.0	0.0	0.0	0.0	0.0	0.0	0.0
	Y'	0.0	0.0	0.0	0.0	0.0	0.0	0.0	0.0	0.0
	Z	0.002961	-0.004055	0.005671	0.173617	-0.008819	-0.099864	-1.008318	0.291531	0.030389
	Z'	0.000529	0.001037	-0.001075	-0.063444	-0.027250	-0.014428	0.164064	0.058291	0.008992
O	S	-0.905151	0.000255	0.176140	0.190280	0.350405	-0.019057	-0.108966	-0.020216	-0.117041
	S'	-0.327167	-0.001541	-0.377810	-0.410308	-0.759958	-0.025418	0.171807	0.031998	0.169190
	S''	0.000203	-0.000188	0.012030	0.013250	0.000637	0.000454	-0.014966	-0.000198	-0.014295
	X	-0.007562	0.001553	0.952167	-0.004346	-0.393632	-0.083639	0.040640	-0.046401	-0.023429
	X'	0.001079	0.002085	-0.294822	0.004764	-0.059959	-0.041291	0.052687	-0.057864	0.281171
	Y	0.0	0.0	0.0	0.0	0.0	0.0	0.0	0.0	0.0
	Y'	0.0	0.0	0.0	0.0	0.0	0.0	0.0	0.0	0.0
	Z	-0.007845	0.000525	-0.110629	0.954696	-0.355709	-0.010071	-0.102859	-0.008297	0.017934
	Z'	0.000241	0.000163	0.012113	-0.265282	-0.044297	-0.008277	0.181487	0.056062	0.019540
H	S	0.002257	-0.000152	-0.239486	-0.050519	0.089906	-0.084406	-0.136087	0.096750	0.920967
	S'	0.001666	-0.000585	0.068754	-0.023868	0.062787	-0.005239	-0.080805	-0.005239	-0.246007

Table 20b. Transformation from sigma NROs to sigma DLROs for singlet HNO geometry D

		(O 1s)	(N 1s)	(O-hydr)	(O-sigma)	(O-lone)	(N-hydr)	(N-sigma)	(N-lone)	(H)
O 1s		1.0								
N 1s			1.0							
NRO	1			-0.22357	0.69450	-0.05674	0.06591	0.60017	-0.21941	-0.22755
	2			0.71559	0.23552	-0.13945	-0.10996	0.14983	-0.18069	0.58807
	3			0.13627	0.10928	0.54886	0.71806	0.08113	0.35437	0.14306
	4			0.01791	0.09053	0.75193	-0.64287	0.07637	0.08327	0.00617
	5			0.00640	0.17183	-0.33270	-0.23343	0.13624	0.88613	0.03842
	6			0.15917	-0.63259	-0.00180	0.00235	0.74714	0.01209	-0.12698
	7			-0.62744	-0.11127	-0.00201	-0.01308	0.16775	-0.03645	0.75120

Table 21a. Sigma DLROs and occupation numbers for singlet HNO geometry E

		(O 1s)	(N 1s)	(O-hydr)	(O-sigma)	(O-lone)	(N-hydr)	(N-sigma)	(N-lone)	(H)
ETCGAO		2.000000	2.000000	1.238907	1.116334	1.996317	1.926968	0.890258	1.989987	0.828828
N	S	-0.000630	0.891360	0.002292	-0.091056	0.024097	0.153366	0.123884	0.377729	-0.042174
	S'	0.002528	0.374963	-0.002274	0.152896	-0.010643	-0.312127	-0.276842	-0.774295	0.072437
	S''	0.000489	0.000306	0.007136	0.014230	-0.007352	0.000183	-0.005154	0.004255	-0.003174
	X	0.002858	0.000401	-0.004997	0.027016	0.021917	0.996819	-0.008661	-0.374227	-0.138396
	X'	0.000133	0.000134	-0.041870	0.008751	-0.003540	0.010336	0.022087	-0.025557	-0.014022
	Y	0.0	0.0	0.0	0.0	0.0	0.0	0.0	0.0	0.0
	Y'	0.0	0.0	0.0	0.0	0.0	0.0	0.0	0.0	0.0
	Z	0.001180	-0.006435	0.015346	0.181622	-0.006648	0.051363	-0.982480	0.289929	0.031144
	Z'	0.000264	0.000509	-0.007495	-0.071537	-0.035873	0.018824	0.187734	0.054829	0.017362
O	S	-0.905498	-0.001179	0.164022	0.166749	0.357174	-0.000040	-0.089568	-0.020651	-0.102323
	S'	-0.334048	0.005440	-0.344513	-0.352818	-0.788161	0.005000	0.133686	0.033630	0.146279
	S''	0.000147	-0.000186	0.012732	0.004738	0.000258	0.005223	-0.003592	-0.001182	-0.014738
	X	-0.003549	0.001878	0.948803	-0.127714	-0.310238	-0.123595	0.005266	0.016531	0.011420
	X'	0.000525	0.000532	-0.303617	0.024158	-0.037646	-0.128860	-0.008211	-0.007435	0.313167
	Y	0.0	0.0	0.0	0.0	0.0	0.0	0.0	0.0	0.0
	Y'	0.0	0.0	0.0	0.0	0.0	0.0	0.0	0.0	0.0
	Z	-0.004411	0.002025	0.050431	0.965709	-0.351942	-0.017683	-0.074467	-0.012516	-0.032513
	Z'	0.001070	0.000555	-0.025014	-0.264808	-0.050998	0.019899	0.183525	0.036079	0.003422
H	S	-0.000221	-0.003485	-0.204496	-0.049105	0.086202	-0.056232	-0.165261	0.133365	0.883044
	S'	0.000612	-0.001459	0.062767	-0.025315	0.063956	0.059126	-0.086429	0.085531	-0.288846

Table 21b. Transformation from sigma NROs to sigma DLROs for singlet HNO geometry E

		(O 1s)	(N 1s)	(O-hydr)	(O-sigma)	(O-lone)	(N-hydr)	(N-sigma)	(N-lone)	(H)
O	1s	1.0								
N	1s		1.0							
NRO	1			-0.17491	0.70548	-0.09111	-0.01531	0.62664	-0.22585	-0.13957
	2			0.73061	0.13030	-0.12520	-0.42458	0.11873	-0.05069	0.48644
	3			0.21862	0.03083	-0.00257	0.85582	0.02902	-0.28021	0.37344
	4			0.09411	0.13954	0.93117	0.02650	0.12629	0.28472	0.08290
	5			0.03831	0.15505	-0.33004	0.23433	0.13158	0.88702	0.08083
	6			0.10016	-0.65444	-0.00253	0.03036	0.73763	0.00344	-0.12896
	7			-0.60620	-0.11206	-0.00224	-0.17472	0.12256	0.00385	0.75789

Table 22a. Sigma DLROs and occupation numbers for singlet HNO geometry F

		(O 1s)	(N 1s)	(O-hydr)	(O-sigma)	(O-lone)	(N-hydr)	(N-sigma)	(N-lone)	(H)
ETCGAO		2.000000	2.000000	1.505933	1.078291	1.995984	1.649939	0.927603	1.990515	0.839231
N	S	0.000980	0.906697	0.013988	-0.090409	0.009335	0.130104	0.120924	0.357225	-0.074645
	S'	-0.001541	0.336772	-0.021499	0.142639	-0.002152	-0.283987	-0.281441	-0.807104	0.109041
	S''	-0.000503	0.000362	0.009620	0.015339	-0.005549	0.004087	-0.007699	0.002017	-0.007934
	X	-0.000809	0.000647	-0.041523	0.021542	0.005297	1.034630	-0.063412	-0.301153	-0.102006
	X'	-0.000397	-0.000794	-0.137482	0.002953	-0.009914	-0.071952	0.018257	-0.033216	0.115994
	Y	0.0	0.0	0.0	0.0	0.0	0.0	0.0	0.0	0.0
	Y'	0.0	0.0	0.0	0.0	0.0	0.0	0.0	0.0	0.0
	Z	-0.002976	-0.001553	0.002857	0.170731	-0.009552	-0.027873	-0.960607	0.301669	0.047465
	Z'	-0.000794	0.002420	-0.013924	-0.092818	-0.046404	0.024861	0.229320	0.052372	0.019637
O	S	0.910583	0.000708	0.138404	0.155284	0.350143	-0.001138	-0.085410	-0.015089	-0.088376
	S'	0.323671	-0.001082	-0.298625	-0.332035	-0.807868	0.002529	0.125546	0.028888	0.126386
	S''	-0.000142	-0.000188	0.004967	0.001370	0.001227	0.009064	0.001463	-0.001346	-0.007434
	X	0.000951	-0.001467	0.995262	-0.110117	-0.270207	-0.137357	0.003311	0.015215	-0.018913
	X'	-0.000898	-0.000487	-0.201017	0.023087	-0.018825	-0.201825	-0.025176	-0.007197	0.249088
	Y	0.0	0.0	0.0	0.0	0.0	0.0	0.0	0.0	0.0
	Y'	0.0	0.0	0.0	0.0	0.0	0.0	0.0	0.0	0.0
	Z	0.000291	0.003146	0.049936	0.973318	-0.328280	-0.014287	-0.076624	-0.019791	-0.054910
	Z'	-0.002348	0.000464	-0.025795	-0.277248	-0.047848	0.019884	0.176212	0.028333	-0.014010
H	S	0.002264	0.002119	-0.186631	-0.072204	0.090421	-0.116237	-0.157367	0.124453	0.895420
	S'	0.000239	-0.000268	-0.055686	0.038157	-0.064963	-0.061244	0.071028	-0.083923	0.322767

Table 22b. Transformation from sigma NROs to sigma DLROs for singlet HNO geometry F

		(O 1s)	(N 1s)	(O-hydr)	(O-sigma)	(O-lone)	(N-hydr)	(N-sigma)	(N-lone)	(H)
O 1s		1.0								
N 1s			1.0							
NRO	1			0.06568	0.69628	-0.13608	-0.16976	0.65000	-0.20252	-0.00576
	2			0.72602	-0.13293	-0.02838	-0.65682	-0.08813	0.06218	0.10663
	3			0.46507	0.01569	-0.09856	0.59317	0.00918	-0.21420	0.61313
	4			0.09905	0.15022	0.90557	0.07057	0.14142	0.33169	0.11208
	5			0.03902	0.11821	-0.38844	0.12297	0.09963	0.89398	0.09679
	6			-0.11253	-0.67019	-0.00372	-0.05977	0.71550	0.00411	0.15046
	7			-0.47781	0.10763	-0.00089	-0.40526	-0.16668	-0.00104	0.75372

Table 23a. Sigma DLPOs and occupation numbers for singlet HNO geometry M

		(O 1s)	(N 1s)	(O-hydr)	(O-sigma)	(O-lone)	(N-hydr)	(N-sigma)	(N-lone)	(H)
ETCGAO		2.000000	2.000000	1.641849	1.061299	1.995824	1.495834	0.948371	1.989963	0.851194
N	S	-0.010149	-0.908189	0.012479	-0.097383	0.006326	0.131574	0.139390	0.361333	-0.082402
	S'	-0.001160	-0.320018	-0.021843	0.161483	-0.000965	-0.293836	-0.323579	-0.804561	0.124135
	S''	0.000435	0.000133	0.007086	0.012931	-0.005272	0.003542	-0.005281	-0.000440	-0.005745
	X	0.000225	-0.005147	-0.031750	0.021061	0.004683	1.044899	-0.058233	-0.310534	-0.123602
	X'	0.000243	0.000141	-0.121663	0.011171	-0.010372	-0.054602	0.020442	-0.051133	0.092705
	Y	0.0	0.0	0.0	0.0	0.0	0.0	0.0	0.0	0.0
	Y'	0.0	0.0	0.0	0.0	0.0	0.0	0.0	0.0	0.0
	Z	0.001636	0.006114	0.013400	0.183867	-0.008164	-0.009283	-0.967769	0.322586	0.023223
	Z'	0.000416	-0.000792	-0.013224	-0.092001	-0.050396	0.031092	0.217336	0.059034	-0.004166
O	S	-0.905277	0.007427	0.150063	0.161335	0.359552	0.001437	-0.094737	-0.013133	-0.082436
	S'	-0.335929	0.005992	-0.320311	-0.338367	-0.796977	-0.002667	0.141589	0.025021	0.122895
	S''	0.000229	0.000173	0.006848	-0.000160	0.001342	0.014217	0.004000	-0.001663	-0.013513
	X	-0.002764	0.001239	0.992665	-0.128556	-0.287730	-0.158611	0.007186	0.018882	0.002096
	X'	0.000414	0.000315	-0.148697	0.030807	-0.019600	-0.237880	-0.022421	-0.006661	0.260971
	Y	0.0	0.0	0.0	0.0	0.0	0.0	0.0	0.0	0.0
	Y'	0.0	0.0	0.0	0.0	0.0	0.0	0.0	0.0	0.0
	Z	-0.003275	-0.000683	0.065560	0.987938	-0.331538	-0.012747	-0.095808	-0.025548	-0.060704
	Z'	0.001445	-0.000226	-0.020687	-0.251696	-0.052526	0.027607	0.165017	0.020689	-0.039741
H	S	-0.000582	0.000127	-0.192835	-0.068632	0.091455	-0.131233	-0.155549	0.124509	0.921741
	S'	0.000385	0.000813	0.031216	-0.054310	0.073361	0.030916	-0.075546	0.093643	-0.198608

Table 23b. Transformation from sigma NRCs to sigma DLROs for singlet HNO geometry M

		(O 1s)	(N 1s)	(O-hydr)	(O-sigma)	(O-lone)	(N-hydr)	(N-sigma)	(N-lone)	(H)
O	1s	1.0								
N	1s		1.0							
NRO	1			0.33090	0.57452	-0.13258	-0.44304	0.56504	-0.13770	-0.09130
	2			-0.57624	0.40609	-0.04085	0.58680	0.34427	-0.17930	0.07985
	3			0.59893	-0.03018	-0.03688	0.41602	0.01016	-0.34027	0.59165
	4			0.10422	0.14848	0.90361	0.06374	0.14896	0.33671	0.10468
	5			0.13041	0.11120	-0.40357	0.19295	0.10604	0.84836	0.19892
	6			-0.24947	-0.59033	-0.00385	-0.24878	0.61375	0.00275	0.38817
	7			-0.33112	0.34815	0.00024	-0.42793	-0.38985	-0.00304	0.65881

Table 24a. Sigma DLPOs and occupation numbers for singlet HNO geometry G

		(O 1s)	(N 1s)	(O-hydr)	(O-sigma)	(O-lone)	(N-hydr)	(N-sigma)	(N-lone)	(H)
ETCGAO		2.000000	2.000000	1.822162	1.100742	1.995946	1.225096	0.905191	1.990191	0.885939
N	S	-0.001157	0.888165	-0.027850	-0.102052	0.046640	0.152313	-0.172462	0.394284	-0.090353
	S'	0.004521	0.372980	0.028561	0.169155	0.021031	-0.310292	0.355416	-0.779871	0.138622
	S''	0.000432	0.000546	-0.003105	0.009915	-0.005064	0.010127	0.000636	0.000065	-0.010291
	X	0.001134	0.010651	0.110225	0.023455	0.015996	1.000980	0.089351	-0.308239	-0.043855
	X'	0.000439	0.002070	0.141999	0.014929	-0.009306	-0.212866	-0.012791	-0.055731	0.243753
	Y	0.0	0.0	0.0	0.0	0.0	0.0	0.0	0.0	0.0
	Y'	0.0	0.0	0.0	0.0	0.0	0.0	0.0	0.0	0.0
	Z	0.001506	-0.009356	0.002612	0.158773	-0.018914	-0.030612	0.970795	0.341632	0.038345
	Z'	0.000404	0.001137	0.014351	-0.108539	-0.057253	0.034459	-0.255650	0.051954	-0.010343
O	S	-0.904573	-0.015345	-0.142329	0.170625	0.348760	-0.001811	0.114114	-0.010310	-0.064377
	S'	-0.340982	0.038498	0.310558	-0.360671	-0.774765	0.001079	-0.173298	0.015449	0.100586
	S''	0.000038	-0.000230	-0.000529	-0.001131	0.000991	0.011399	-0.005690	-0.002124	-0.006973
	X	-0.002346	0.007473	-1.010078	-0.039541	-0.339705	-0.071397	-0.020036	0.019387	-0.097400
	X'	0.000235	0.000602	0.022260	0.006116	-0.014915	-0.131037	-0.014152	-0.001972	0.071512
	Y	0.0	0.0	0.0	0.0	0.0	0.0	0.0	0.0	0.0
	Y'	0.0	0.0	0.0	0.0	0.0	0.0	0.0	0.0	0.0
	Z	-0.003035	0.010954	0.054947	1.003882	-0.327018	-0.025421	0.154097	-0.025461	-0.045062
	Z'	0.001651	0.003242	0.015214	-0.224059	-0.050219	0.017897	-0.139796	0.016392	-0.023573
H	S	-0.000679	-0.010548	0.125932	-0.089580	0.103700	-0.179131	0.125383	0.116205	0.929500
	S'	-0.000060	-0.005195	-0.037349	-0.058533	0.074864	0.049888	0.060363	0.091727	-0.235002

Table 24b. Transformation from sigma NPOs to sigma DLPOs for singlet HNO geometry G

		(O 1s)	(N 1s)	(O-hydr)	(O-sigma)	(O-lone)	(N-hydr)	(N-sigma)	(N-lone)	(H)
O 1s		1.0								
N 1s			1.0							
NRO	1			-0.29396	0.43123	-0.10172	-0.62298	-0.38999	-0.01553	-0.42053
	2			0.29055	0.57381	-0.10087	0.42673	-0.51775	-0.23459	0.26635
	3			-0.86452	0.04156	-0.16739	0.19692	-0.03469	0.02249	0.42704
	4			-0.10522	0.15799	0.90016	0.04448	-0.14517	0.35386	0.07350
	5			0.13344	0.09556	-0.37570	0.07622	-0.08079	0.90498	0.02420
	6			0.17296	-0.44213	-0.00383	-0.46642	-0.48495	0.00042	0.56733
	7			0.15157	0.50347	0.00137	-0.40704	0.56201	-0.00365	0.49193

Table 25a. Sigma DLROs and occupation numbers for singlet HNO geometry H

		(O 1s)	(N 1s)	(O-hydr)	(O-sigma)	(O-lone)	(N-hydr)	(N-sigma)	(N-lone)	(H)
ETCGAO		2.000000	2.000000	1.996660	1.069246	1.992694	1.078179	0.935424	1.990675	0.927128
N	S	-0.003859	0.910026	0.007808	-0.131232	0.008009	0.173576	0.187118	0.343637	-0.117544
	S'	0.008366	0.318935	-0.009271	0.200019	-0.015728	-0.368863	-0.418711	-0.775391	0.175505
	S''	0.000678	0.000172	0.002087	0.007481	-0.004674	0.006866	0.002529	-0.000649	-0.004688
	X	0.003166	0.002957	-0.091629	0.022275	-0.072941	1.011279	-0.041758	-0.366579	-0.091718
	X'	0.002157	-0.001094	-0.041181	0.039137	-0.067802	-0.206475	0.018448	-0.078329	0.193545
	Y	0.0	0.0	0.0	0.0	0.0	0.0	0.0	0.0	0.0
	Y'	0.0	0.0	0.0	0.0	0.0	0.0	0.0	0.0	0.0
	Z	0.000561	-0.006026	0.021492	0.180489	-0.020314	0.027880	-0.961678	0.364369	0.015530
	Z'	0.000379	0.000785	0.031874	-0.104830	-0.065779	0.006178	0.258174	0.043322	-0.012099
O	S	-0.908308	0.004006	-0.136185	0.175845	0.334443	-0.011331	-0.128544	-0.010521	-0.033661
	S'	-0.329445	-0.008140	0.312761	-0.377003	-0.762914	0.012545	0.191137	0.006781	0.058588
	S''	0.000100	-0.000303	-0.001319	-0.001123	-0.000852	0.003561	0.007479	-0.003032	0.000733
	X	-0.001972	-0.003003	0.953219	-0.044503	0.431048	-0.064897	0.014838	0.040397	-0.098781
	X'	-0.000814	0.000004	0.015595	0.014432	0.001626	-0.036626	-0.000814	0.009474	-0.022809
	Y	0.0	0.0	0.0	0.0	0.0	0.0	0.0	0.0	0.0
	Y'	0.0	0.0	0.0	0.0	0.0	0.0	0.0	0.0	0.0
	Z	-0.002710	0.000103	0.184715	1.018328	-0.295333	-0.021449	-0.163156	-0.028234	-0.028114
	Z'	0.001545	0.000127	0.022368	-0.223154	-0.052003	0.006061	0.142528	0.008979	-0.016140
H	S	-0.002063	0.001297	-0.110748	-0.061781	0.039574	-0.253336	-0.124934	0.117724	0.994680
	S'	-0.000639	0.000018	-0.034352	-0.037368	0.081744	0.088193	-0.077469	0.095979	-0.237820

Table 25b. Transformation from sigma NROs to sigma DLROs for singlet HNO geometry H

		(O 1s)	(N 1s)	(O-hydr)	(O-sigma)	(O-lone)	(N-hydr)	(N-sigma)	(N-lone)	(H)
O 1s		1.0								
N 1s			1.0							
NRO	1			0.13825	0.35604	0.02539	-0.63237	0.30168	0.04277	-0.60061
	2			-0.02611	0.61194	-0.19704	0.33898	0.58521	-0.23780	0.26851
	3			0.93775	-0.07405	0.01035	0.05483	-0.06682	-0.32276	0.05812
	4			0.06769	0.14202	0.94261	0.09204	0.14228	0.20364	0.12868
	5			0.31021	0.08876	-0.26523	0.11793	0.08289	0.89217	0.09382
	6			-0.00175	-0.37554	-0.03460	-0.56463	0.43735	-0.00032	0.58965
	7			-0.00282	0.56939	-0.01935	-0.37550	-0.58623	-0.00324	0.43674

Table 26a. Sigma DLROs and occupation numbers for singlet HNO geometry I

		(O 1s)	(N 1s)	(O-hydr)	(O-sigma)	(O-lone)	(N-hydr)	(N-sigma)	(N-lone)	(H)
ETCGAO		2.000000	2.000000	1.993037	1.077203	1.996730	1.045990	0.926486	1.992560	0.960444
N	S	0.003089	0.827969	0.225365	-0.103239	0.027502	0.206318	0.222317	0.451489	-0.136216
	S'	-0.006425	0.379550	0.124018	0.223765	-0.003186	-0.464818	-0.444037	-0.681808	0.224239
	S''	0.000454	0.000745	-0.001564	0.003219	-0.004759	0.010940	0.004757	-0.000692	-0.008267
	X	-0.004157	0.062964	0.096535	0.036913	-0.101800	1.000332	0.021331	-0.463667	-0.112007
	X'	0.004594	0.008547	0.010330	0.053247	-0.066994	-0.227984	0.029584	-0.099516	0.189630
	Y	0.0	0.0	0.0	0.0	0.0	0.0	0.0	0.0	0.0
	Y'	0.0	0.0	0.0	0.0	0.0	0.0	0.0	0.0	0.0
	Z	0.005604	-0.027236	-0.036815	0.189197	-0.028068	0.132770	-0.957973	0.348157	-0.022787
	Z'	0.000278	0.008680	-0.058773	-0.090467	-0.067525	-0.030064	0.264366	0.025443	-0.009830
O	S	-0.901381	-0.084061	0.276061	0.193972	0.234840	-0.015106	-0.135076	0.017642	-0.021112
	S'	-0.326131	0.135035	-0.423929	-0.409769	-0.676459	0.006489	0.208739	0.006956	0.035930
	S''	-0.000001	-0.000195	0.000516	-0.001304	-0.001007	0.002737	0.008140	-0.003123	0.000470
	X	-0.109442	0.200153	-0.796818	-0.048811	0.622914	-0.076739	-0.012548	0.049975	-0.058562
	X'	-0.000624	-0.001353	-0.011856	0.006268	0.008137	-0.036673	-0.004781	0.024809	-0.009785
	Y	0.0	0.0	0.0	0.0	0.0	0.0	0.0	0.0	0.0
	Y'	0.0	0.0	0.0	0.0	0.0	0.0	0.0	0.0	0.0
	Z	-0.009225	0.052889	-0.251745	1.014356	-0.274886	-0.027437	-0.175563	-0.026471	-0.007489
	Z'	0.000990	0.013365	-0.033862	-0.226335	-0.047997	0.003246	0.147516	0.004343	-0.015874
H	S	0.008552	-0.053281	0.085779	-0.059772	0.058400	-0.314758	-0.104966	0.139457	1.019252
	S'	0.001058	-0.025527	0.043185	-0.047557	0.078807	0.081450	-0.062530	0.104714	-0.217484

Table 26b. Transformation from sigma NROs to sigma DLEOs for singlet HNO geometry I

		(O 1s)	(N 1s)	(O-hydr)	(O-sigma)	(O-lone)	(N-hydr)	(N-sigma)	(N-lone)	(H)
O 1s		1.0								
N 1s			1.0							
NRO	1			-0.10481	0.62484	-0.08317	-0.35949	0.54393	-0.06283	-0.40328
	2			0.02154	0.34704	-0.15994	0.60895	0.37146	-0.19532	0.55369
	3			-0.87849	-0.07726	0.20154	0.04765	-0.07340	-0.41703	-0.00945
	4			0.08746	0.13976	0.94216	0.09283	0.13827	0.22994	0.06743
	5			-0.45482	0.05154	-0.19770	0.11014	0.05018	0.85505	0.07510
	6			-0.02230	-0.61354	0.00275	-0.29353	0.68997	0.00140	0.24665
	7			-0.04239	0.29077	0.01116	-0.62512	-0.25115	-0.00178	0.67800

Table 27a. Sigma DLROs and occupation numbers for singlet HNO geometry J

		(O 1s)	(N 1s)	(O-hydr)	(O-sigma)	(O-lone)	(N-hydr)	(N-sigma)	(N-lone)	(H)
ETCGAO		2.000000	2.000000	1.968101	1.050102	1.996133	1.076793	0.951783	1.991641	0.955097
N	S	0.001611	0.936438	-0.005152	-0.131998	-0.004913	0.240609	0.190839	0.254249	-0.163497
	S'	-0.000242	0.223566	0.010957	0.222015	-0.007107	-0.567644	-0.497734	-0.677673	0.267197
	S''	-0.000310	0.000016	-0.003702	0.002156	-0.004421	0.017621	0.001880	-0.001488	-0.016180
	X	0.001242	0.001257	-0.139454	0.020867	-0.085242	0.946701	0.102132	-0.619028	-0.124947
	X'	0.000605	-0.002862	-0.027128	0.048879	-0.070488	-0.185149	0.041326	-0.116107	0.139625
	Y	0.0	0.0	0.0	0.0	0.0	0.0	0.0	0.0	0.0
	Y'	0.0	0.0	0.0	0.0	0.0	0.0	0.0	0.0	0.0
	Z	-0.001734	-0.005465	0.008052	0.205260	-0.065135	0.320092	-0.918687	0.313310	-0.098880
	Z'	-0.000009	-0.000384	0.031874	-0.074948	-0.108491	-0.079671	0.282615	-0.008461	-0.000177
O	S	0.911308	0.005071	-0.079391	0.194544	0.336934	0.009631	-0.137077	-0.003727	-0.022514
	S'	0.310234	-0.013667	0.196947	-0.421976	-0.775807	-0.014450	0.215784	0.010691	0.038209
	S''	0.000037	-0.000438	-0.001380	0.000418	-0.000807	0.005734	0.004651	-0.002582	-0.003610
	X	-0.006315	0.001138	1.007605	0.009146	0.251755	-0.076069	-0.018012	0.094399	-0.046993
	X'	-0.000159	0.000471	0.001195	-0.004116	0.010990	0.010758	-0.014611	0.048813	-0.058623
	Y	0.0	0.0	0.0	0.0	0.0	0.0	0.0	0.0	0.0
	Y'	0.0	0.0	0.0	0.0	0.0	0.0	0.0	0.0	0.0
	Z	0.006262	-0.000826	0.072511	1.009107	-0.382146	-0.003665	-0.154824	-0.024582	-0.006312
	Z'	-0.001123	-0.000186	0.021923	-0.252328	-0.064052	0.001140	0.168975	0.004505	-0.020716
H	S	-0.000704	0.004589	0.003935	-0.042881	0.132342	-0.378456	-0.075654	0.154499	1.093388
	S'	0.000522	-0.001409	0.016021	0.039707	-0.090791	-0.093319	0.056358	-0.104231	0.216184

Table 27b. Transformation from sigma NROs to sigma DLROs for singlet HNO geometry J

		(O 1s)	(N 1s)	(O-hydr)	(O-sigma)	(O-lone)	(N-hydr)	(N-sigma)	(N-lone)	(H)
O	1s	1.0								
N	1s		1.0							
NRO	1			0.00916	0.69021	0.16745	-0.15571	0.62881	-0.12358	-0.24608
	2			-0.14252	0.13075	0.09880	0.68192	0.21347	-0.18906	0.63757
	3			0.77707	-0.08292	0.18730	0.06492	-0.08855	-0.58272	-0.05090
	4			0.24049	0.13241	-0.94732	0.09254	0.13337	-0.01481	0.02539
	5			0.55169	0.08317	0.17230	0.19044	0.08606	0.78051	0.07851
	6			-0.00256	-0.68893	0.00277	0.02960	0.71255	0.00183	-0.12940
	7			0.11648	-0.02356	-0.00193	-0.67883	0.13512	-0.00027	0.71190

Table 28a. Sigma DLROs and occupation numbers for singlet HNO geometry K

		(O 1s)	(N 1s)	(O-hydr)	(O-sigma)	(O-lone)	(N-hydr)	(N-sigma)	(N-lone)	(H)
ETCGAO		2.000000	2.000000	1.974075	1.012415	1.996480	1.121244	0.986300	1.992873	0.909062
N	S	-0.000849	0.951833	-0.017581	-0.120410	-0.006841	0.256205	0.193213	0.195520	-0.162032
	S'	0.000940	0.164984	-0.004047	0.217803	0.005287	-0.675336	-0.560728	-0.540327	0.284211
	S''	0.000230	-0.000144	-0.005064	-0.002266	-0.002581	0.025991	0.000564	-0.002513	-0.028873
	X	-0.000555	0.012735	-0.132912	0.041164	-0.107862	0.710211	0.185993	-0.821633	-0.037810
	X'	0.000132	-0.002274	-0.028492	0.062538	-0.077892	-0.204962	0.017445	-0.097684	0.175893
	Y	0.0	0.0	0.0	0.0	0.0	0.0	0.0	0.0	0.0
	Y'	0.0	0.0	0.0	0.0	0.0	0.0	0.0	0.0	0.0
	Z	0.003106	-0.007657	0.012182	0.188815	-0.135233	0.516920	-0.821350	0.205715	-0.145678
	Z'	0.000776	-0.000179	0.058618	-0.103718	-0.154207	-0.205351	0.353369	-0.046187	0.060482
O	S	-0.923788	0.001503	-0.096665	0.166167	0.294513	0.009164	-0.110089	-0.008348	-0.009943
	S'	-0.266008	-0.003484	0.248731	-0.391576	-0.745801	-0.013462	0.183460	0.013949	0.018809
	S''	0.000012	-0.000391	0.000124	-0.005255	-0.001000	-0.001343	0.008841	-0.000954	0.001068
	X	0.002873	0.016867	0.990926	0.020515	0.324646	-0.053821	-0.042248	0.132711	-0.046749
	X'	-0.000065	-0.000423	-0.003049	-0.011502	0.020129	-0.008601	-0.014140	0.072605	-0.036494
	Y	0.0	0.0	0.0	0.0	0.0	0.0	0.0	0.0	0.0
	Y'	0.0	0.0	0.0	0.0	0.0	0.0	0.0	0.0	0.0
	Z	-0.005257	0.002486	0.073202	0.999911	-0.386107	0.002889	-0.142179	-0.001621	-0.014138
	Z'	0.001597	0.001071	0.036689	-0.269020	-0.067606	-0.023837	0.183813	0.009158	-0.003689
H	S	-0.000478	0.001075	-0.012844	-0.039909	0.186813	-0.319455	-0.035497	0.149360	1.082721
	S'	0.000152	-0.000394	0.022070	0.015253	-0.080677	-0.121064	0.054937	-0.072709	0.219131

Table 28b. Transformation from sigma NROs to sigma DLROs for singlet HNO geometry K

		(O 1s)	(N 1s)	(O-hydr)	(O-sigma)	(O-lone)	(N-hydr)	(N-sigma)	(N-lone)	(H)
O	1s	1.0								
N	1s		1.0							
NRO	1			0.02831	0.69090	-0.20406	-0.02749	0.66553	-0.11368	-0.15364
	2			-0.27981	-0.00677	-0.08640	0.65276	0.10615	-0.31946	0.61219
	3			0.74603	-0.05474	0.09987	0.06167	-0.06169	-0.64909	-0.03931
	4			-0.06143	0.15111	0.96836	0.06658	0.16367	0.05405	0.03909
	5			0.59166	0.05099	-0.05643	0.35400	0.08704	0.67880	0.22470
	6			-0.02854	-0.67095	-0.00322	0.19966	0.62690	0.00332	-0.34078
	7			0.09844	-0.20978	-0.00123	-0.63225	0.33858	-0.00140	0.65721

Table 29a. Sigma DLROs and occupation numbers for singlet HNO geometry L

		(O 1s)	(N 1s)	(O-hydr)	(O-sigma)	(O-lone)	(N-hydr)	(N-sigma)	(N-lone)	(H)
ETCGAO		2.000000	2.000000	1.986001	0.935817	1.993291	1.194860	1.081615	1.981499	0.794868
N	S	0.000138	0.997835	-0.000014	-0.030453	0.000096	-0.033174	-0.048393	0.000019	-0.047504
	S'	0.001312	0.051954	0.000063	-0.240559	-0.019366	0.783258	0.684303	-0.000146	-0.320988
	S''	-0.000296	-0.000088	-0.000008	-0.006658	0.001990	0.049480	-0.004687	-0.000000	-0.062684
	X	0.000000	-0.000001	-0.158475	0.000242	-0.000142	0.000053	0.000250	1.056145	0.000014
	X'	0.000000	-0.000000	-0.371842	-0.000018	-0.000074	-0.000016	0.000050	0.012996	0.000006
	Y	0.0	0.0	0.0	0.0	0.0	0.0	0.0	0.0	0.0
	Y'	0.0	0.0	0.0	0.0	0.0	0.0	0.0	0.0	0.0
	Z	-0.008611	-0.005324	0.000111	0.139743	-0.258139	0.700463	-0.686853	0.000086	-0.188532
	Z'	-0.004331	-0.001703	0.000335	-0.137022	-0.258114	-0.342676	0.389241	-0.000034	0.089985
O	S	0.996534	0.001781	0.000085	-0.025481	-0.092462	0.005391	-0.020293	0.000011	-0.001736
	S'	-0.070902	-0.001668	0.000707	-0.358452	-0.721438	-0.042099	0.170840	0.000047	0.028662
	S''	-0.000100	-0.000130	-0.000000	-0.000877	0.000056	-0.001537	0.000037	0.000000	0.001142
	X	-0.000000	0.000001	1.048502	-0.000209	0.001062	0.000052	-0.000238	-0.154511	-0.000020
	X'	-0.000000	0.000000	-0.016766	-0.000061	-0.000019	-0.000005	0.000030	-0.073655	-0.000015
	Y	0.0	0.0	0.0	0.0	0.0	0.0	0.0	0.0	0.0
	Y'	0.0	0.0	0.0	0.0	0.0	0.0	0.0	0.0	0.0
	Z	-0.000474	0.003714	0.000530	0.994948	-0.385384	0.062326	-0.140613	-0.000157	-0.032923
	Z'	-0.002798	0.001172	0.000058	-0.295947	-0.073174	-0.017267	0.176036	0.000021	-0.023676
H	S	0.006341	0.004692	-0.000287	0.020657	0.320948	-0.277387	0.004223	-0.000003	1.269894
	S'	-0.004436	-0.003434	0.000240	-0.004577	-0.235763	-0.001977	0.033111	0.000000	-0.352122

Table 29b. Transformation from sigma NROs to sigma DLROs for singlet HNO geometry L

		(O 1s)	(N 1s)	(O-hydr)	(O-sigma)	(O-lone)	(N-hydr)	(N-sigma)	(N-lone)	(H)
O	1s	1.0								
N	1s		1.0							
NRO	1			-0.00026	0.66049	-0.22032	-0.13852	0.65472	0.00062	-0.25958
	2			0.00017	0.06480	-0.15856	0.75826	0.26743	-0.00010	0.56937
	3			0.75880	-0.00002	0.00076	0.00008	-0.00002	0.65132	-0.00000
	4			-0.00090	0.15923	0.96180	0.06989	0.20225	-0.00007	0.06166
	5			0.65132	0.00050	0.00040	-0.00015	0.00046	-0.75880	-0.00030
	6			-0.00003	-0.70276	0.00624	0.13254	0.59138	-0.00000	-0.37255
	7			0.00011	-0.20085	-0.03500	-0.61920	0.33044	-0.00000	0.68252

Table 30a. Sigma DLROs and occupation numbers for triplet HNO geometry A

		(O 1s)	(N 1s)	(O-hydr)	(O-sigma)	(O-lone)	(N-hydr)	(N-sigma)	(N-lone)	(H)
ETCGAO		2.000000	2.000000	1.081992	1.585221	1.839735	1.159465	0.652814	1.980697	0.700887
N	S	-0.000109	0.995949	0.005677	-0.001086	-0.000000	-0.000000	-0.038300	-0.108532	-0.006407
	S'	0.000163	0.072654	0.092632	-0.047744	-0.000001	0.000001	0.209198	0.657376	-0.091425
	S''	-0.000229	-0.000339	0.004913	0.008806	0.000000	-0.000000	-0.013064	0.000350	-0.017262
	X	0.0	0.0	-0.000002	0.000003	-0.156878	1.036796	-0.000002	-0.000000	0.000013
	X'	0.0	0.0	0.000004	-0.000004	-0.033354	-0.049459	0.000010	0.000000	0.000003
	Y	0.0	0.0	0.0	0.0	0.0	0.0	0.0	0.0	0.0
	Y'	0.0	0.0	0.0	0.0	0.0	0.0	0.0	0.0	0.0
	Z	-0.002179	0.002330	-0.149530	0.071990	-0.000002	-0.000006	-0.984056	0.397212	0.101014
	Z'	-0.000837	0.003469	-0.029143	-0.120334	-0.000003	0.000002	0.251262	0.097415	0.150780
O	S	0.997836	-0.000147	-0.019354	-0.057209	-0.000003	-0.000000	-0.029573	-0.003615	-0.034549
	S'	0.056392	0.000786	0.302821	0.979089	0.000041	-0.000003	-0.272604	-0.035320	-0.264860
	S''	-0.000079	-0.000248	0.021256	0.003669	0.000000	-0.000000	-0.001598	0.003455	-0.026705
	X	0.0	0.0	-0.000018	-0.000039	1.038039	-0.111370	-0.000006	0.000001	-0.000017
	X'	0.0	0.0	0.000027	0.000012	0.003406	-0.058088	-0.000012	0.000003	-0.000044
	Y	0.0	0.0	0.0	0.0	0.0	0.0	0.0	0.0	0.0
	Y'	0.0	0.0	0.0	0.0	0.0	0.0	0.0	0.0	0.0
	Z	0.001732	0.009633	-0.971498	0.234414	-0.000007	0.000001	-0.032048	0.279769	0.228956
	Z'	0.002040	0.007809	0.432549	-0.198660	0.000001	0.000001	0.240771	0.363938	-0.019619
H	S	0.005085	0.009090	-0.222857	-0.118274	0.000005	0.000002	0.110556	0.363870	1.142282
	S'	-0.000167	-0.001619	-0.130060	-0.032019	0.000000	0.000001	0.017684	-0.100996	0.329685

Table 30b. Transformation from sigma NROs to sigma DLROs for triplet HNO geometry A

		(O 1s)	(N 1s)	(O-hydr)	(O-sigma)	(O-lone)	(N-hydr)	(N-sigma)	(N-lone)	(H)
O	1s	1.0								
N	1s		1.0							
NRO	1			-0.57721	0.37220	0.00001	0.00001	0.50296	-0.30935	-0.42384
	2			-0.45810	-0.61291	0.00033	0.00016	-0.08220	0.51004	-0.38418
	3			0.00017	0.00019	0.92048	0.39078	0.00001	-0.00023	0.00014
	4			0.01627	0.52920	0.00006	0.00002	0.24221	0.79976	0.14627
	5			0.00001	0.00002	-0.39078	0.92048	-0.00000	0.00000	0.00000
	6			0.25820	-0.44875	-0.00001	0.00001	0.82358	-0.00011	0.23168
	7			-0.62454	-0.06617	-0.00001	0.00000	-0.05775	-0.06742	0.77311

Table 31a. Sigma DLROs and occupation numbers for triplet HNO geometry B

		(O 1s)	(N 1s)	(O-hydr)	(O-sigma)	(O-lone)	(N-hydr)	(N-sigma)	(N-lone)	(H)
ETCGAO		2.000000	2.000000	1.149225	1.254034	1.931646	1.099818	0.779737	1.990816	0.795483
N	S	0.001512	0.910150	0.031030	-0.104397	-0.019406	-0.011509	0.171414	0.362588	-0.013101
	S'	-0.003400	0.305731	-0.051801	0.178767	0.018500	0.026010	-0.371497	-0.837094	0.021987
	S''	-0.000740	-0.000039	-0.009385	0.022381	-0.002482	0.000050	-0.019476	-0.002427	0.001757
	X	0.000420	-0.000442	-0.032605	-0.043862	0.106222	1.026076	0.047165	0.003695	-0.068529
	X'	-0.000599	-0.000501	0.004814	-0.010095	-0.032889	0.026981	0.030938	-0.012102	0.020473
	Y	0.0	0.0	0.0	0.0	0.0	0.0	0.0	0.0	0.0
	Y'	0.0	0.0	0.0	0.0	0.0	0.0	0.0	0.0	0.0
	Z	-0.001155	-0.003845	-0.051142	0.180106	0.007536	0.094162	-1.048315	0.323195	0.026127
	Z'	0.001080	-0.002194	-0.002430	0.060037	0.017729	0.013858	-0.138352	-0.052012	-0.014608
O	S	0.936850	0.003045	0.194662	0.224054	0.244662	0.009950	-0.120283	-0.027736	-0.135437
	S'	0.224146	-0.007200	-0.475026	-0.558743	-0.663836	-0.019173	0.207408	0.046146	0.224054
	S''	-0.000238	-0.000222	0.017328	0.006201	0.000026	-0.002432	-0.010759	0.002180	-0.022004
	X	-0.002362	-0.006158	0.727549	0.341765	-0.694453	-0.113166	0.073765	-0.038666	-0.006354
	X'	-0.002193	-0.001828	-0.203873	-0.017309	-0.120805	-0.042081	0.115308	-0.058945	0.233035
	Y	0.0	0.0	0.0	0.0	0.0	0.0	0.0	0.0	0.0
	Y'	0.0	0.0	0.0	0.0	0.0	0.0	0.0	0.0	0.0
	Z	0.001476	0.000756	-0.621168	0.832125	-0.163673	0.028439	-0.210604	0.052088	0.118653
	Z'	0.001305	0.002720	0.177879	-0.191957	0.032784	0.001445	0.036366	0.128402	-0.043281
H	S	0.004063	0.003635	-0.295393	0.009153	0.131586	0.027694	-0.140556	0.129773	1.014617
	S'	-0.001100	-0.001372	-0.107571	-0.010580	-0.068277	-0.010745	0.074866	-0.069105	0.234894

Table 31b. Transformation from sigma NROs to sigma DLROs for triplet HNO geometry B

		(O 1s)	(N 1s)	(O-hydr)	(O-sigma)	(O-lone)	(N-hydr)	(N-sigma)	(N-lone)	(H)
O	1s	1.0								
N	1s		1.0							
NRO	1			-0.19018	0.70776	-0.07117	0.07580	0.59940	-0.19626	-0.23301
	2			-0.11372	0.04031	-0.62828	0.14070	0.03383	0.74931	-0.09114
	3			0.71139	0.26813	-0.23009	0.24695	0.03710	-0.08079	0.54791
	4			0.13034	0.21595	0.69666	-0.11703	0.14826	0.62615	0.15268
	5			-0.09121	-0.12870	0.24578	0.94594	-0.01988	0.00546	-0.13957
	6			0.03644	-0.59219	-0.03465	-0.02419	0.78207	0.00017	0.18589
	7			-0.64668	0.10803	-0.01791	0.06626	-0.06465	-0.03748	0.74823

Table 32a. Sigma DLROs and occupation numbers for triplet HNO geometry C

		(O 1s)	(N 1s)	(O-hydr)	(O-sigma)	(O-lone)	(N-hydr)	(N-sigma)	(N-lone)	(H)
ETCGAO		2.000000	2.000000	1.119620	1.157270	1.967452	1.065978	0.853599	1.992867	0.843921
N	S	0.001694	0.900098	0.022138	-0.109150	0.006753	-0.006596	0.153534	0.390791	-0.035559
	S'	-0.003063	0.345925	-0.033339	0.178488	-0.013261	0.016244	-0.330526	-0.843698	0.053197
	S''	-0.000741	0.000161	-0.004219	0.017851	-0.008366	-0.001129	-0.007983	-0.000382	0.004571
	X	0.000392	-0.000500	-0.043880	-0.013262	0.067574	1.022697	0.022247	0.009443	-0.073927
	X'	0.000326	0.000076	-0.011045	0.010048	0.016321	-0.024488	-0.014829	0.004450	-0.008684
	Y	0.0	0.0	0.0	0.0	0.0	0.0	0.0	0.0	0.0
	Y'	0.0	0.0	0.0	0.0	0.0	0.0	0.0	0.0	0.0
	Z	-0.001806	-0.004355	-0.009228	0.169653	0.003307	0.039846	-1.028938	0.322677	0.021662
	Z'	-0.000870	0.001376	0.006806	-0.067660	-0.023191	-0.011319	0.146987	0.057609	0.001554
O	S	0.924459	-0.004333	0.184095	0.181534	0.301695	0.009401	-0.108761	-0.018532	-0.127486
	S'	0.271636	-0.008303	-0.413439	-0.420888	-0.757413	-0.017575	0.178451	0.031954	0.193300
	S''	-0.000258	-0.000211	0.009923	0.007730	0.000159	-0.001001	-0.010556	-0.000234	-0.012300
	X	-0.001356	-0.002554	0.947843	0.133156	-0.486052	-0.091021	0.062544	-0.038099	-0.055629
	X'	-0.002096	-0.000972	-0.247657	-0.002448	-0.106283	-0.032683	0.092160	-0.054595	0.253206
	Y	0.0	0.0	0.0	0.0	0.0	0.0	0.0	0.0	0.0
	Y'	0.0	0.0	0.0	0.0	0.0	0.0	0.0	0.0	0.0
	Z	-0.000172	-0.000754	-0.298236	0.956826	-0.282636	0.001828	-0.155776	0.011261	0.085745
	Z'	-0.000866	0.000786	0.034782	-0.196781	-0.027415	-0.002288	0.090134	0.074590	0.038030
H	S	0.003262	0.001473	-0.292808	-0.027012	0.114409	-0.014392	-0.138678	0.108880	0.965674
	S'	-0.000432	-0.000540	-0.103807	0.007115	-0.071150	-0.009915	0.077949	-0.079310	0.250770

Table 32b. Transformation from sigma NROs to sigma DLROs for triplet HNO geometry C

		(O 1s)	(N 1s)	(O-hydr)	(O-sigma)	(O-lone)	(N-hydr)	(N-sigma)	(N-lone)	(H)
O	1s	1.0								
N	1s		1.0							
NRO	1			-0.12123	0.72218	-0.10573	0.03562	0.63233	-0.15414	-0.16649
	2			-0.06712	0.04411	-0.53555	0.07755	0.03395	0.83506	-0.04728
	3			0.72028	0.15995	-0.19486	0.22356	0.05268	-0.06442	0.60061
	4			0.12680	0.16861	0.79775	-0.08788	0.13426	0.52348	0.13894
	5			-0.11863	-0.07048	0.16485	0.96589	-0.00650	0.00231	-0.14420
	6			0.07231	-0.64606	-0.01308	-0.02718	0.75882	0.00465	0.02515
	7			-0.65315	0.01182	-0.01675	0.03646	0.04849	-0.02653	0.75405

Table 33a. Sigma DLROs and occupation numbers for triplet HNO geometry D

		(O 1s)	(N 1s)	(O-hydr)	(O-sigma)	(O-lone)	(N-hydr)	(N-sigma)	(N-lone)	(H)
ETCGAO		2.000000	2.000000	1.112205	1.133082	1.978105	1.064151	0.875246	1.992534	0.845298
N	S	0.001407	0.902751	0.012588	-0.095311	0.019238	-0.004448	0.128291	0.383611	-0.044025
	S'	-0.002121	0.348929	-0.018089	0.150159	-0.018888	0.012652	-0.288337	-0.847738	0.069018
	S''	-0.000788	0.000480	-0.000644	0.015632	-0.008816	-0.003212	-0.005973	0.001806	0.003939
	X	-0.000036	0.000050	-0.039961	0.012501	0.038243	1.029444	-0.010757	0.024385	-0.086140
	X'	-0.000129	-0.000093	-0.011613	0.005735	-0.003275	-0.025318	0.008892	-0.006290	-0.002244
	Y	0.0	0.0	0.0	0.0	0.0	0.0	0.0	0.0	0.0
	Y'	0.0	0.0	0.0	0.0	0.0	0.0	0.0	0.0	0.0
	Z	-0.002211	-0.000309	0.002754	0.148112	-0.005317	-0.026257	-1.001931	0.308174	0.036582
	Z'	-0.001030	0.002351	0.004980	-0.079968	-0.029297	-0.005103	0.171695	0.060085	0.003755
O	S	0.916373	0.000708	0.169187	0.158109	0.333885	0.008747	-0.097868	-0.013813	-0.124291
	S'	0.302604	-0.001247	-0.360276	-0.349528	-0.796829	-0.015604	0.155062	0.026441	0.179767
	S''	-0.000317	-0.000219	0.004138	0.003912	-0.000664	0.000217	-0.004064	-0.000823	-0.003506
	X	-0.000690	-0.000579	1.002377	-0.025785	-0.351231	-0.079405	0.040793	-0.030787	-0.079509
	X'	-0.001260	-0.000868	-0.233559	-0.000104	-0.076178	-0.044787	0.051950	-0.044543	0.224938
	Y	0.0	0.0	0.0	0.0	0.0	0.0	0.0	0.0	0.0
	Y'	0.0	0.0	0.0	0.0	0.0	0.0	0.0	0.0	0.0
	Z	-0.000939	0.002534	-0.074064	0.975173	-0.319036	-0.008271	-0.114891	-0.005385	0.035159
	Z'	-0.001852	0.001292	-0.025790	-0.214019	-0.055053	-0.003270	0.143454	0.049931	0.053724
H	S	0.002327	0.001948	-0.271510	-0.055935	0.089978	-0.060075	-0.133828	0.100205	0.956987
	S'	0.000082	0.001059	0.094543	-0.032852	0.066033	0.006827	-0.065090	0.089589	-0.277088

Table 33b. Transformation from sigma NROs to sigma DLROs for triplet HNO geometry D

		(O 1s)	(N 1s)	(O-hydr)	(O-sigma)	(O-lone)	(N-hydr)	(N-sigma)	(N-lone)	(H)
O 1s		1.0								
N 1s			1.0							
NRO	1			-0.12778	0.72261	-0.12311	-0.01305	0.63709	-0.13989	-0.14394
	2			-0.05401	0.03560	-0.53454	0.05977	0.02559	0.83979	-0.02450
	3			0.71186	0.13151	-0.18818	0.23478	0.08209	-0.08099	0.61002
	4			0.12450	0.16360	0.80427	-0.06229	0.13912	0.51733	0.14148
	5			-0.17940	-0.02185	0.12821	0.96773	0.00597	-0.00156	-0.11985
	6			0.10051	-0.65404	-0.00411	-0.00928	0.74604	0.00736	-0.07340
	7			-0.64515	-0.06524	-0.01958	-0.02593	0.10366	-0.03055	0.75285

Table 34a. Sigma DLROs and occupation numbers for triplet HNO geometry E

		(O 1s)	(N 1s)	(O-hydr)	(O-sigma)	(O-lone)	(N-hydr)	(N-sigma)	(N-lone)	(H)
ETCGAO		2.000000	2.000000	1.131854	1.125832	1.980193	1.067911	0.881581	1.987407	0.825899
N	S	0.001210	0.902886	0.004732	-0.090586	0.016068	0.004040	0.132418	0.384094	-0.054668
	S'	-0.001775	0.350462	-0.008886	0.141450	-0.012753	-0.002642	-0.292604	-0.847887	0.085948
	S''	-0.000610	0.000391	-0.000074	0.011806	-0.007148	-0.003347	-0.004894	0.002778	0.006248
	X	-0.000196	-0.000057	-0.047040	0.033368	0.017927	1.043912	-0.024741	0.026785	-0.098422
	X'	-0.000234	-0.000340	-0.073263	-0.000397	-0.019055	-0.036379	0.027684	-0.021200	0.060758
	Y	0.0	0.0	0.0	0.0	0.0	0.0	0.0	0.0	0.0
	Y'	0.0	0.0	0.0	0.0	0.0	0.0	0.0	0.0	0.0
	Z	-0.002181	-0.000269	0.000220	0.142750	-0.007373	-0.073155	-0.986125	0.295982	0.049626
	Z'	-0.000835	0.002142	0.004289	-0.082078	-0.036636	0.004714	0.196175	0.058861	0.005523
O	S	0.911799	0.008315	0.139243	0.146462	0.355144	0.007372	-0.090086	-0.012370	-0.110588
	S'	0.319705	0.001575	-0.291250	-0.315628	-0.823254	-0.011687	0.140607	0.024695	0.158247
	S''	-0.000199	-0.000245	-0.001274	0.000835	-0.000923	0.001317	0.000205	-0.000970	0.002626
	X	-0.000310	-0.000427	1.023311	-0.142716	-0.238173	-0.074918	0.009975	-0.026674	-0.089775
	X'	-0.001313	-0.000597	-0.186500	0.015442	-0.052494	-0.077637	-0.002733	-0.042763	0.186483
	Y	0.0	0.0	0.0	0.0	0.0	0.0	0.0	0.0	0.0
	Y'	0.0	0.0	0.0	0.0	0.0	0.0	0.0	0.0	0.0
	Z	-0.000669	0.001974	0.091694	0.976172	-0.323850	-0.015940	-0.108714	-0.016087	-0.014849
	Z'	-0.002069	0.000854	-0.050450	-0.210287	-0.060260	-0.000780	0.145263	0.035514	0.037570
H	S	0.002530	0.002039	-0.233432	-0.068856	0.076671	-0.109204	-0.149189	0.095106	0.942887
	S'	-0.000031	0.000749	0.100135	-0.036830	0.067531	0.024141	-0.063527	0.096447	-0.345135

Table 34b. Transformation from sigma NROs to sigma DLROs for triplet HNO geometry E

		(O 1s)	(N 1s)	(O-hydr)	(O-sigma)	(O-lone)	(N-hydr)	(N-sigma)	(N-lone)	(H)
O 1s		1.0								
N 1s			1.0							
NRO	1			-0.11269	0.72615	-0.13894	-0.06350	0.63678	-0.14076	-0.10664
	2			-0.05181	0.03961	-0.51561	0.05975	0.02919	0.85168	0.01077
	3			0.69851	0.08960	-0.18667	0.28448	0.08759	-0.10534	0.60787
	4			0.12763	0.16328	0.81635	-0.04335	0.14608	0.49035	0.16418
	5			-0.31108	0.03551	0.11243	0.94103	0.00910	-0.01811	-0.05809
	6			0.07062	-0.65301	0.00318	0.03407	0.74577	0.00997	-0.10559
	7			-0.61535	-0.09363	-0.03020	-0.15128	0.09164	-0.05350	0.75995

Table 35a. Sigma DLROs and occupation numbers for triplet HNO geometry F

		(O 1s)	(N 1s)	(O-hydr)	(O-sigma)	(O-lone)	(N-hydr)	(N-sigma)	(N-lone)	(H)
ETCGAO		2.000000	2.000000	1.182945	1.084626	1.981593	1.018555	0.923491	1.966943	0.842660
N	S	0.001178	0.906813	0.012641	-0.091454	0.010534	0.037811	0.136839	0.378559	-0.079011
	S'	-0.001735	0.336662	-0.020565	0.145885	-0.004046	-0.070547	-0.305178	-0.851978	0.115978
	S''	-0.000536	0.000380	-0.002118	0.012253	-0.005908	-0.007370	-0.007569	-0.000471	0.012529
	X	-0.000439	-0.000165	-0.044239	0.024962	-0.003927	1.061806	-0.087822	-0.015565	-0.102022
	X'	-0.000388	-0.000679	-0.111249	0.001310	-0.030598	-0.082334	0.016937	-0.044206	0.108620
	Y	0.0	0.0	0.0	0.0	0.0	0.0	0.0	0.0	0.0
	Y'	0.0	0.0	0.0	0.0	0.0	0.0	0.0	0.0	0.0
	Z	-0.001893	-0.000222	0.005253	0.167477	-0.006509	-0.129603	-0.964610	0.297844	0.046677
	Z'	-0.000969	0.002148	0.008476	-0.078468	-0.041651	0.035485	0.211030	0.053841	-0.015465
O	S	0.910574	0.000655	0.094941	0.157638	0.365847	0.007298	-0.085315	-0.011473	-0.092792
	S'	0.323809	-0.001139	-0.194640	-0.333312	-0.841229	-0.012205	0.130251	0.023184	0.135130
	S''	-0.000223	-0.000229	-0.003286	0.002301	0.000255	0.001004	-0.001094	-0.001215	0.006631
	X	-0.000191	-0.000659	1.027976	-0.134081	-0.135100	-0.099614	0.010771	-0.018214	-0.053722
	X'	-0.000847	-0.000502	-0.170208	0.017771	-0.038032	-0.138854	-0.027792	-0.045189	0.199107
	Y	0.0	0.0	0.0	0.0	0.0	0.0	0.0	0.0	0.0
	Y'	0.0	0.0	0.0	0.0	0.0	0.0	0.0	0.0	0.0
	Z	-0.001062	0.001682	0.111087	0.978455	-0.320455	-0.013627	-0.090520	-0.021705	-0.043855
	Z'	-0.002126	0.000626	-0.041936	-0.239250	-0.053302	0.002373	0.147307	0.026893	0.011983
H	S	0.002187	0.002323	-0.195615	-0.076188	0.072984	-0.161815	-0.154290	0.087126	0.914425
	S'	-0.000174	-0.000524	-0.071311	0.039396	-0.072110	-0.050819	0.057254	-0.099632	0.373190

Table 35b. Transformation from sigma NROs to sigma DLROs for triplet HNO geometry F

		(O 1s)	(N 1s)	(O-hydr)	(O-sigma)	(O-lone)	(N-hydr)	(N-sigma)	(N-lone)	(H)
O 1s		1.0								
N 1s			1.0							
NRO	1			-0.11440	0.70819	-0.14449	-0.06962	0.64857	-0.17852	-0.08449
	2			-0.04348	0.07734	-0.46644	0.10285	0.06662	0.86541	0.10301
	3			0.65424	0.07113	-0.15545	0.37864	0.07270	-0.17947	0.60157
	4			0.10252	0.17007	0.85252	0.00322	0.16143	0.41394	0.19066
	5			-0.53111	0.03957	0.09019	0.83470	-0.04353	-0.08356	0.05119
	6			-0.08659	-0.67513	-0.00380	0.00947	0.72854	-0.01224	0.07536
	7			-0.50686	0.03361	-0.04945	-0.37997	-0.10445	-0.09224	0.75876

Table 36a. Sigma DLROs and occupation numbers for triplet HNO geometry M

		(O 1s)	(N 1s)	(O-hydr)	(O-sigma)	(O-lone)	(N-hydr)	(N-sigma)	(N-lone)	(H)
ETCGAO		2.000000	2.000000	1.217859	1.074325	1.983743	0.995333	0.933630	1.951510	0.844440
N	S	0.001215	0.915298	0.018120	-0.093451	0.010837	0.057420	0.134916	0.364749	-0.090156
	S'	-0.001846	0.303709	-0.032074	0.151728	-0.004922	-0.116908	-0.314746	-0.856919	0.133878
	S''	-0.000525	-0.000124	-0.003487	0.016454	-0.005967	-0.011215	-0.012198	-0.003204	0.016690
	X	-0.000413	-0.000162	-0.039208	0.026326	-0.011023	1.070719	-0.111564	-0.062168	-0.119121
	X'	-0.000450	-0.000888	-0.104025	0.011634	-0.035733	-0.067344	0.005311	-0.056229	0.105944
	Y	0.0	0.0	0.0	0.0	0.0	0.0	0.0	0.0	0.0
	Y'	0.0	0.0	0.0	0.0	0.0	0.0	0.0	0.0	0.0
	Z	-0.001916	-0.000736	-0.000814	0.175353	-0.007664	-0.135596	-0.965518	0.310444	0.035486
	Z'	-0.001096	0.002119	0.007418	-0.085508	-0.048446	0.047741	0.200235	0.068541	-0.023441
O	S	0.910273	0.004121	0.064135	0.170705	0.366069	0.001491	-0.093334	-0.010607	-0.077033
	S'	0.324752	-0.000053	-0.131078	-0.359600	-0.841579	-0.003290	0.141841	0.021869	0.114540
	S''	-0.000290	-0.000238	-0.002658	0.003419	0.000554	0.001920	-0.001652	-0.001325	0.004681
	X	-0.000020	-0.000567	1.036364	-0.083595	-0.086324	-0.120770	0.015532	-0.020255	-0.030193
	X'	-0.000640	-0.000457	-0.128827	0.023660	-0.034681	-0.177784	-0.023460	-0.055913	0.215056
	Y	0.0	0.0	0.0	0.0	0.0	0.0	0.0	0.0	0.0
	Y'	0.0	0.0	0.0	0.0	0.0	0.0	0.0	0.0	0.0
	Z	-0.001094	0.002153	0.078328	0.990875	-0.328666	-0.018652	-0.098475	-0.027514	-0.042069
	Z'	-0.002151	0.000524	-0.022396	-0.222193	-0.056967	0.003810	0.144884	0.018525	0.002397
H	S	0.002012	0.002403	-0.184916	-0.098100	0.066554	-0.165991	-0.137308	0.097110	0.923588
	S'	0.000539	0.000597	0.045048	-0.055660	0.079842	0.044277	-0.060258	0.103934	-0.265759

Table 36b. Transformation from sigma NROs to sigma DLROs for triplet HNO geometry M

		(O 1s)	(N 1s)	(O-hydr)	(O-sigma)	(O-lone)	(N-hydr)	(N-sigma)	(N-lone)	(H)
O 1s		1.0								
N 1s			1.0							
NRO	1			-0.10278	0.69874	-0.13898	-0.07995	0.65023	-0.20843	-0.09616
	2			-0.03764	0.11250	-0.43523	0.14615	0.09765	0.85992	0.16166
	3			0.61779	0.07553	-0.11671	0.44348	0.05778	-0.23413	0.58667
	4			0.07238	0.17284	0.87713	0.02817	0.16152	0.36657	0.18512
	5			-0.65293	0.01997	0.07050	0.73433	-0.04776	-0.13286	0.09560
	6			-0.15438	-0.65536	-0.01812	-0.11143	0.68723	-0.03549	0.24572
	7			-0.38855	0.18340	-0.05453	-0.47236	-0.25232	-0.09480	0.71878

Table 37a. Sigma DLBOs and occupation numbers for triplet HNO geometry G

		(O 1s)	(N 1s)	(O-hydr)	(O-sigma)	(O-lone)	(N-hydr)	(N-sigma)	(N-lone)	(H)
ETCGAO		2.000000	2.000000	1.237777	1.082949	1.987825	0.960205	0.925223	1.939829	0.866995
N	S	0.001235	0.908086	0.022308	-0.101819	0.012472	0.091702	0.144257	0.371779	-0.104183
	S'	-0.001809	0.333206	-0.038208	0.157772	-0.008034	-0.181195	-0.322530	-0.840907	0.148819
	S''	-0.000387	0.000415	-0.002069	0.012868	-0.005935	-0.010266	-0.006851	-0.002319	0.014608
	X	-0.000432	-0.000254	-0.044868	0.018645	-0.013905	1.075530	-0.106531	-0.124228	-0.135672
	X'	-0.000388	-0.001129	-0.085333	0.009964	-0.036605	-0.079728	0.013903	-0.064999	0.094946
	Y	0.0	0.0	0.0	0.0	0.0	0.0	0.0	0.0	0.0
	Y'	0.0	0.0	0.0	0.0	0.0	0.0	0.0	0.0	0.0
	Z	-0.002416	-0.000760	-0.000423	0.174093	-0.015702	-0.113318	-0.962168	0.316394	0.024994
	Z'	-0.001176	0.002103	0.010676	-0.079260	-0.053789	0.059714	0.199577	0.066660	-0.042381
O	S	0.908272	-0.009728	0.040069	0.168593	0.368990	0.002634	-0.098083	-0.008159	-0.065097
	S'	0.332727	-0.005301	-0.079731	-0.354434	-0.840246	-0.005191	0.147369	0.018342	0.099818
	S''	-0.000148	-0.000271	-0.001728	0.002796	0.000237	0.002083	-0.000126	-0.001805	0.003580
	X	-0.000087	-0.000469	1.040033	-0.048719	-0.044180	-0.118117	0.018386	-0.006557	-0.029196
	X'	-0.000446	-0.000354	-0.087751	0.027786	-0.023879	-0.173518	-0.018039	-0.044140	0.182061
	Y	0.0	0.0	0.0	0.0	0.0	0.0	0.0	0.0	0.0
	Y'	0.0	0.0	0.0	0.0	0.0	0.0	0.0	0.0	0.0
	Z	-0.000598	0.002227	0.052104	0.996542	-0.327116	-0.024228	-0.105061	-0.030312	-0.036774
	Z'	-0.002188	0.000517	-0.012260	-0.227100	-0.054802	-0.004698	0.150528	0.016587	0.003461
H	S	0.001566	0.002390	-0.168006	-0.083584	0.062111	-0.195587	-0.144705	0.096613	0.943335
	S'	0.000594	0.000508	0.039640	-0.037132	0.081367	0.051494	-0.071590	0.101313	-0.278916

Table 37b. Transformation from sigma NROs to sigma DLROs for triplet HNO geometry G

		(O 1s)	(N 1s)	(O-hydr)	(O-sigma)	(O-lone)	(N-hydr)	(N-sigma)	(N-lone)	(H)
O 1s		1.0								
N 1s			1.0							
NBO	1			0.33354	0.55893	-0.15362	0.27748	0.50667	-0.34583	0.31534
	2			-0.04650	0.14482	-0.37442	0.17776	0.12452	0.86520	0.20246
	3			0.46433	-0.42487	0.03163	0.43029	-0.40295	-0.03856	0.50386
	4			0.03814	0.16553	0.91119	0.04102	0.15338	0.30121	0.15793
	5			-0.76214	0.00074	0.04239	0.60253	-0.02955	-0.17706	0.14858
	6			-0.13309	-0.62259	-0.02563	-0.22292	0.66455	-0.03833	0.31816
	7			-0.26637	0.26663	-0.04987	-0.54022	-0.31525	-0.08244	0.67635

Table 38a. Sigma DLROs and occupation numbers for triplet HNO geometry H

		(O 1s)	(N 1s)	(O-hydr)	(O-sigma)	(O-lone)	(N-hydr)	(N-sigma)	(N-lone)	(H)
ETCGAO		2.000000	2.000000	1.252031	1.102995	1.994686	0.958844	0.902913	1.913136	0.875978
N	S	0.000897	0.914888	0.012963	-0.100769	0.011223	0.156716	0.140500	0.351772	-0.139367
	S'	-0.001297	0.307715	-0.024308	0.159795	-0.007090	-0.318522	-0.326862	-0.827465	0.203420
	S''	-0.000304	0.000283	0.000288	0.010054	-0.004960	-0.005203	-0.004073	-0.001736	0.009194
	X	-0.000551	-0.000331	-0.084373	0.029574	-0.024449	1.061789	-0.068372	-0.252304	-0.144528
	X'	-0.000893	-0.001659	-0.053059	0.038489	-0.038619	-0.142924	0.004070	-0.093925	0.136916
	Y	0.0	0.0	0.0	0.0	0.0	0.0	0.0	0.0	0.0
	Y'	0.0	0.0	0.0	0.0	0.0	0.0	0.0	0.0	0.0
	Z	-0.001884	-0.000650	0.008910	0.169415	-0.026739	-0.051588	-0.964354	0.310874	0.013708
	Z'	-0.000254	0.001899	0.002213	-0.067914	-0.065958	0.052556	0.187935	0.062866	-0.054850
O	S	0.910644	-0.002575	0.014299	0.165727	0.362273	-0.003513	-0.104988	-0.005999	-0.040357
	S'	0.324700	-0.002884	-0.028335	-0.352874	-0.836772	0.004759	0.160864	0.014966	0.066743
	S''	-0.000003	-0.000369	-0.001236	0.002139	0.000351	0.001836	0.001386	-0.002641	0.002964
	X	0.000048	-0.000126	1.033852	-0.055114	-0.001340	-0.061542	0.020891	0.018560	-0.066676
	X'	-0.000310	-0.000169	-0.019316	0.009432	-0.005307	-0.031407	0.007714	-0.014260	0.019159
	Y	0.0	0.0	0.0	0.0	0.0	0.0	0.0	0.0	0.0
	Y'	0.0	0.0	0.0	0.0	0.0	0.0	0.0	0.0	0.0
	Z	-0.000343	0.002367	0.056698	0.997986	-0.331982	-0.037303	-0.109270	-0.032553	-0.016984
	Z'	-0.001609	0.000524	-0.005598	-0.219737	-0.058193	-0.021667	0.162559	0.012574	0.010532
H	S	0.001528	0.002993	-0.096737	-0.070004	0.074968	-0.291416	-0.140067	0.100124	1.017500
	S'	0.000316	0.000616	0.013108	-0.040587	0.085308	0.090018	-0.070419	0.108200	-0.267830

Table 38b. Transformation from sigma NROs to sigma DLROs for triplet HNO geometry H

		(O 1s)	(N 1s)	(O-hydr)	(O-sigma)	(O-lone)	(N-hydr)	(N-sigma)	(N-lone)	(H)
O	1s	1.0								
N	1s		1.0							
NRO	1			0.03314	0.70053	-0.12957	-0.11245	0.63094	-0.24615	-0.14162
	2			-0.06632	0.19640	-0.26459	0.23233	0.16693	0.85574	0.26997
	3			0.49454	0.02343	-0.04115	0.58484	0.04258	-0.32139	0.55321
	4			0.00910	0.14773	0.95419	0.05045	0.13720	0.18903	0.10251
	5			-0.86311	0.03110	0.00440	0.36781	0.03120	-0.25209	0.23290
	6			-0.02433	-0.64353	-0.01232	-0.18430	0.71923	-0.00628	0.18391
	7			-0.06549	0.18225	-0.02924	-0.64772	-0.18745	-0.06715	0.70884

Table 39a. Sigma DLROs and occupation numbers for triplet HNO geometry I

		(O 1s)	(N 1s)	(O-hydr)	(O-sigma)	(O-lone)	(N-hydr)	(N-sigma)	(N-lone)	(H)
ETCGAO		2.000000	2.000000	1.278375	1.086384	1.996321	0.979934	0.904380	1.864469	0.890770
N	S	0.001045	0.924783	0.003883	-0.099701	0.009728	0.168247	0.132387	0.322400	-0.138221
	S'	-0.001629	0.270038	-0.008946	0.165441	-0.005063	-0.367985	-0.328890	-0.808867	0.208683
	S''	-0.000587	0.000281	-0.000026	0.009911	-0.004740	-0.000535	-0.005641	-0.001902	0.005230
	X	-0.000240	-0.000959	-0.094122	0.042028	-0.031559	1.054360	0.029055	-0.359151	-0.145307
	X'	-0.000452	-0.002218	-0.033095	0.068890	-0.042595	-0.200217	0.004364	-0.124879	0.184654
	Y	0.0	0.0	0.0	0.0	0.0	0.0	0.0	0.0	0.0
	Y'	0.0	0.0	0.0	0.0	0.0	0.0	0.0	0.0	0.0
	Z	-0.002789	-0.000489	0.018178	0.173998	-0.039663	0.094632	-0.959307	0.274465	-0.026252
	Z'	-0.001132	0.001599	-0.006436	-0.062584	-0.081184	-0.010040	0.199114	0.046372	-0.025676
O	S	0.913422	0.000740	0.014770	0.167232	0.351791	-0.003666	-0.109023	-0.009758	-0.019522
	S'	0.312806	-0.002177	-0.032695	-0.362201	-0.831430	0.004525	0.170187	0.019981	0.034803
	S''	-0.000175	-0.000418	-0.000295	0.004404	-0.000540	-0.000447	-0.000638	-0.003140	0.004313
	X	-0.000221	0.000177	1.022829	-0.067205	-0.014811	-0.069226	0.016263	0.039425	-0.043723
	X'	-0.000817	0.000169	-0.021707	-0.021605	-0.001084	-0.032143	0.035903	-0.001345	0.022731
	Y	0.0	0.0	0.0	0.0	0.0	0.0	0.0	0.0	0.0
	Y'	0.0	0.0	0.0	0.0	0.0	0.0	0.0	0.0	0.0
	Z	-0.000792	0.002941	0.049926	0.996225	-0.348375	-0.014448	-0.105417	-0.032822	-0.016360
	Z'	-0.002214	0.000894	-0.009671	-0.223215	-0.062805	0.006596	0.170267	0.017294	-0.027943
H	S	0.001642	0.003527	-0.040371	-0.063207	0.094957	-0.322480	-0.115129	0.118728	1.014506
	S'	0.001981	0.000533	0.010243	-0.044599	0.086568	0.113642	-0.066172	0.113168	-0.265751

Table 39b. Transformation from sigma NROs to sigma DLROs for triplet HNO geometry I

		(O 1s)	(N 1s)	(O-hydr)	(O-sigma)	(O-lone)	(N-hydr)	(N-sigma)	(N-lone)	(H)
O 1s		1.0								
N 1s			1.0							
NRO	1			-0.36197	-0.58592	0.12419	-0.14672	-0.57306	0.39683	-0.05340
	2			0.04259	-0.21494	0.21598	-0.33497	-0.18684	-0.78926	-0.36782
	3			-0.36794	0.35719	-0.06182	-0.56261	0.24683	0.28936	-0.52156
	4			-0.01225	-0.14357	-0.96632	-0.04557	-0.13541	-0.14241	-0.06908
	5			0.85481	-0.10686	0.00155	-0.27691	-0.10672	0.33212	-0.24394
	6			0.02396	0.66104	0.00707	0.13058	-0.73484	-0.02642	-0.06831
	7			-0.01904	-0.11793	0.01671	0.67374	0.07783	0.06765	-0.72173

Table 40a. Sigma DLROs and occupation numbers for triplet HNO geometry J

		(O 1s)	(N 1s)	(O-hydr)	(O-sigma)	(O-lone)	(N-hydr)	(N-sigma)	(N-lone)	(H)
ETCGAO		2.000000	2.000000	1.396863	1.050127	1.996237	1.005325	0.929061	1.731114	0.892099
N	S	0.001314	0.940997	-0.003070	-0.122422	0.009726	0.204212	0.107226	0.300090	-0.165928
	S'	-0.002350	0.210301	0.006885	0.202593	0.000237	-0.485520	-0.286416	-0.834899	0.265770
	S''	-0.000461	0.000085	-0.003255	0.007822	-0.003101	0.024921	-0.007940	-0.000691	-0.023496
	X	-0.001417	-0.001796	-0.126126	0.053513	-0.049019	0.986632	0.227101	-0.474272	-0.126557
	X'	-0.000899	-0.003144	-0.018972	0.064871	-0.055272	-0.168144	0.042668	-0.123642	0.134836
	Y	0.0	0.0	0.0	0.0	0.0	0.0	0.0	0.0	0.0
	Y'	0.0	0.0	0.0	0.0	0.0	0.0	0.0	0.0	0.0
	Z	-0.004420	-0.001595	0.023703	0.202120	-0.065232	0.287762	-0.965185	0.090926	-0.030514
	Z'	-0.001765	0.001569	-0.001002	-0.037646	-0.110026	-0.172043	0.222955	0.029796	0.103258
O	S	0.918538	0.009412	0.023102	0.186781	0.333087	-0.009632	-0.124528	-0.038619	0.014015
	S'	0.292978	0.002260	-0.051363	-0.410375	-0.817413	0.012835	0.196125	0.063590	-0.016354
	S''	-0.000120	-0.000612	-0.000901	-0.007745	-0.000896	0.001300	0.011807	0.000702	-0.001333
	X	0.000095	0.000014	1.023802	-0.047173	-0.034482	-0.077366	-0.007454	0.069878	-0.035771
	X'	0.000105	0.000600	-0.010422	-0.078414	0.006072	-0.027365	0.073270	0.037683	-0.009186
	Y	0.0	0.0	0.0	0.0	0.0	0.0	0.0	0.0	0.0
	Y'	0.0	0.0	0.0	0.0	0.0	0.0	0.0	0.0	0.0
	Z	0.000573	0.008839	0.012291	1.011554	-0.374680	0.006983	-0.127325	-0.058166	-0.006107
	Z'	-0.002619	0.000792	-0.012226	-0.205212	-0.071324	0.002695	0.138543	0.039290	-0.029509
H	S	0.001311	0.006749	0.009920	-0.064724	0.128883	-0.366922	-0.072892	0.096524	1.060865
	S'	-0.001429	-0.000727	-0.008682	0.050056	-0.084669	-0.075716	0.059709	-0.101558	0.201231

Table 40b. Transformation from sigma NROs to sigma DLROs for triplet HNO geometry J

		(O 1s)	(N 1s)	(O-hydr)	(O-sigma)	(O-lone)	(N-hydr)	(N-sigma)	(N-lone)	(H)
O 1s		1.0								
N 1s			1.0							
NRO	1			0.57894	0.39759	-0.09180	0.22413	0.53067	-0.40600	0.04055
	2			-0.02396	0.22333	-0.18993	0.44622	0.13540	0.69664	0.45905
	3			0.25594	-0.52886	0.13505	0.47283	-0.33591	-0.31690	0.44692
	4			0.01206	0.15306	0.96794	0.03158	0.12992	0.13998	0.04520
	5			-0.76805	0.16084	-0.00463	0.24318	0.25290	-0.44714	0.24734
	6			-0.04580	-0.68036	-0.00465	-0.03849	0.70634	0.16240	-0.09069
	7			0.08127	0.01296	-0.01736	-0.68226	0.00639	-0.05943	0.71864

Table 41a. Sigma DLROs and occupation numbers for triplet HNO geometry K

		(O 1s)	(N 1s)	(O-hydr)	(O-sigma)	(O-lone)	(N-hydr)	(N-sigma)	(N-lone)	(H)
ETCGAO		2.000000	2.000000	1.516968	0.989863	1.994833	1.059946	1.022021	1.547518	0.869825
N	S	0.001644	0.956115	-0.001513	-0.137499	0.002130	0.243888	0.222529	0.187368	-0.179140
	S'	-0.003537	0.152340	0.008083	0.243871	0.006330	-0.619298	-0.652632	-0.566314	0.318239
	S''	-0.000400	-0.000106	-0.006832	0.004604	-0.000501	0.039160	-0.008259	0.003718	-0.042209
	X	-0.002045	-0.003922	-0.155981	0.030837	-0.062682	0.794954	0.126788	-0.754299	-0.086500
	X'	-0.001004	-0.002139	-0.037595	0.018578	-0.062291	-0.115751	0.029399	-0.101771	0.070789
	Y	0.0	0.0	0.0	0.0	0.0	0.0	0.0	0.0	0.0
	Y'	0.0	0.0	0.0	0.0	0.0	0.0	0.0	0.0	0.0
	Z	-0.006707	-0.005423	0.003366	0.174691	-0.134257	0.537041	-0.754923	0.322206	-0.128118
	Z'	-0.003505	0.000270	-0.001896	-0.101107	-0.165048	-0.233790	0.328155	-0.106572	0.086589
O	S	0.928532	0.005551	0.004444	0.160673	0.295679	0.015114	-0.107519	-0.005578	-0.000420
	S'	0.253287	-0.000595	-0.010593	-0.385791	-0.791746	-0.026710	0.174147	0.008317	0.002995
	S''	-0.000602	-0.000421	-0.000285	-0.009902	-0.000928	-0.002874	0.012454	-0.001565	-0.000007
	X	0.000393	-0.000236	1.037820	0.021167	-0.005871	-0.087334	0.000985	0.115016	-0.015634
	X'	0.000753	0.000943	-0.003160	-0.102796	0.017252	-0.047221	0.091358	0.037940	-0.004486
	Y	0.0	0.0	0.0	0.0	0.0	0.0	0.0	0.0	0.0
	Y'	0.0	0.0	0.0	0.0	0.0	0.0	0.0	0.0	0.0
	Z	0.000797	0.007948	-0.045611	1.005308	-0.386828	0.021852	-0.133667	-0.006177	-0.006785
	Z'	-0.003235	0.000983	0.002963	-0.249390	-0.078411	-0.035413	0.169761	-0.007566	-0.002785
H	S	0.003830	0.002996	0.034860	-0.007486	0.181942	-0.353006	-0.048372	0.090445	1.121204
	S'	-0.000858	-0.001279	-0.008147	0.013044	-0.080845	-0.076753	0.037016	-0.088686	0.170402

Table 41b. Transformation from sigma NROs to sigma DLROs for triplet HNO geometry K

		(O 1s)	(N 1s)	(O-hydr)	(O-sigma)	(O-lone)	(N-hydr)	(N-sigma)	(N-lone)	(H)
O 1s		1.0								
N 1s			1.0							
NBO	1			0.64674	0.37491	-0.09976	0.18433	0.37149	-0.50737	-0.04267
	2			-0.05459	0.16225	-0.19683	0.55476	0.33294	0.49040	0.52235
	3			0.33052	-0.53659	0.19188	0.39936	-0.46317	-0.23791	0.36795
	4			-0.01316	0.17785	0.95582	0.03530	0.20753	0.08712	0.05199
	5			-0.67804	0.11537	-0.00796	0.23690	0.07763	-0.65146	0.20083
	6			-0.05559	-0.68616	0.00250	0.13136	0.64232	-0.03443	-0.30833
	7			0.08065	-0.17152	-0.02882	-0.65126	0.27377	-0.11095	0.67219

Table 42a. Sigma DLROs and occupation numbers for triplet HNO geometry L

		(O 1s)	(N 1s)	(O-hydr)	(O-sigma)	(O-lone)	(N-hydr)	(N-sigma)	(N-lone)	(H)
ETCGAO		2.000000	2.000000	1.567934	0.925736	1.993474	1.175614	1.097433	1.431108	0.809894
N	S	0.000011	0.997728	0.000008	-0.031504	-0.000035	-0.030431	-0.049621	0.000209	-0.051553
	S'	0.001765	0.052918	0.001265	-0.243699	-0.019976	0.792856	0.692842	-0.009637	-0.332021
	S''	-0.000290	-0.000073	-0.000112	-0.002626	0.002468	0.062217	-0.010133	-0.000329	-0.075905
	X	-0.000057	0.000036	-0.154523	0.008050	0.000066	0.004068	0.007477	1.047713	-0.001164
	X'	-0.000011	0.000003	-0.045715	0.025252	0.000931	0.013251	-0.025236	-0.005519	-0.007674
	Y	0.0	0.0	0.0	0.0	0.0	0.0	0.0	0.0	0.0
	Y'	0.0	0.0	0.0	0.0	0.0	0.0	0.0	0.0	0.0
	Z	-0.008381	-0.005340	-0.000416	0.125816	-0.260665	0.707785	-0.663895	0.000225	-0.188917
	Z'	-0.004300	-0.001628	0.003403	-0.150871	-0.258710	-0.337421	0.394401	-0.003528	0.074752
O	S	0.996548	-0.000278	0.000070	-0.026525	-0.092366	0.005447	-0.019645	0.000116	-0.003067
	S'	-0.070820	-0.001490	-0.001423	-0.340079	-0.721909	-0.044268	0.158628	0.002261	0.033191
	S''	-0.000120	-0.000134	-0.000066	-0.001469	0.000041	-0.001409	0.000542	0.000090	0.000794
	X	0.000035	0.000035	1.042522	-0.011385	0.001107	-0.001770	0.001286	-0.148140	0.000856
	X'	0.000217	-0.000006	-0.017926	0.003181	0.000023	0.002066	-0.003583	-0.051293	-0.001951
	Y	0.0	0.0	0.0	0.0	0.0	0.0	0.0	0.0	0.0
	Y'	0.0	0.0	0.0	0.0	0.0	0.0	0.0	0.0	0.0
	Z	0.000119	0.004343	0.004247	0.993003	-0.381393	0.052864	-0.131498	-0.003730	-0.023093
	Z'	-0.002545	0.001132	-0.002769	-0.303130	-0.075183	-0.038733	0.186445	0.002471	-0.002499
H	S	0.005835	0.004325	-0.001012	0.036205	0.285483	-0.253470	-0.019202	0.004298	1.126329
	S'	-0.001487	-0.001161	0.000992	-0.006141	-0.085713	-0.130731	0.042628	-0.000051	0.234826

Table 42b. Transformation from sigma NROs to sigma DLROs for triplet HNO geometry L

		(O 1s)	(N 1s)	(O-hydr)	(O-sigma)	(O-lone)	(N-hydr)	(N-sigma)	(N-lone)	(H)
O 1s		1.0								
N 1s			1.0							
NRO	1			-0.54006	0.45162	-0.17365	-0.11615	0.44606	-0.47504	-0.18998
	2			-0.00232	0.07157	-0.19497	0.74578	0.27752	-0.00731	0.56885
	3			-0.53041	-0.46636	0.17986	0.11065	-0.46614	-0.44874	0.19473
	4			0.00110	0.18263	0.94777	0.08763	0.23558	-0.00309	0.07201
	5			-0.65344	0.00793	-0.00027	0.00206	0.00723	0.75690	-0.00027
	6			-0.00274	-0.69986	0.00643	0.14986	0.57987	-0.00112	-0.38914
	7			0.00103	-0.22405	-0.03423	-0.62284	0.33900	0.00192	0.66766

Table 43a. Pi DLROs and occupation numbers for singlet HNO geometry A

		(O-pi)	(N-pi)
ETCGAO		1.344109	0.662902
N	S	0.0	0.0
	S'	0.0	0.0
	S''	0.0	0.0
	X	0.0	0.0
	X'	0.0	0.0
	Y	-0.126629	0.780302
	Y'	0.016833	-0.087186
	Z	0.0	0.0
	Z'	0.0	0.0
O	S	0.0	0.0
	S'	0.0	0.0
	S''	0.0	0.0
	X	0.0	0.0
	X'	0.0	0.0
	Y	0.966118	0.123013
	Y'	-0.293623	0.390976
	Z	0.0	0.0
	Z'	0.0	0.0
H	S	0.0	0.0
	S'	0.0	0.0

Table 43b. Transformation from pi NROs to pi DLROS for singlet HNO geometry A

		(O-pi)	(N-pi)
NRO	1	0.82435	0.56608
	2	-0.56608	0.82435

Table 44a. Pi DLROs and occupation numbers for singlet HNO geometry B

		(O-pi)	(N-pi)
ETCGAO		1.562642	0.987059
N	S	0.0	0.0
	S'	0.0	0.0
	S''	0.0	0.0
	X	0.0	0.0
	X'	0.0	0.0
	Y	-0.134005	0.846489
	Y'	-0.019943	0.081455
	Z	0.0	0.0
	Z'	0.0	0.0
O	S	0.0	0.0
	S'	0.0	0.0
	S''	0.0	0.0
	X	0.0	0.0
	X'	0.0	0.0
	Y	0.989215	0.058852
	Y'	-0.167157	0.323277
	Z	0.0	0.0
	Z'	0.0	0.0
H	S	0.0	0.0
	S'	0.0	0.0

Table 44b. Transformation from pi NROs to pi DLROS for singlet HNO geometry B

		(O-pi)	(N-pi)
NRO	1	0.84410	0.53619
	2	-0.53619	0.84410

Table 45a. Pi DLROs and occupation numbers for singlet HNO geometry C

		(O-pi)	(N-pi)
ETCGAO		1.381637	0.626073
N	S	0.0	0.0
	S'	0.0	0.0
	S''	0.0	0.0
	X	0.0	0.0
	X'	0.0	0.0
	Y	-0.132268	0.807238
	Y'	0.019344	-0.066728
	Z	0.0	0.0
	Z'	0.0	0.0
O	S	0.0	0.0
	S'	0.0	0.0
	S''	0.0	0.0
	X	0.0	0.0
	X'	0.0	0.0
	Y	0.979412	0.096795
	Y'	-0.202151	0.369274
	Z	0.0	0.0
	Z'	0.0	0.0
H	S	0.0	0.0
	S'	0.0	0.0

Table 45b. Transformation from pi NROs to pi DLROS for singlet HNO geometry C

		(O-pi)	(N-pi)
NRO	1	0.83602	0.54870
	2	-0.54870	0.83602

Table 46a. Pi DLROs and occupation numbers for singlet HNO geometry D

		(O-pi)	(N-pi)
ETCGAO		1.371662	0.636026
N	S	0.0	0.0
	S'	0.0	0.0
	S''	0.0	0.0
	X	0.0	0.0
	X'	0.0	0.0
	Y	-0.132851	0.818809
	Y'	0.019816	-0.059012
	Z	0.0	0.0
	Z'	0.0	0.0
O	S	0.0	0.0
	S'	0.0	0.0
	S''	0.0	0.0
	X	0.0	0.0
	X'	0.0	0.0
	Y	0.980834	0.089650
	Y'	-0.199957	0.352740
	Z	0.0	0.0
	Z'	0.0	0.0
H	S	0.0	0.0
	S'	0.0	0.0

Table 46b. Transformation from pi NROs to pi DLROS for singlet HNO geometry D

		(O-pi)	(N-pi)
NRO	1	0.83322	0.55295
	2	-0.55295	0.83322

Table 47a. Pi DLROs and occupation numbers for singlet HNO geometry E

		(O-pi)	(N-pi)
ETCGAO		1.358226	0.654100
N	S	0.0	0.0
	S'	0.0	0.0
	S''	0.0	0.0
	X	0.0	0.0
	X'	0.0	0.0
	Y	-0.128287	0.877910
	Y'	0.026875	-0.068089
	Z	0.0	0.0
	Z'	0.0	0.0
O	S	0.0	0.0
	S'	0.0	0.0
	S''	0.0	0.0
	X	0.0	0.0
	X'	0.0	0.0
	Y	0.990257	0.039163
	Y'	-0.163996	0.273078
	Z	0.0	0.0
	Z'	0.0	0.0
H	S	0.0	0.0
	S'	0.0	0.0

Table 47b. Transformation from pi NROs to pi DLROS for singlet HNO geometry E

		(O-pi)	(N-pi)
NRO	1	0.83003	0.55772
	2	-0.55772	0.83003

Table 48a. Pi DLROs and occupation numbers for singlet HNO geometry F

		(O-pi)	(N-pi)
ETCGAO		1.234449	0.778021
N	S	0.0	0.0
	S'	0.0	0.0
	S''	0.0	0.0
	X	0.0	0.0
	X'	0.0	0.0
	Y	-0.119544	0.903872
	Y'	0.034057	-0.063283
	Z	0.0	0.0
	Z'	0.0	0.0
O	S	0.0	0.0
	S'	0.0	0.0
	S''	0.0	0.0
	X	0.0	0.0
	X'	0.0	0.0
	Y	0.986205	0.021227
	Y'	-0.188177	0.231719
	Z	0.0	0.0
	Z'	0.0	0.0
H	S	0.0	0.0
	S'	0.0	0.0

Table 48b. Transformation from pi NBOs to pi DLROS for singlet HNO geometry F

		(O-pi)	(N-pi)
NBO	1	0.79069	0.61222
	2	-0.61222	0.79069

Table 49a. Pi DLROs and occupation numbers for singlet HNO geometry M

		(O-pi)	(N-pi)
ETCGAO		1.191327	0.824323
N	S	0.0	0.0
	S'	0.0	0.0
	S''	0.0	0.0
	X	0.0	0.0
	X'	0.0	0.0
	Y	-0.112726	0.947210
	Y'	0.040412	-0.056189
	Z	0.0	0.0
	Z'	0.0	0.0
O	S	0.0	0.0
	S'	0.0	0.0
	S''	0.0	0.0
	X	0.0	0.0
	X'	0.0	0.0
	Y	0.994929	-0.029268
	Y'	-0.131380	0.158081
	Z	0.0	0.0
	Z'	0.0	0.0
H	S	0.0	0.0
	S'	0.0	0.0

Table 49b. Transformation from pi NROs to pi DLROS for singlet HNO geometry M

		(O-pi)	(N-pi)
NRO	1	0.77610	0.63061
	2	-0.63061	0.77610

Table 50a. Pi DLROs and occupation numbers for singlet HNO geometry G

		(O-pi)	(N-pi)
ETCGAO		1.143175	0.870545
N	S	0.0	0.0
	S'	0.0	0.0
	S''	0.0	0.0
	X	0.0	0.0
	X'	0.0	0.0
	Y	-0.106812	0.966971
	Y'	0.055422	-0.072454
	Z	0.0	0.0
	Z'	0.0	0.0
O	S	0.0	0.0
	S'	0.0	0.0
	S''	0.0	0.0
	X	0.0	0.0
	X'	0.0	0.0
	Y	0.995377	-0.056749
	Y'	-0.106796	0.117910
	Z	0.0	0.0
	Z'	0.0	0.0
H	S	0.0	0.0
	S'	0.0	0.0

Table 50b. Transformation from pi NROs to pi DLROS for singlet HNO geometry G

		(O-pi)	(N-pi)
NRO	1	0.75936	0.65067
	2	-0.65067	0.75936

Table 51a. Pi DLROs and occupation numbers for singlet HNO geometry H

		(O-pi)	(N-pi)
ETCGAO		1.080223	0.929907
N	S	0.0	0.0
	S'	0.0	0.0
	S''	0.0	0.0
	X	0.0	0.0
	X'	0.0	0.0
	Y	-0.108537	0.977815
	Y'	0.057241	-0.065334
	Z	0.0	0.0
	Z'	0.0	0.0
O	S	0.0	0.0
	S'	0.0	0.0
	S''	0.0	0.0
	X	0.0	0.0
	X'	0.0	0.0
	Y	0.997046	-0.072187
	Y'	-0.097450	0.096614
	Z	0.0	0.0
	Z'	0.0	0.0
H	S	0.0	0.0
	S'	0.0	0.0

Table 51b. Transformation from pi NROs to pi DLROS for singlet HNO geometry H

		(O-pi)	(N-pi)
NRO	1	0.73632	0.67664
	2	-0.67664	0.73632

Table 52a. Pi DLROs and occupation numbers for singlet HNO geometry I

		(O-pi)	(N-pi)
ETCGAO		1.069396	0.938194
N	S	0.0	0.0
	S'	0.0	0.0
	S''	0.0	0.0
	X	0.0	0.0
	X'	0.0	0.0
	Y	-0.110597	0.982219
	Y'	0.056106	-0.065989
	Z	0.0	0.0
	Z'	0.0	0.0
O	S	0.0	0.0
	S'	0.0	0.0
	S''	0.0	0.0
	X	0.0	0.0
	X'	0.0	0.0
	Y	0.998284	-0.078638
	Y'	-0.098022	0.088160
	Z	0.0	0.0
	Z'	0.0	0.0
H	S	0.0	0.0
	S'	0.0	0.0

Table 52b. Transformation from pi NROs to pi DLROS for singlet HNO geometry I

		(O-pi)	(N-pi)
NRO	1	0.73257	0.68069
	2	-0.68069	0.73257

Table 53a. Pi DLROs and occupation numbers for singlet HNO geometry J

		(O-pi)	(N-pi)
ETCGAO		1.061724	0.948586
N	S	0.0	0.0
	S'	0.0	0.0
	S''	0.0	0.0
	X	0.0	0.0
	X'	0.0	0.0
	Y	-0.117939	0.981852
	Y'	0.046647	-0.061072
	Z	0.0	0.0
	Z'	0.0	0.0
O	S	0.0	0.0
	S'	0.0	0.0
	S''	0.0	0.0
	X	0.0	0.0
	X'	0.0	0.0
	Y	1.000952	-0.078174
	Y'	-0.112347	0.092294
	Z	0.0	0.0
	Z'	0.0	0.0
H	S	0.0	0.0
	S'	0.0	0.0

Table 53b. Transformation from pi NROs to pi DLROS for singlet HNO geometry J

		(O-pi)	(N-pi)
NRO	1	0.72906	0.68445
	2	-0.68445	0.72906

Table 54a. Pi DLROs and occupation numbers for singlet HNO geometry K

		(O-pi)	(N-pi)
ETCGAO		1.065244	0.942346
N	S	0.0	0.0
	S'	0.0	0.0
	S''	0.0	0.0
	X	0.0	0.0
	X'	0.0	0.0
	Y	-0.121385	0.984807
	Y'	0.042966	-0.064756
	Z	0.0	0.0
	Z'	0.0	0.0
O	S	0.0	0.0
	S'	0.0	0.0
	S''	0.0	0.0
	X	0.0	0.0
	X'	0.0	0.0
	Y	1.002403	-0.081527
	Y'	-0.119596	0.088359
	Z	0.0	0.0
	Z'	0.0	0.0
H	S	0.0	0.0
	S'	0.0	0.0

Table 54b. Transformation from pi NROs to pi DLROS for singlet HNO geometry K

		(O-pi)	(N-pi)
NRO	1	0.73099	0.68239
	2	-0.68239	0.73099

Table 55a. Pi DLROs and occupation numbers for singlet HNO geometry L

		(O-pi)	(N-pi)
ETCGAO		1.076366	0.955694
N	S	0.0	0.0
	S'	0.0	0.0
	S''	0.0	0.0
	X	0.0	0.0
	X'	0.0	0.0
	Y	-0.125018	0.986359
	Y'	0.039318	-0.096407
	Z	0.0	0.0
	Z'	0.0	0.0
O	S	0.0	0.0
	S'	0.0	0.0
	S''	0.0	0.0
	X	0.0	0.0
	X'	0.0	0.0
	Y	1.005014	-0.082608
	Y'	-0.132042	0.081375
	Z	0.0	0.0
	Z'	0.0	0.0
H	S	0.0	0.0
	S'	0.0	0.0

Table 55b. Transformation from pi NROs to pi DLROS for singlet HNO geometry L

		(O-pi)	(N-pi)
NRO	1	0.73089	0.68249
	2	-0.68249	0.73089

Table 56a. Pi DLROs and occupation numbers for triplet HNO geometry A

		(O-pi)	(N-pi)
ETCGAO		1.854408	1.144792
N	S	0.0	0.0
	S'	0.0	0.0
	S''	0.0	0.0
	X	0.0	0.0
	X'	0.0	0.0
	Y	-0.133346	1.040124
	Y'	-0.034080	-0.049850
	Z	0.0	0.0
	Z'	0.0	0.0
O	S	0.0	0.0
	S'	0.0	0.0
	S''	0.0	0.0
	X	0.0	0.0
	X'	0.0	0.0
	Y	1.035170	-0.134639
	Y'	0.002334	-0.058887
	Z	0.0	0.0
	Z'	0.0	0.0
H	S	0.0	0.0
	S'	0.0	0.0

Table 56b. Transformation from pi NROs to pi DLROS for triplet HNO geometry A

		(O-pi)	(N-pi)
NRO	1	0.92867	0.37092
	2	-0.37092	0.92867

Table 57a. Pi DLROs and occupation numbers for triplet HNO geometry B

		(O-pi)	(N-pi)
ETCGAO		1.858710	1.140490
N	S	0.0	0.0
	S'	0.0	0.0
	S''	0.0	0.0
	X	0.0	0.0
	X'	0.0	0.0
	Y	-0.123888	1.032362
	Y'	0.027066	0.027073
	Z	0.0	0.0
	Z'	0.0	0.0
O	S	0.0	0.0
	S'	0.0	0.0
	S''	0.0	0.0
	X	0.0	0.0
	X'	0.0	0.0
	Y	1.030276	-0.121227
	Y'	0.061891	-0.046714
	Z	0.0	0.0
	Z'	0.0	0.0
H	S	0.0	0.0
	S'	0.0	0.0

Table 57b. Transformation from pi NBOs to pi DLROS for triplet HNO geometry B

		(O-pi)	(N-pi)
NRO	1	0.93111	0.36474
	2	-0.36474	0.93111

Table 58a. Pi DLROs and occupation numbers for triplet HNO geometry C

		(O-pi)	(N-pi)
ETCGAO		1.858954	1.140346
N	S	0.0	0.0
	S'	0.0	0.0
	S''	0.0	0.0
	X	0.0	0.0
	X'	0.0	0.0
	Y	-0.118511	1.029433
	Y'	-0.023571	-0.020441
	Z	0.0	0.0
	Z'	0.0	0.0
O	S	0.0	0.0
	S'	0.0	0.0
	S''	0.0	0.0
	X	0.0	0.0
	X'	0.0	0.0
	Y	1.027199	-0.116057
	Y'	0.057672	-0.041986
	Z	0.0	0.0
	Z'	0.0	0.0
H	S	0.0	0.0
	S'	0.0	0.0

Table 58b. Transformation from pi NROs to pi DLROS for triplet HNO geometry C

		(O-pi)	(N-pi)
NRO	1	0.93156	0.36359
	2	-0.36359	0.93156

Table 59a. Pi DLROs and occupation numbers for triplet HNO geometry D

		(O-pi)	(N-pi)
ETCGAO		1.850631	1.148769
N	S	0.0	0.0
	S'	0.0	0.0
	S''	0.0	0.0
	X	0.0	0.0
	X'	0.0	0.0
	Y	-0.114183	1.027145
	Y'	-0.019277	-0.018709
	Z	0.0	0.0
	Z'	0.0	0.0
O	S	0.0	0.0
	S'	0.0	0.0
	S''	0.0	0.0
	X	0.0	0.0
	X'	0.0	0.0
	Y	1.024481	-0.112553
	Y'	0.048522	-0.037540
	Z	0.0	0.0
	Z'	0.0	0.0
H	S	0.0	0.0
	S'	0.0	0.0

Table 59b. Transformation from pi NROs to pi DLROS for triplet HNO geometry D

		(O-pi)	(N-pi)
NRO	1	0.92760	0.37357
	2	-0.37357	0.92760

Table 60a. Pi DLROs and occupation numbers for triplet HNO geometry E

		(O-pi)	(N-pi)
ETCGAO		1.829185	1.170115
N	S	0.0	0.0
	S'	0.0	0.0
	S''	0.0	0.0
	X	0.0	0.0
	X'	0.0	0.0
	Y	-0.110349	1.024348
	Y'	-0.013334	-0.027367
	Z	0.0	0.0
	Z'	0.0	0.0
O	S	0.0	0.0
	S'	0.0	0.0
	S''	0.0	0.0
	X	0.0	0.0
	X'	0.0	0.0
	Y	1.021747	-0.109259
	Y'	0.031944	-0.031081
	Z	0.0	0.0
	Z'	0.0	0.0
H	S	0.0	0.0
	S'	0.0	0.0

Table 60b. Transformation from pi NROs to pi DLROS for triplet HNO geometry E

		(O-pi)	(N-pi)
NRO	1	0.91704	0.39880
	2	-0.39880	0.91704

Table 61a. Pi DLROs and occupation numbers for triplet HNO geometry F

		(O-pi)	(N-pi)
ETCGAO		1.779394	1.219806
N	S	0.0	0.0
	S'	0.0	0.0
	S''	0.0	0.0
	X	0.0	0.0
	X'	0.0	0.0
	Y	-0.111776	1.024836
	Y'	-0.013652	-0.019883
	Z	0.0	0.0
	Z'	0.0	0.0
O	S	0.0	0.0
	S'	0.0	0.0
	S''	0.0	0.0
	X	0.0	0.0
	X'	0.0	0.0
	Y	1.021616	-0.111147
	Y'	-0.001915	-0.026781
	Z	0.0	0.0
	Z'	0.0	0.0
H	S	0.0	0.0
	S'	0.0	0.0

Table 61b. Transformation from pi NROs to pi DLROS for triplet HNO geometry F

		(O-pi)	(N-pi)
NRO	1	0.89063	0.45473
	2	-0.45473	0.89063

Table 62a. Pi DLROs and occupation numbers for triplet HNO geometry M

		(O-pi)	(N-pi)
ETCGAO		1.741254	1.257946
N	S	0.0	0.0
	S'	0.0	0.0
	S''	0.0	0.0
	X	0.0	0.0
	X'	0.0	0.0
	Y	-0.117887	1.025503
	Y'	-0.020626	0.016292
	Z	0.0	0.0
	Z'	0.0	0.0
O	S	0.0	0.0
	S'	0.0	0.0
	S''	0.0	0.0
	X	0.0	0.0
	X'	0.0	0.0
	Y	1.024033	-0.113068
	Y'	0.008571	-0.022811
	Z	0.0	0.0
	Z'	0.0	0.0
H	S	0.0	0.0
	S'	0.0	0.0

Table 62b. Transformation from pi NROs to pi DLROS for triplet HNO geometry M

		(O-pi)	(N-pi)
NRO	1	0.86879	0.49517
	2	-0.49517	0.86879

Table 63a. Pi DLROs and occupation numbers for triplet HNO geometry G

		(O-pi)	(N-pi)
ETCGAO		1.718129	1.281071
N	S	0.0	0.0
	S'	0.0	0.0
	S''	0.0	0.0
	X	0.0	0.0
	X'	0.0	0.0
	Y	-0.119717	1.026704
	Y'	-0.022538	0.022588
	Z	0.0	0.0
	Z'	0.0	0.0
O	S	0.0	0.0
	S'	0.0	0.0
	S''	0.0	0.0
	X	0.0	0.0
	X'	0.0	0.0
	Y	1.024828	-0.115095
	Y'	0.001823	-0.023743
	Z	0.0	0.0
	Z'	0.0	0.0
H	S	0.0	0.0
	S'	0.0	0.0

Table 63b. Transformation from pi NROs to pi DLROS for triplet HNO geometry G

		(O-pi)	(N-pi)
NRO	1	0.85539	0.51799
	2	-0.51799	0.85539

Table 64a. Pi DLROs and occupation numbers for triplet HNO geometry H

		(O-pi)	(N-pi)
ETCGAO		1.697119	1.302281
N	S	0.0	0.0
	S'	0.0	0.0
	S''	0.0	0.0
	X	0.0	0.0
	X'	0.0	0.0
	Y	-0.120191	1.027507
	Y'	-0.025867	0.042770
	Z	0.0	0.0
	Z'	0.0	0.0
O	S	0.0	0.0
	S'	0.0	0.0
	S''	0.0	0.0
	X	0.0	0.0
	X'	0.0	0.0
	Y	1.025273	-0.115970
	Y'	0.004644	-0.025170
	Z	0.0	0.0
	Z'	0.0	0.0
H	S	0.0	0.0
	S'	0.0	0.0

Table 64b. Transformation from pi NROs to pi DLROS for triplet HNO geometry H

		(O-pi)	(N-pi)
NRO	1	0.84297	0.53796
	2	-0.53796	0.84297

Table 65a. Pi DLROs and occupation numbers for triplet HNO geometry I

		(O-pi)	(N-pi)
ETCGAO		1.672102	1.327299
N	S	0.0	0.0
	S'	0.0	0.0
	S''	0.0	0.0
	X	0.0	0.0
	X'	0.0	0.0
	Y	-0.122586	1.029597
	Y'	-0.029099	0.050211
	Z	0.0	0.0
	Z'	0.0	0.0
O	S	0.0	0.0
	S'	0.0	0.0
	S''	0.0	0.0
	X	0.0	0.0
	X'	0.0	0.0
	Y	1.026702	-0.119561
	Y'	0.004285	-0.029127
	Z	0.0	0.0
	Z'	0.0	0.0
H	S	0.0	0.0
	S'	0.0	0.0

Table 65b. Transformation from pi NROs to pi DLROS for triplet HNO geometry I

		(O-pi)	(N-pi)
NRO	1	0.82785	0.56095
	2	-0.56095	0.82785

Table 66a. Pi DLROs and occupation numbers for triplet HNO geometry J

		(O-pi)	(N-pi)
ETCGAO		1.620786	1.378414
N	S	0.0	0.0
	S'	0.0	0.0
	S''	0.0	0.0
	X	0.0	0.0
	X'	0.0	0.0
	Y	-0.132860	1.035907
	Y'	-0.036158	0.046090
	Z	0.0	0.0
	Z'	0.0	0.0
O	S	0.0	0.0
	S'	0.0	0.0
	S''	0.0	0.0
	X	0.0	0.0
	X'	0.0	0.0
	Y	1.032085	-0.130880
	Y'	0.004607	-0.038268
	Z	0.0	0.0
	Z'	0.0	0.0
H	S	0.0	0.0
	S'	0.0	0.0

Table 66b. Transformation from pi NROs to pi DLROS for triplet HNO geometry J

		(O-pi)	(N-pi)
NRO	1	0.79440	0.60740
	2	-0.60740	0.79440

Table 67a. Pi DLROs and occupation numbers for triplet HNO geometry K

		(O-pi)	(N-pi)
ETCGAO		1.575590	1.423511
N	S	0.0	0.0
	S'	0.0	0.0
	S''	0.0	0.0
	X	0.0	0.0
	X'	0.0	0.0
	Y	-0.149625	1.046624
	Y'	-0.048813	0.036722
	Z	0.0	0.0
	Z'	0.0	0.0
O	S	0.0	0.0
	S'	0.0	0.0
	S''	0.0	0.0
	X	0.0	0.0
	X'	0.0	0.0
	Y	1.041528	-0.148239
	Y'	0.000100	-0.051768
	Z	0.0	0.0
	Z'	0.0	0.0
H	S	0.0	0.0
	S'	0.0	0.0

Table 67b. Transformation from pi NROs to pi DLROS for triplet HNO geometry K

		(O-pi)	(N-pi)
NRO	1	0.76246	0.64703
	2	-0.64703	0.76246

Table 68a. Pi DLROs and occupation numbers for triplet HNO geometry L

		(O-pi)	(N-pi)
ETCGAO		1.568300	1.430600
N	S	0.0	0.0
	S'	0.0	0.0
	S''	0.0	0.0
	X	0.0	0.0
	X'	0.0	0.0
	Y	-0.153048	1.047707
	Y'	-0.046559	-0.003976
	Z	0.0	0.0
	Z'	0.0	0.0
O	S	0.0	0.0
	S'	0.0	0.0
	S''	0.0	0.0
	X	0.0	0.0
	X'	0.0	0.0
	Y	1.042431	-0.149624
	Y'	-0.018949	-0.049983
	Z	0.0	0.0
	Z'	0.0	0.0
H	S	0.0	0.0
	S'	0.0	0.0

Table 68b. Transformation from pi NROs to pi DLROS for triplet HNO geometry L

		(O-pi)	(N-pi)
NRO	1	0.75725	0.65313
	2	-0.65313	0.75725

V. THE ISOMERIZATION OF HNO: INTERPRETATION

A. Contour Plots of DLRO's

We start by discussing the directed localized reaction orbitals, because these are the orbitals by which we can visualize the participation of the atoms in the bonding. The numerical expansions have been given in Tables 17 to 68. The character of these orbitals is best recognized by the contour diagrams which are displayed in Figures 7 to 10.

In these figures, each column shows the various DLRO's in the molecule for one geometry as indicated at the top. Each row shows how one particular orbital changes as the hydrogen moves along the reaction path described in Section IVB. The contours of the sigma orbitals are drawn in the plane containing the molecule, those of the pi orbitals in a plane perpendicular to the molecule. Positive contours are given by solid lines, negative contours by dashed lines, and nodes by dotted lines. The maximum contour has the value 0.96 $\text{bohr}^{-3/2}$, the minimum contour is -0.96 $\text{bohr}^{-3/2}$, and the increment is 0.08 $\text{bohr}^{-3/2}$. Superimposed on the contour plots are straight lines connecting the nuclei indicating chemical bonds in the usual manner.

Each of the Figures 7 to 10 is divided into two parts, a and b. The "a" part includes all those geometries with the H bonded to oxygen (points A, B, C, D, E, F, M), starting with the linear HON molecule on the left and ending with the midpoint of the isomerization on the

Figure 7a. Contours of DLRO's for the singlet state NO bonds for geometries A to M

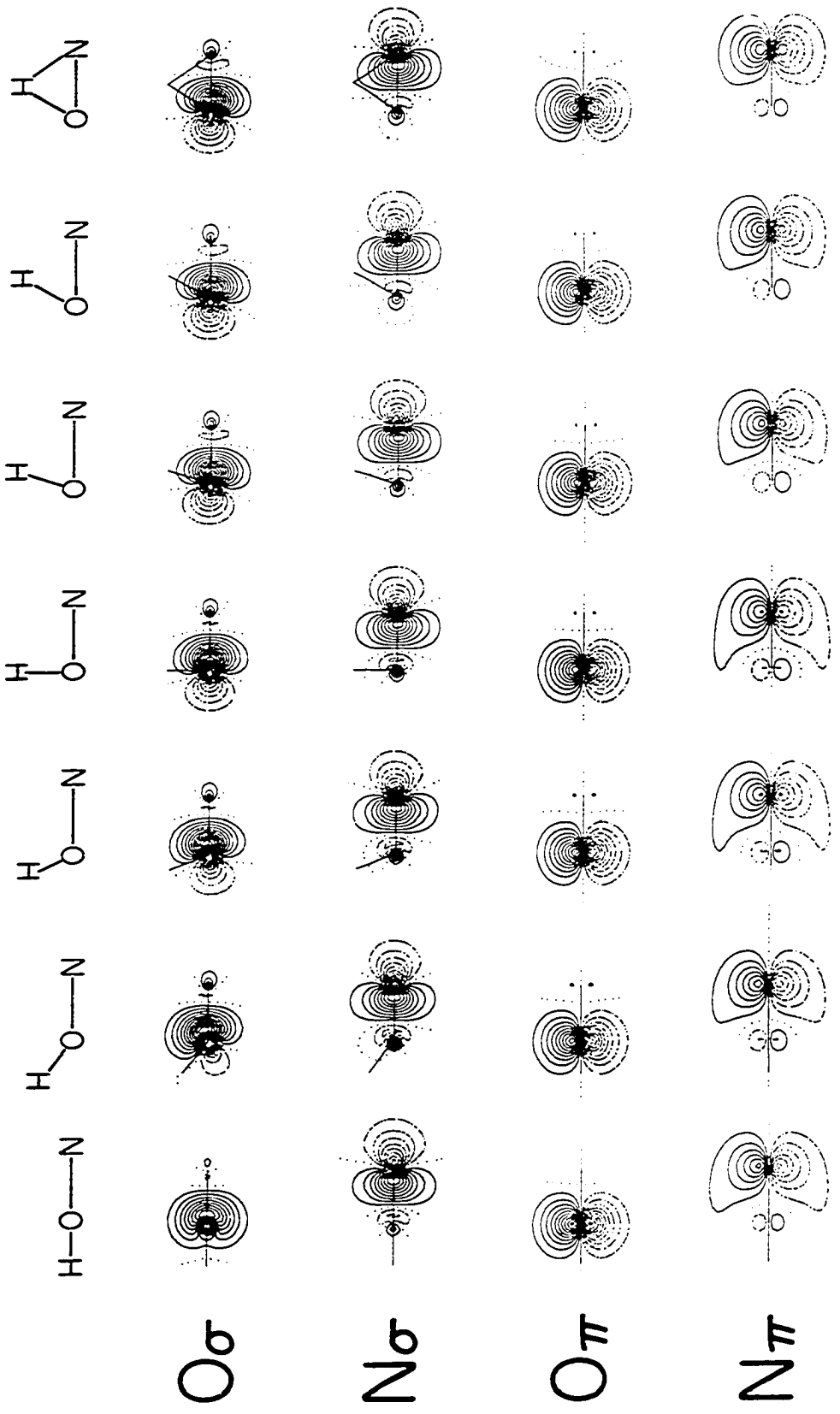
O σ
N σ
O π
N π

Figure 7b. Contours of DLRO's for the singlet state NO bonds for geometries M to L

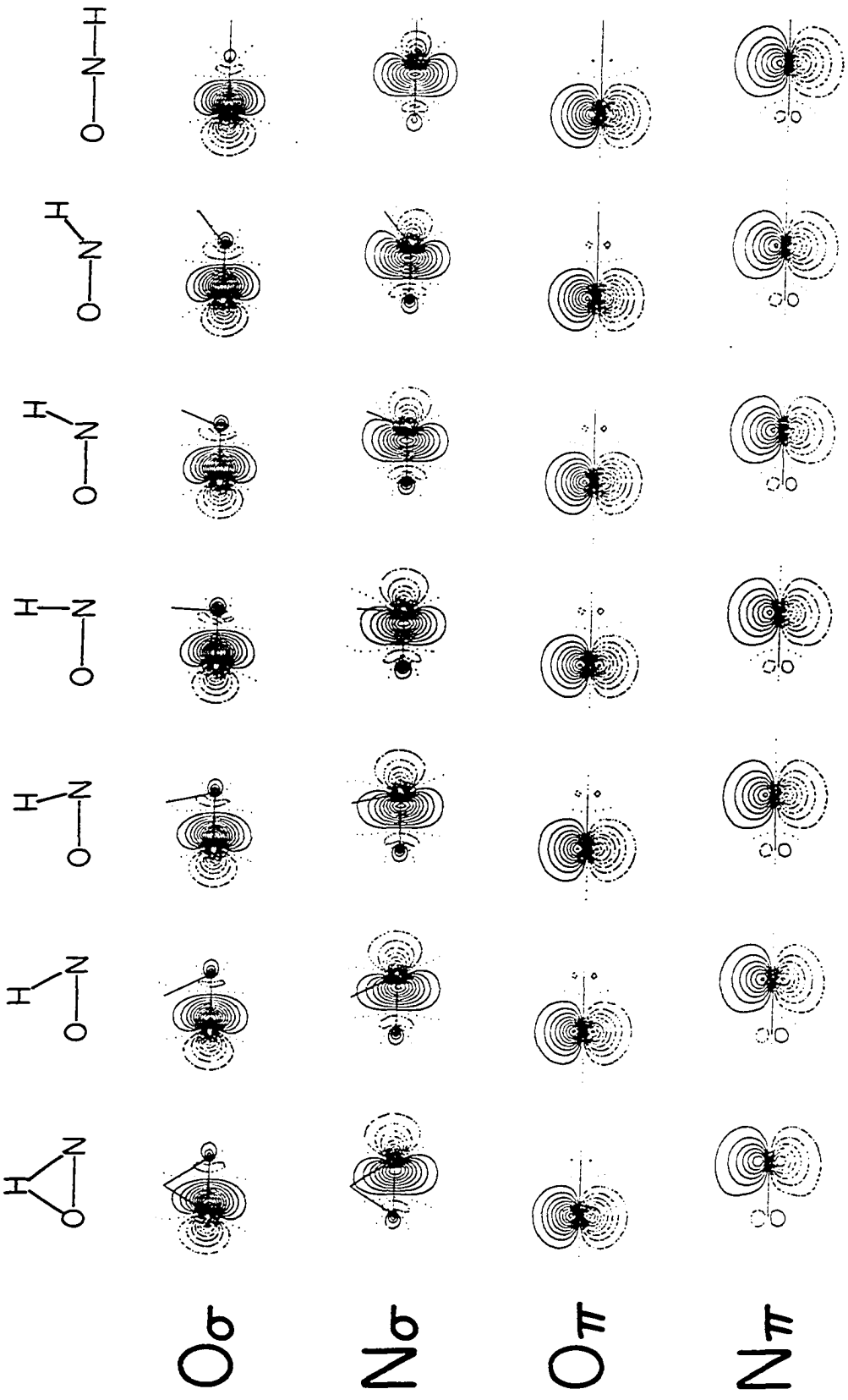
O 6b
N 6b
O 1π
N 1π

Figure 8a. Contours of DLRO's for the triplet state NO bonds for geometries A to M

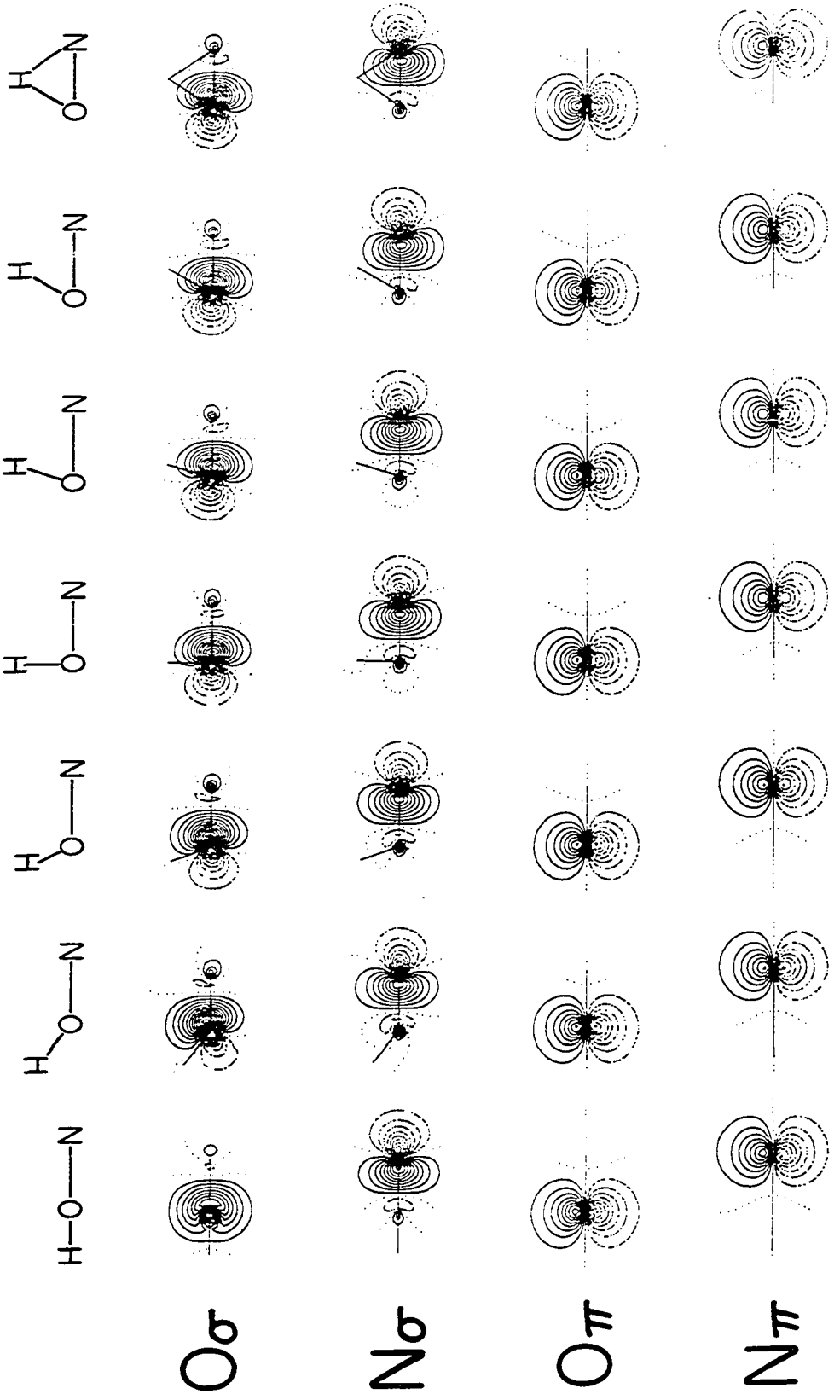
O σ
N σ
O π
N π

Figure 8b. Contours of DLRO's for the triplet state NO bonds for geometries M to L

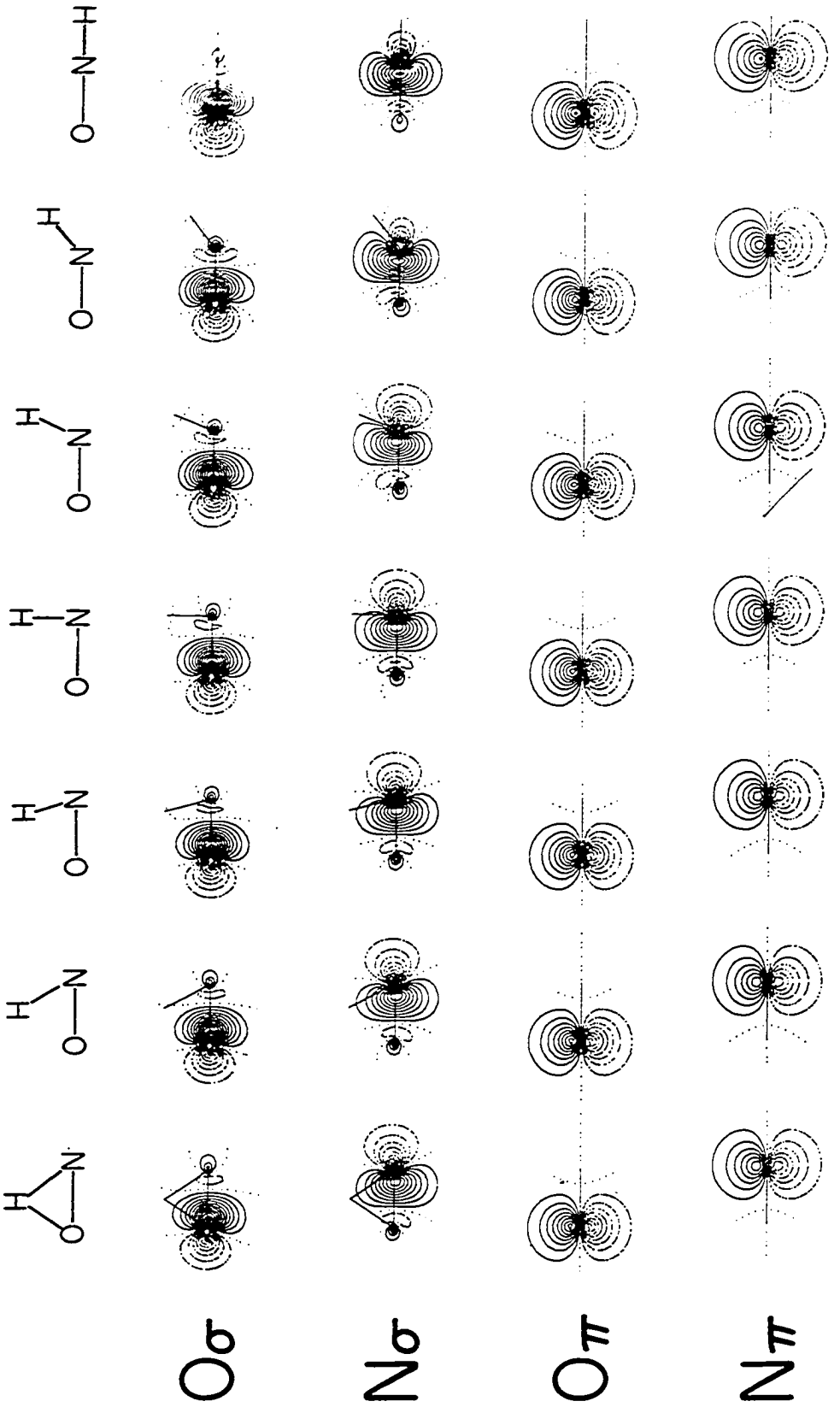
O σ
N σ
O π
N π

Figure 9a. Contours of DLRO's for the singlet state lone pairs and bonds to hydrogen for geometries A to M

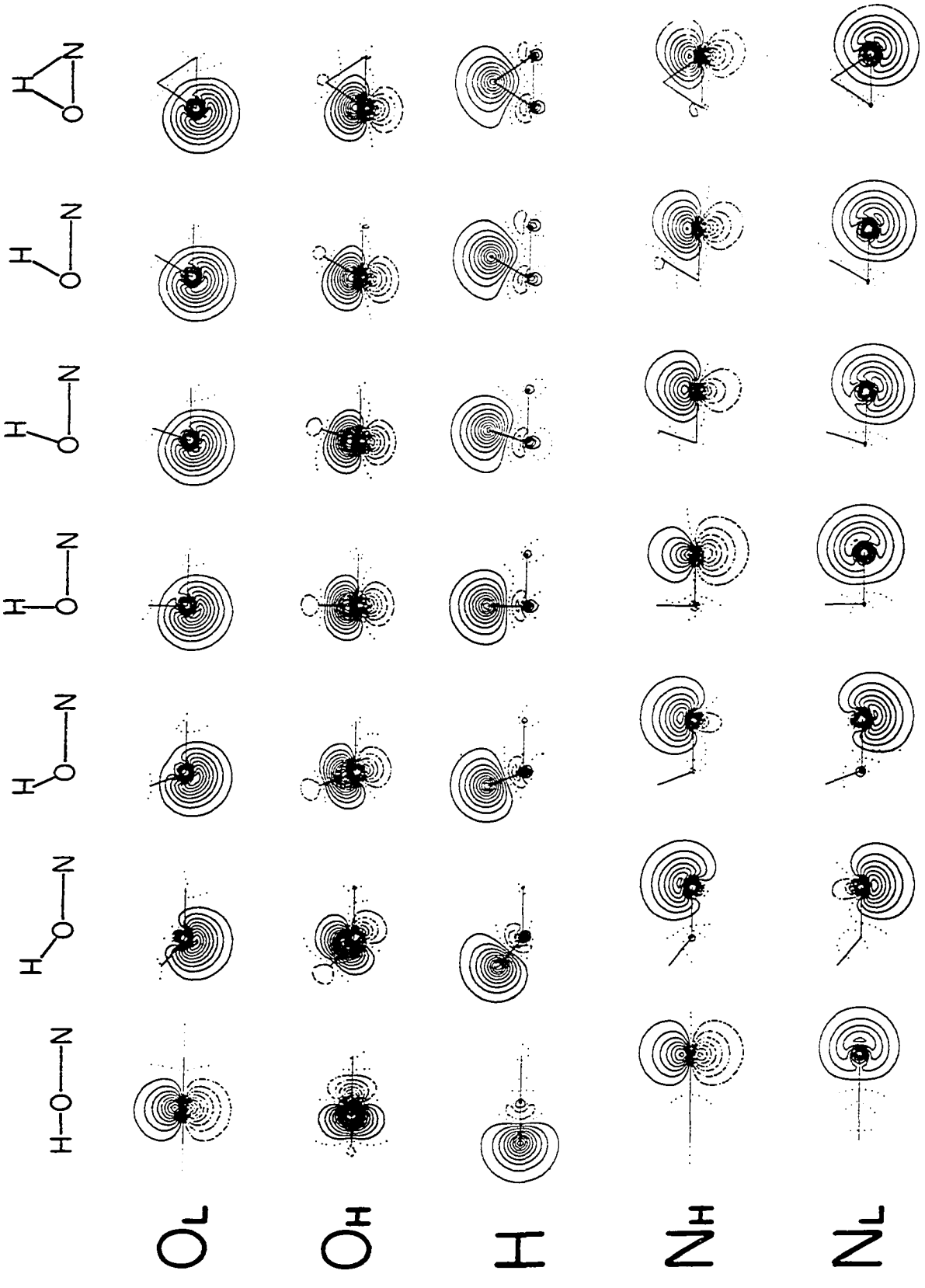
1a'
2a'
3a'
4a'
5a'
6a'
7a'

Figure 9b. Contours of DLRO's for the singlet state lone pairs and bonds to hydrogen for geometries M to L

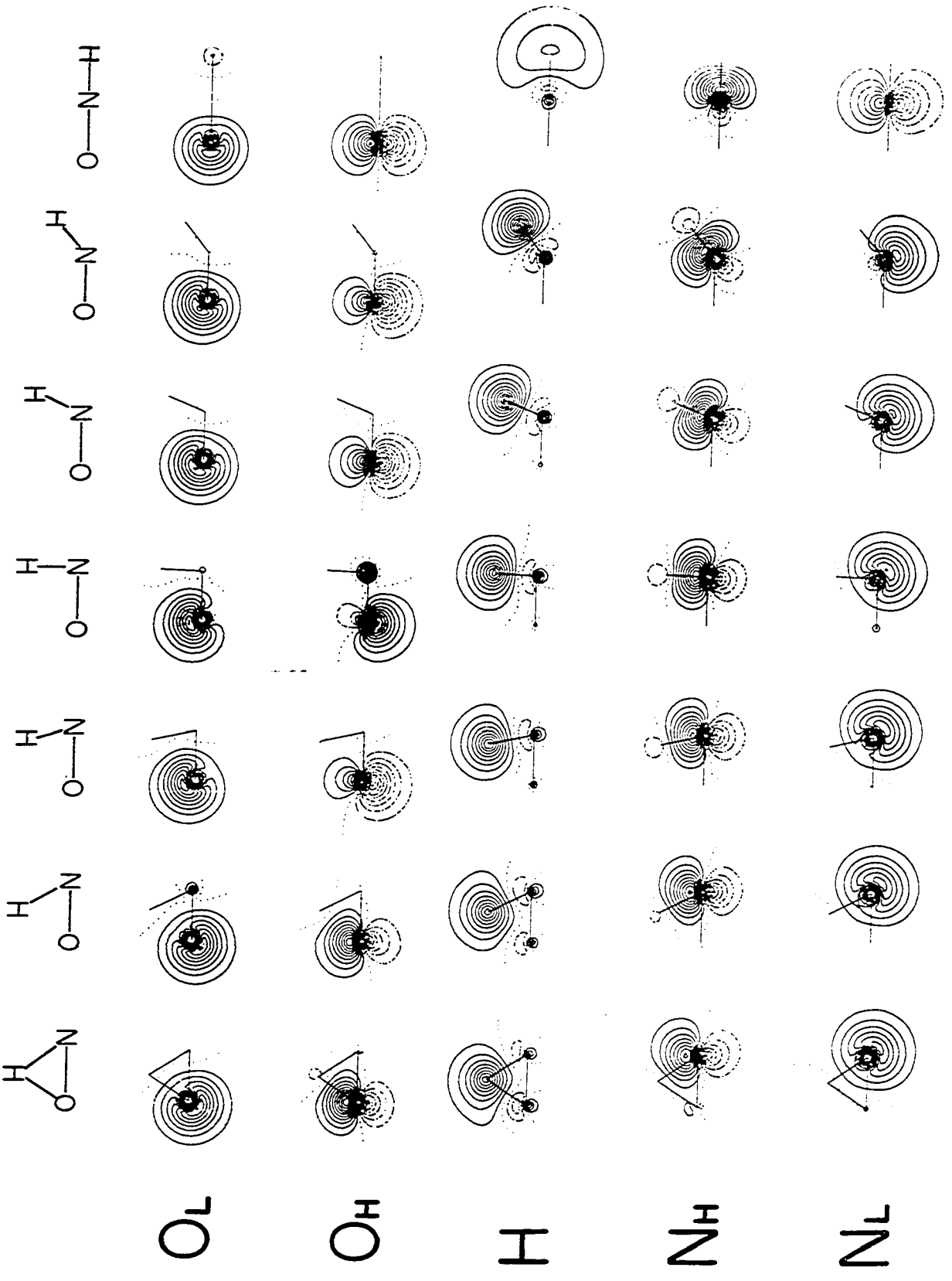
H
N
O
1a'
2a'
1a"
2a"

Figure 10a. Contours of DLRO's for the triplet state lone pairs and bonds to hydrogen for geometries A to M

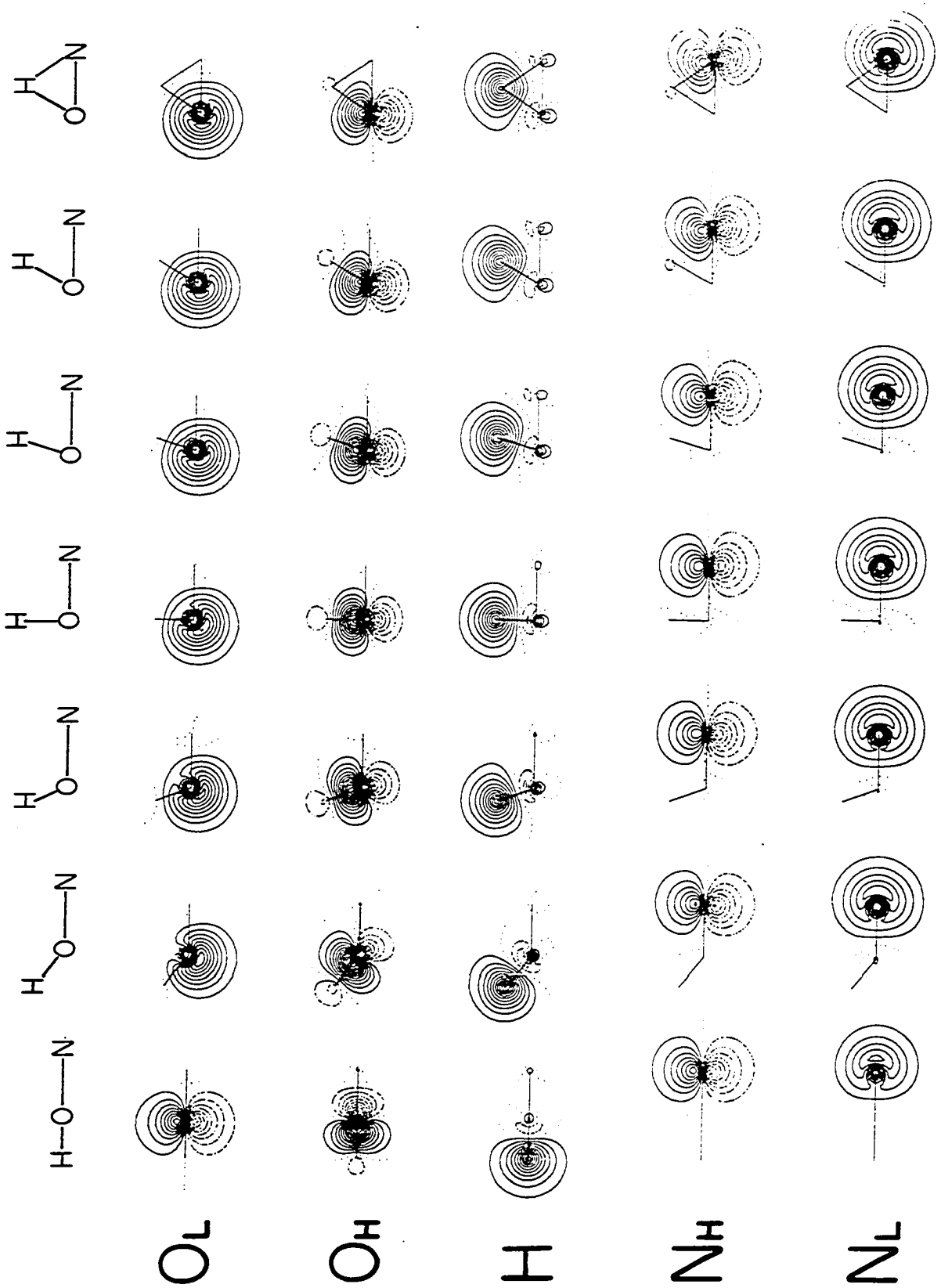
N
H
O
O
H
N
H
O
H
N
H
O
H
N
H
O
H
N
H
O
H
N
H
O
H
N
O
H
O
H
H
N
N

Figure 10b. Contours of DLRO's for the triplet state lone pairs and bonds to hydrogen for geometries M to L

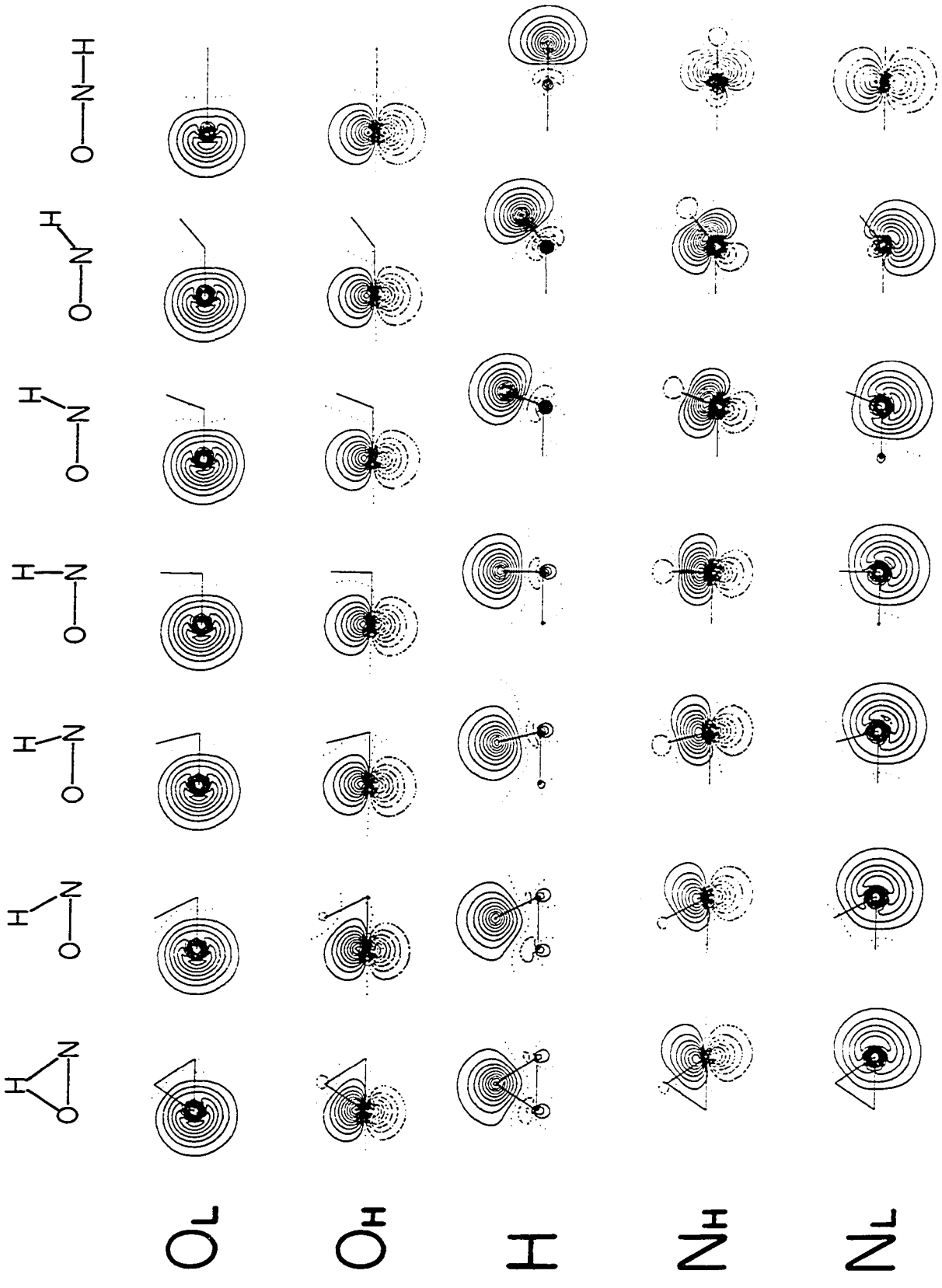
H
N
O
O
H
N
H
N
O
H
N
O
H
N
O
H
N
O
H
N
O
O
H
N
O

right. The "b" part begins with the middle geometry (point M) on the left and proceeds through points G, H, I, J and K to end with point L, the linear HNO molecule, on the right.

Figures 7 and 8 show the orbitals on oxygen and nitrogen which establish the N-O bond, Figure 7 for the singlet and Figure 8 for the triplet. The orbitals denoted by O_σ and N_σ establish the sigma bond; the orbitals denoted by O_π and N_π establish the pi bond.

The remaining five sigma DLRO's which form lone pairs and are involved in bonding to the hydrogen are shown in Figures 9 and 10, Figure 9 giving the singlet and Figure 10 giving the triplet. The lone pairs are denoted by O_L and N_L; the orbitals denoted by N_H and O_H always point more or less toward the H. They form a bond with hydrogen if the latter is on their side of the molecule; if not, they are nonbonding. Figure 11 gives a schematic picture summarizing the orbital changes which occur for these five orbitals in the singlet isomerization. The corresponding picture for the triplet state looks very similar.

B. Bond Orders and Populations

An examination of the orbital shapes is not sufficient for providing a full understanding of the role played by the orbitals. We must also take into account how the orbital occupations and bond orders change during the isomerization process.

The spinless first-order density matrix $\rho(x, x')$ can be expressed

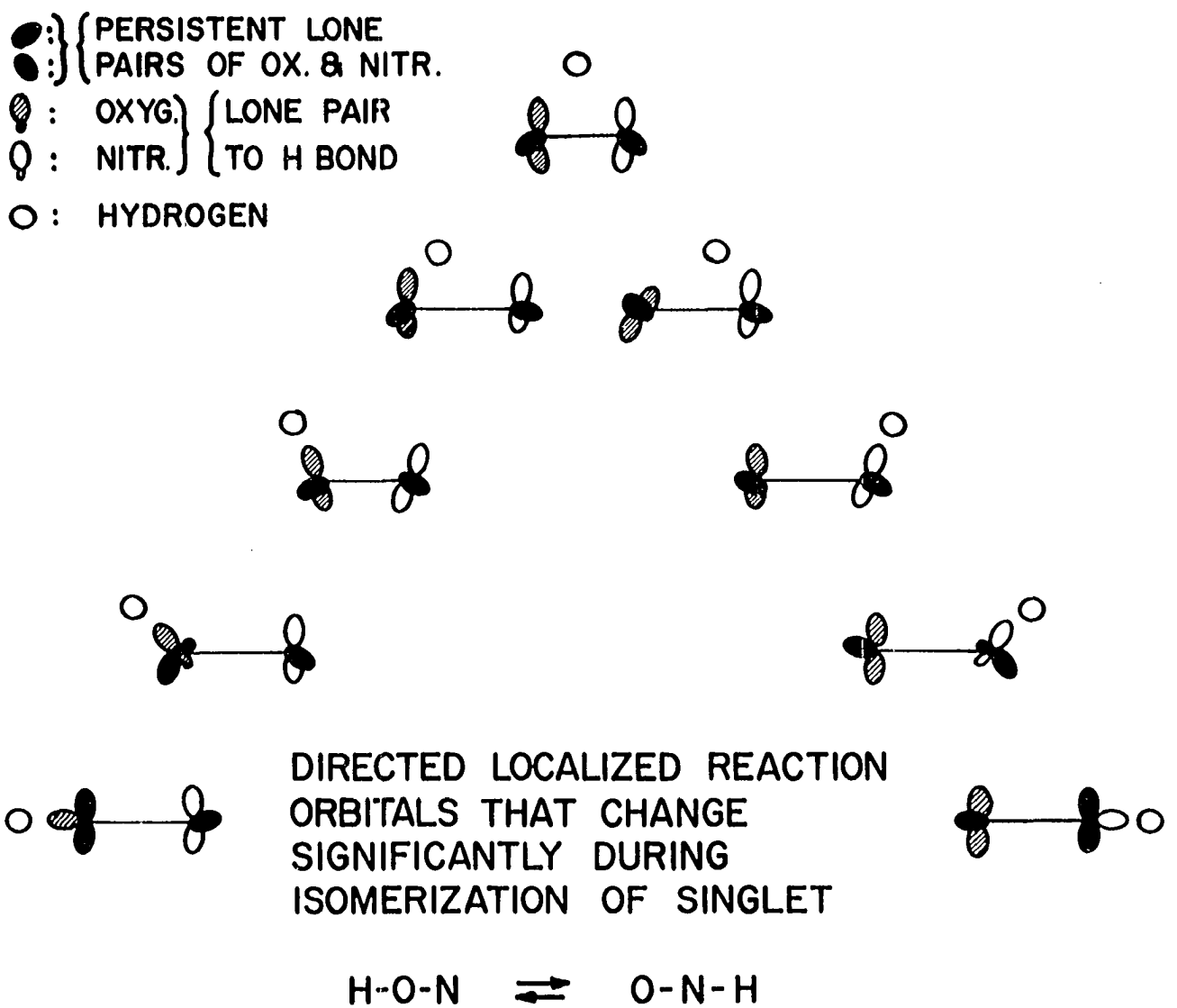

Figure 11. Schematic summary of bonding changes in DLRO's plotted in Figure 9 for points A, C, E, F, M, G, H, J, L

in terms of the DLRO's (χ_i). In the resulting expansion,

$$\rho(x, x') = \sum_{ij} p_{ij} \chi_i(x) \chi_j(x) \tag{5.1}$$

the off-diagonal terms vanish upon integration because of the orbital orthogonality. They represent therefore interference terms, whereas the diagonal terms contain the orbital occupation numbers. Consequently the diagonal coefficients p_{ii} are the orbital occupation numbers. The off-diagonal coefficients p_{ij} play the roles of bond orders. Care has been taken to choose the phases of the DLRO's such that positive bond orders correspond to bonding interactions and negative bond orders to an antibonding interaction. The entire matrix p_{ij} is usually called the bond order matrix. For the singlet the bond order matrices are given in Tables 69-81. For the triplet they are given in Tables 82-94.

The orbital occupation numbers p_{ii} are furthermore plotted against the hydrogen path length in Figures 12 and 13 for the singlet and the triplet. Both of these figures are divided into five sections, three of them corresponding to the total atomic populations, one of them giving the O orbital populations, the other the N orbital populations. The dashed lines on the total atomic population portions give the neutral atom populations. The filled dots correspond to the stable and metastable points.

Table 69a. Bond order matrix between sigma DLROs for singlet HNO geometry A

	(O-hydr)	(O-sigma)	(O-lone)	(N-hydr)	(N-sigma)	(N-lone)	(H)
O-hydr	1.11939						
O-sigma	0.16622	1.51653					
O-lone	0.0	0.0	1.99788				
N-hydr	-0.00000	-0.00000	0.00181	1.99642			
N-sigma	-0.40746	0.77364	-0.00000	0.0	0.66222		
N-lone	-0.07779	0.00224	0.00000	0.0	-0.00284	1.98335	
H	0.86624	0.25634	0.0	0.00000	-0.24955	0.09261	0.71701

Table 69b. Bond order matrix between pi DLROs for singlet HNO geometry A

	(O-pi)	(N-pi)
O-pi	1.34411	
N-pi	0.88523	0.66290

Table 70a. Bond order matrix between sigma DLROs for singlet HNO geometry B

	(O-hydr)	(O-sigma)	(O-lone)	(N-hydr)	(N-sigma)	(N-lone)	(H)
O-hydr	1.14529						
O-sigma	0.16085	1.29177					
O-lone	0.00010	-0.00008	1.99735				
N-hydr	0.01922	0.00777	-0.00065	1.99103			
N-sigma	-0.14480	0.90813	0.00417	-0.00002	0.75309		
N-lone	-0.11505	0.01372	0.00185	-0.00000	-0.00264	1.97620	
H	0.93720	0.07108	0.00309	-0.02316	-0.16886	0.13198	0.83342

Table 70b. Bond order matrix between pi DLROs for singlet HNO geometry B

	(O-pi)	(N-pi)
O-pi	1.56264	
N-pi	0.61295	0.98706

Table 71a. Bond order matrix between sigma DLROs for singlet HNO geometry C

	(O-hydr)	(O-sigma)	(O-lone)	(N-hydr)	(N-sigma)	(N-lone)	(H)
O-hydr	1.13312						
O-sigma	0.10469	1.19320					
O-lone	0.00009	-0.00010	1.99704				
N-hydr	0.03365	0.00453	-0.00047	1.99394			
N-sigma	-0.05340	0.94034	0.00471	0.00006	0.82094		
N-lone	-0.07398	0.01323	0.00101	-0.00000	-0.00114	1.98661	
H	0.95647	0.02277	0.00333	-0.03706	-0.10450	0.08288	0.86742

Table 71b. Bond order matrix between pi DLROs for singlet HNO geometry C

	(O-pi)	(N-pi)
O-pi	1.38164	
N-pi	0.87116	0.62607

Table 72a. Bond order matrix between sigma DLROs for singlet HNO geometry D

	(O-hydr)	(O-sigma)	(O-lone)	(N-hydr)	(N-sigma)	(N-lone)	(H)
O-hydr	1.15833						
O-sigma	0.06097	1.17141					
O-lone	0.00008	-0.00011	1.99676				
N-hydr	-0.01443	-0.00083	-0.00099	1.99673			
N-sigma	-0.02307	0.94501	0.00530	-0.00004	0.83654		
N-lone	-0.04744	0.01283	0.00029	0.00000	-0.00074	1.98828	
H	0.95554	0.00983	0.00413	0.02211	-0.05982	0.05755	0.84435

Table 72b. Bond order matrix between pi DLROs for singlet HNO geometry D

	(O-pi)	(N-pi)
O-pi	1.37166	
N-pi	0.87239	0.63603

Table 73a. Bond order matrix between sigma DLROs for singlet HNO geometry E

	(O-hydr)	(O-sigma)	(O-lone)	(N-hydr)	(N-sigma)	(N-lone)	(H)
O-hydr	1.23891						
O-sigma	-0.00333	1.11633					
O-lone	0.00004	-0.00015	1.99632				
N-hydr	-0.20543	0.00208	-0.00178	1.92697			
N-sigma	0.00373	0.94898	0.00733	0.00001	0.89026		
N-lone	0.00342	0.01130	0.00093	-0.00000	-0.00045	1.98999	
H	0.91504	0.00429	0.00420	0.27232	0.00491	-0.00545	0.82883

Table 73b. Bond order matrix between pi DLROs for singlet HNO geometry E

	(O-pi)	(N-pi)
O-pi	1.35823	
N-pi	0.86255	0.65410

Table 74a. Bond order matrix between sigma DLROs for singlet HNO geometry F

	(O-hydr)	(O-sigma)	(O-lone)	(N-hydr)	(N-sigma)	(N-lone)	(H)
O-hydr	1.50593						
O-sigma	-0.04496	1.07829					
O-lone	-0.00001	-0.00022	1.99598				
N-hydr	-0.37663	0.00938	-0.00204	1.64994			
N-sigma	0.00128	0.94747	0.00906	-0.04603	0.92760		
N-lone	-0.00043	0.01164	0.00081	-0.00002	-0.00044	1.99051	
H	0.73191	0.03818	0.00323	0.61401	0.03652	0.00065	0.83923

Table 74b. Bond order matrix between pi DLROs for singlet HNO geometry F

	(O-pi)	(N-pi)
O-pi	1.23445	
N-pi	0.88243	0.77802

Table 75a. Bond order matrix between sigma DLROs for singlet HNO geometry M

	(O-hydr)	(O-sigma)	(O-lone)	(N-hydr)	(N-sigma)	(N-lone)	(H)
O-hydr	1.64185						
O-sigma	-0.06118	1.06130					
O-lone	-0.00002	-0.00024	1.99582				
N-hydr	-0.38158	0.00866	-0.00282	1.49583			
N-sigma	0.04390	0.95087	0.00899	-0.02536	0.94837		
N-lone	-0.00120	0.01074	0.00108	-0.00001	-0.00040	1.98996	
H	0.61507	-0.00162	0.00289	0.73368	0.04009	0.00246	0.85119

Table 75b. Bond order matrix between pi DLROs for singlet HNO geometry M

	(O-pi)	(N-pi)
O-pi	1.19133	
N-pi	0.87760	0.82432

Table 76a. Bond order matrix between sigma DLROs for singlet HNO geometry G

	(O-hydr)	(O-sigma)	(O-lone)	(N-hydr)	(N-sigma)	(N-lone)	(H)
O-hydr	1.88316						
O-sigma	-0.00038	1.10074					
O-lone	0.0	-0.00021	1.99595				
N-hydr	0.26555	0.00404	-0.00348	1.22510			
N-sigma	-0.00382	-0.95253	-0.00912	0.00415	0.90519		
N-lone	0.00240	0.00843	0.00153	0.00005	0.00033	1.99019	
H	-0.34339	0.00621	0.00231	0.88984	-0.00884	0.00475	0.88594

Table 76b. Bond order matrix between pi DLROs for singlet HNO geometry G

	(O-pi)	(N-pi)
O-pi	1.14318	
N-pi	0.87893	0.87054

Table 77a. Bond order matrix between sigma DLROs for singlet HNO geometry H

	(O-hydr)	(O-sigma)	(O-lone)	(N-hydr)	(N-sigma)	(N-lone)	(H)
O-hydr	1.99666						
O-sigma	0.00007	1.06925					
O-lone	0.00000	-0.00035	1.99269				
N-hydr	-0.00030	0.00880	-0.04953	1.07818			
N-sigma	-0.00324	0.96048	0.01056	0.05190	0.93542		
N-lone	-0.00244	0.00664	-0.00011	0.00013	-0.00027	1.99068	
H	0.00796	-0.05190	0.05879	0.95316	0.00188	0.00559	0.92713

Table 77b. Bond order matrix between pi DLROs for singlet HNO geometry H

	(O-pi)	(N-pi)
O-pi	1.08022	
N-pi	0.88816	0.92991

Table 78a. Bond order matrix between sigma DLROs for singlet HNO geometry I

	(O-hydr)	(O-sigma)	(O-lone)	(N-hydr)	(N-sigma)	(N-lone)	(H)
O-hydr	1.99304						
O-sigma	-0.00009	1.07720					
O-lone	0.0	-0.00043	1.99673				
N-hydr	-0.06630	0.00662	0.01685	1.04599			
N-sigma	0.01110	0.96116	0.00468	0.08905	0.92649		
N-lone	0.00288	0.00533	0.00007	0.00009	-0.00021	1.99256	
H	0.06603	-0.08795	-0.01511	0.96455	0.00343	0.00305	0.96044

Table 78b. Bond order matrix between pi DLROs for singlet HNO geometry I

	(O-pi)	(N-pi)
O-pi	1.06940	
N-pi	0.89220	0.93819

Table 79a. Bond order matrix between sigma DLROs for singlet HNO geometry J

	(O-hydr)	(O-sigma)	(O-lone)	(N-hydr)	(N-sigma)	(N-lone)	(H)
O-hydr	1.96810						
O-sigma	0.00171	1.05010					
O-lone	-0.00000	0.00017	1.99613				
N-hydr	0.15719	0.00971	-0.00347	1.07679			
N-sigma	-0.02753	0.95880	-0.00671	0.13958	0.95178		
N-lone	-0.00405	0.00473	-0.00025	0.00008	-0.00018	1.99164	
H	-0.16305	-0.13901	0.00331	0.95269	-0.00692	0.00168	0.95510

Table 79b. Bond order matrix between pi DLROs for singlet HNO geometry J

	(O-pi)	(N-pi)
O-pi	1.06172	
N-pi	0.89546	0.94859

Table 80a. Bond order matrix between sigma DLROs for singlet HNO geometry K

	(O-hydr)	(O-sigma)	(O-lone)	(N-hydr)	(N-sigma)	(N-lone)	(H)
O-hydr	1.97408						
O-sigma	0.00217	1.01241					
O-lone	0.00000	-0.00030	1.99648				
N-hydr	0.13691	0.00225	0.00103	1.12124			
N-sigma	-0.03084	0.95116	0.00931	0.17477	0.98630		
N-lone	-0.00490	0.00605	-0.00123	0.00019	-0.00026	1.99287	
H	-0.14327	-0.17385	-0.00022	0.94213	-0.01744	0.00718	0.90906

Table 80b. Bond order matrix between pi DLROs for singlet HNO geometry K

	(O-pi)	(N-pi)
O-pi	1.06524	
N-pi	0.89249	0.94235

Table 81a. Bond order matrix between sigma DLROs for singlet HNO geometry L

	(O-hydr)	(O-sigma)	(O-lone)	(N-hydr)	(N-sigma)	(N-lone)	(H)
O-hydr	1.98600						
O-sigma	0.00000	0.93582					
O-lone	0.0	-0.00129	1.99329				
N-hydr	0.00014	-0.06201	-0.04406	1.19486			
N-sigma	-0.00005	0.93585	0.02009	0.25223	1.08161		
N-lone	0.01468	-0.00000	0.00001	-0.00000	0.00000	1.98150	
H	-0.00017	-0.23784	0.05147	0.92964	-0.01213	-0.00000	0.79487

Table 81b. Bond order matrix between pi DLROs for singlet HNO geometry L

	(O-pi)	(N-pi)
O-pi	1.07637	
N-pi	0.87990	0.95569

Table 82a. Bond order matrix between sigma DLROs for triplet HNO geometry A

	(O-hydr)	(O-sigma)	(O-lone)	(N-hydr)	(N-sigma)	(N-lone)	(H)
O-hydr	1.08199						
O-sigma	0.14906	1.58522					
O-lone	0.00000	-0.00000	1.83973				
N-hydr	-0.00001	-0.00001	0.35230	1.15947			
N-sigma	-0.48042	0.71084	0.00001	-0.00000	0.65281		
N-lone	-0.08656	-0.00445	-0.00000	0.0	-0.00340	1.98070	
H	0.83087	0.30747	0.00001	-0.00001	-0.27995	0.10082	0.70089

Table 82b. Bond order matrix between pi DLROs for singlet HNO geometry A

	(O-pi)	(N-pi)
O-pi	1.85441	
N-pi	0.33723	1.14479

Table 83a. Bond order matrix between sigma DLROs for triplet HNO geometry B

	(O-hydr)	(O-sigma)	(O-lone)	(N-hydr)	(N-sigma)	(N-lone)	(H)
O-hydr	1.14922						
O-sigma	0.17012	1.25403					
O-lone	0.00365	-0.00243	1.93165				
N-hydr	0.16969	0.07560	-0.22812	1.09982			
N-sigma	-0.13713	0.90417	0.05710	0.06254	0.77974		
N-lone	-0.04752	0.01349	-0.00205	0.00029	-0.00131	1.99082	
H	0.92416	0.04058	0.07433	0.03989	-0.18747	0.05563	0.79548

Table 83b. Bond order matrix between pi DLROs for singlet HNO geometry B

	(O-pi)	(N-pi)
O-pi	1.85871	
N-pi	0.33235	1.14049

Table 84a. Bond order matrix between sigma DLROs for triplet HNO geometry C

	(O-hydr)	(O-sigma)	(O-lone)	(N-hydr)	(N-sigma)	(N-lone)	(H)
O-hydr	1.11962						
O-sigma	0.09923	1.15727					
O-lone	0.00176	-0.00103	1.96745				
N-hydr	0.16174	0.03079	-0.15647	1.06598			
N-sigma	-0.04312	0.93799	0.02480	0.04192	0.85360		
N-lone	-0.03427	0.01092	-0.00069	0.00023	-0.00068	1.99287	
H	0.94359	0.00670	0.05070	0.08294	-0.10708	0.03952	0.84392

Table 84b. Bond order matrix between pi DLROs for singlet HNO geometry C

	(O-pi)	(N-pi)
O-pi	1.85895	
N-pi	0.33088	1.14035

Table 85a. Bond order matrix between sigma DLROs for triplet HNO geometry D

	(O-hydr)	(O-sigma)	(O-lone)	(N-hydr)	(N-sigma)	(N-lone)	(H)
O-hydr	1.11221						
O-sigma	0.04279	1.13308					
O-lone	0.00124	-0.00047	1.97810				
N-hydr	0.13722	0.00552	-0.12327	1.06415			
N-sigma	-0.01093	0.94322	0.01300	0.01291	0.87525		
N-lone	-0.03981	0.00994	-0.00069	0.00030	-0.00050	1.99253	
H	0.93937	0.00333	0.04574	0.14886	-0.04384	0.04661	0.84530

Table 85b. Bond order matrix between pi DLROs for singlet HNO geometry D

	(O-pi)	(N-pi)
O-pi	1.85063	
N-pi	0.33737	1.14877

Table 86a. Bond order matrix between sigma DLROs for triplet HNO geometry E

	(O-hydr)	(O-sigma)	(O-lone)	(N-hydr)	(N-sigma)	(N-lone)	(H)
O-hydr	1.13185						
O-sigma	-0.01076	1.12583					
O-lone	0.00113	-0.00009	1.98019				
N-hydr	0.09662	-0.01645	-0.11290	1.06791			
N-sigma	0.01278	0.93992	0.00460	-0.02949	0.88158		
N-lone	-0.06987	0.00847	-0.00110	0.00071	-0.00019	1.98741	
H	0.90094	0.00986	0.05515	0.28126	0.01817	0.08216	0.82590

Table 86b. Bond order matrix between pi DLROs for singlet HNO geometry E

	(O-pi)	(N-pi)
O-pi	1.82918	
N-pi	0.35346	1.17012

Table 87a. Bond order matrix between sigma DLROs for triplet HNO geometry F

	(O-hydr)	(O-sigma)	(O-lone)	(N-hydr)	(N-sigma)	(N-lone)	(H)
O-hydr	1.18295						
O-sigma	-0.05735	1.08463					
O-lone	0.00103	0.00028	1.98159				
N-hydr	0.05364	0.00589	-0.10910	1.01855			
N-sigma	-0.00236	0.94129	0.00427	-0.05403	0.92349		
N-lone	-0.13348	-0.00049	-0.00178	0.00247	0.00064	1.96694	
H	0.77546	0.04797	0.07285	0.51065	0.05145	0.14613	0.84266

Table 87b. Bond order matrix between pi DLROs for singlet HNO geometry F

	(O-pi)	(N-pi)
O-pi	1.77939	
N-pi	0.38644	1.21981

Table 88a. Bond order matrix between sigma DLROs for triplet HNO geometry M

	(O-hydr)	(O-sigma)	(O-lone)	(N-hydr)	(N-sigma)	(N-lone)	(H)
O-hydr	1.21786						
O-sigma	-0.04291	1.07433					
O-lone	0.00090	0.00022	1.98374				
N-hydr	0.06855	0.01425	-0.10338	0.99533			
N-sigma	-0.01504	0.94561	0.00526	-0.04874	0.93363		
N-lone	-0.16296	-0.00169	-0.00242	0.00398	0.00058	1.95151	
H	0.66604	0.05397	0.08150	0.63686	0.03276	0.16709	0.84444

Table 88b. Bond order matrix between pi DLROs for singlet HNO geometry M

	(O-pi)	(N-pi)
O-pi	1.74125	
N-pi	0.40801	1.25795

Table 89a. Bond order matrix between sigma DLROs for triplet HNO geometry G

	(O-hydr)	(O-sigma)	(O-lone)	(N-hydr)	(N-sigma)	(N-lone)	(H)
O-hydr	1.23778						
O-sigma	-0.02050	1.08295					
O-lone	0.00067	-0.00003	1.98783				
N-hydr	0.09891	0.01339	-0.08719	0.96021			
N-sigma	-0.01371	0.94715	0.00801	-0.02671	0.92522		
N-lone	-0.17929	0.00394	-0.00254	0.00518	-0.00010	1.93983	
H	0.53079	0.03326	0.07772	0.75076	0.01326	0.16335	0.86700

Table 89b. Bond order matrix between pi DLROs for singlet HNO geometry G

	(O-pi)	(N-pi)
O-pi	1.71813	
N-pi	0.41791	1.28107

Table 90a. Bond order matrix between sigma DLROs for triplet HNO geometry H

	(O-hydr)	(O-sigma)	(O-lone)	(N-hydr)	(N-sigma)	(N-lone)	(H)
O-hydr	1.25203						
O-sigma	0.01772	1.10300					
O-lone	0.00027	-0.00030	1.99469				
N-hydr	0.20493	-0.00688	-0.04233	0.95884			
N-sigma	0.03433	0.94556	0.01064	0.00961	0.90291		
N-lone	-0.21317	0.03067	-0.00287	0.00748	-0.00180	1.91314	
H	0.28447	-0.02748	0.04500	0.87057	-0.00017	0.15701	0.87598

Table 90b. Bond order matrix between pi DLROs for singlet HNO geometry H

	(O-pi)	(N-pi)
O-pi	1.69712	
N-pi	0.42509	1.30228

Table 91a. Bond order matrix between sigma DLROs for triplet HNO geometry I

	(O-hydr)	(O-sigma)	(O-lone)	(N-hydr)	(N-sigma)	(N-lone)	(H)
O-hydr	1.27837						
O-sigma	0.04836	1.08638					
O-lone	0.00013	-0.00039	1.99632				
N-hydr	0.23794	-0.03698	-0.02340	0.97993			
N-sigma	0.11946	0.93505	0.01201	0.05577	0.90438		
N-lone	-0.25976	0.08925	-0.00226	0.01196	-0.00767	1.86447	
H	0.16964	-0.10038	0.02500	0.89972	-0.00927	0.17516	0.89077

Table 91b. Bond order matrix between pi DLROs for singlet HNO geometry I

	(O-pi)	(N-pi)
O-pi	1.67210	
N-pi	0.43197	1.32730

Table 92a. Bond order matrix between sigma DLROs for triplet HNO geometry J

	(O-hydr)	(O-sigma)	(O-lone)	(N-hydr)	(N-sigma)	(N-lone)	(H)
O-hydr	1.39686						
O-sigma	0.05019	1.05013					
O-lone	0.00008	-0.00054	1.99624				
N-hydr	0.27626	-0.06809	-0.02295	1.00532			
N-sigma	0.22563	0.88373	0.01449	0.11010	0.92906		
N-lone	-0.29290	0.28663	-0.00121	0.04196	-0.10081	1.73111	
H	0.05424	-0.17146	0.02413	0.89575	-0.05427	0.22143	0.89210

Table 92b. Bond order matrix between pi DLROs for singlet HNO geometry J

	(O-pi)	(N-pi)
O-pi	1.62079	
N-pi	0.44613	1.37841

Table 93a. Bond order matrix between sigma DLROs for triplet HNO geometry K

	(O-hydr)	(O-sigma)	(O-lone)	(N-hydr)	(N-sigma)	(N-lone)	(H)
O-hydr	1.51697						
O-sigma	0.02467	0.98986					
O-lone	0.00005	-0.00099	1.99483				
N-hydr	0.26640	-0.06863	-0.03613	1.05995			
N-sigma	0.07321	0.93711	0.01765	0.17044	1.02202		
N-lone	-0.39924	-0.00921	-0.01050	0.01742	0.15411	1.54752	
H	-0.01142	-0.20418	0.04066	0.89397	0.01188	0.25202	0.86983

Table 93b. Bond order matrix between pi DLROs for singlet HNO geometry K

	(O-pi)	(N-pi)
O-pi	1.57559	
N-pi	0.46112	1.42351

Table 94a. Bond order matrix between sigma DLROs for triplet HNO geometry L

	(O-hydr)	(O-sigma)	(O-lone)	(N-hydr)	(N-sigma)	(N-lone)	(H)
O-hydr	1.56793						
O-sigma	0.00154	0.92574					
O-lone	0.00000	-0.00133	1.99347				
N-hydr	0.00330	-0.06901	-0.04331	1.17561			
N-sigma	0.00674	0.93341	0.02133	0.24877	1.09743		
N-lone	0.46379	-0.00639	0.00030	0.00111	-0.00527	1.43111	
H	-0.00355	-0.23231	0.04982	0.93219	-0.00384	-0.00320	0.80989

Table 94b. Bond order matrix between pi DLROs for singlet HNO geometry L

	(O-pi)	(N-pi)
O-pi	1.56830	
N-pi	0.46377	1.43060

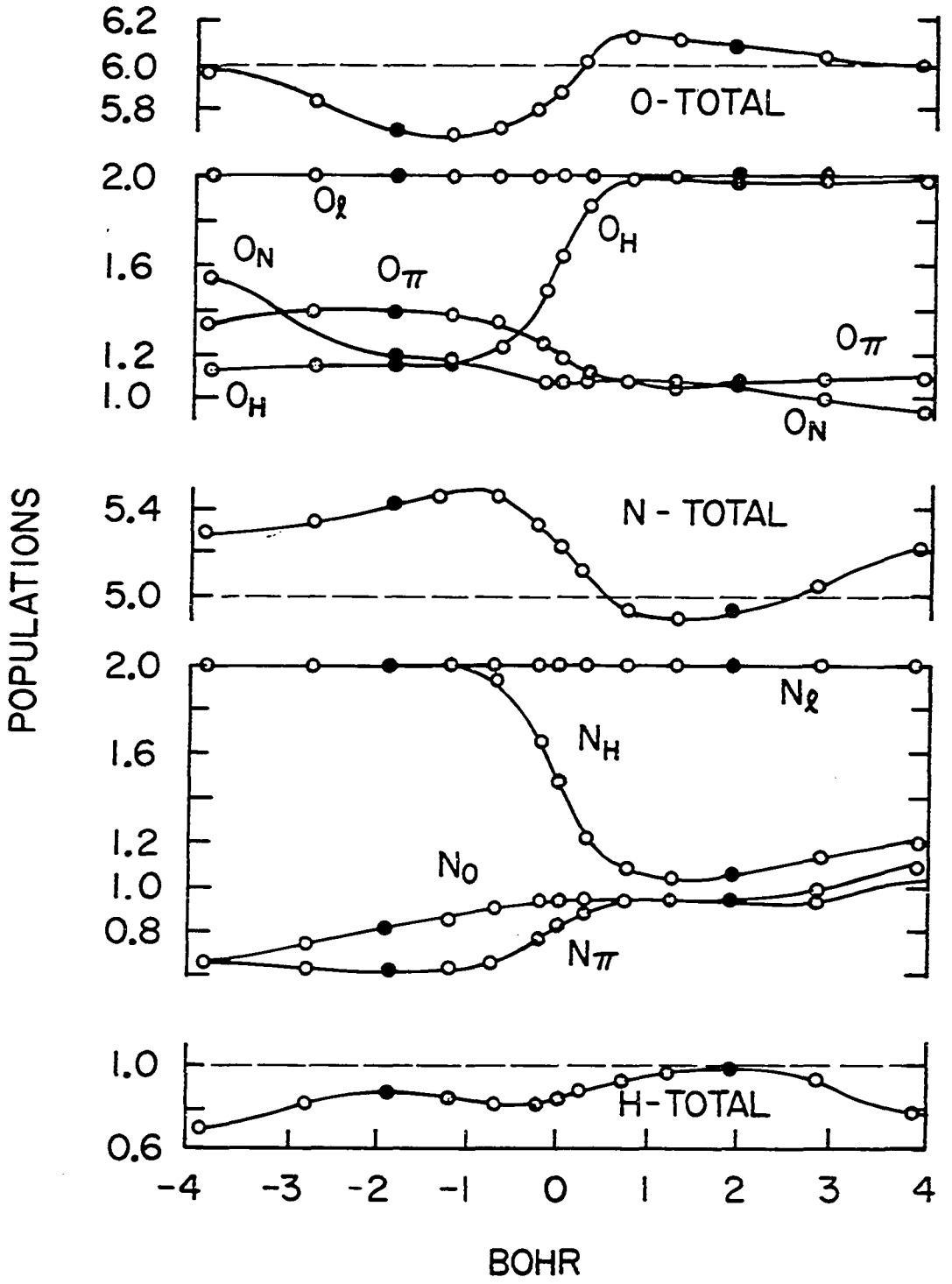

Figure 12. Occupation numbers of the DLRO's for the singlet state

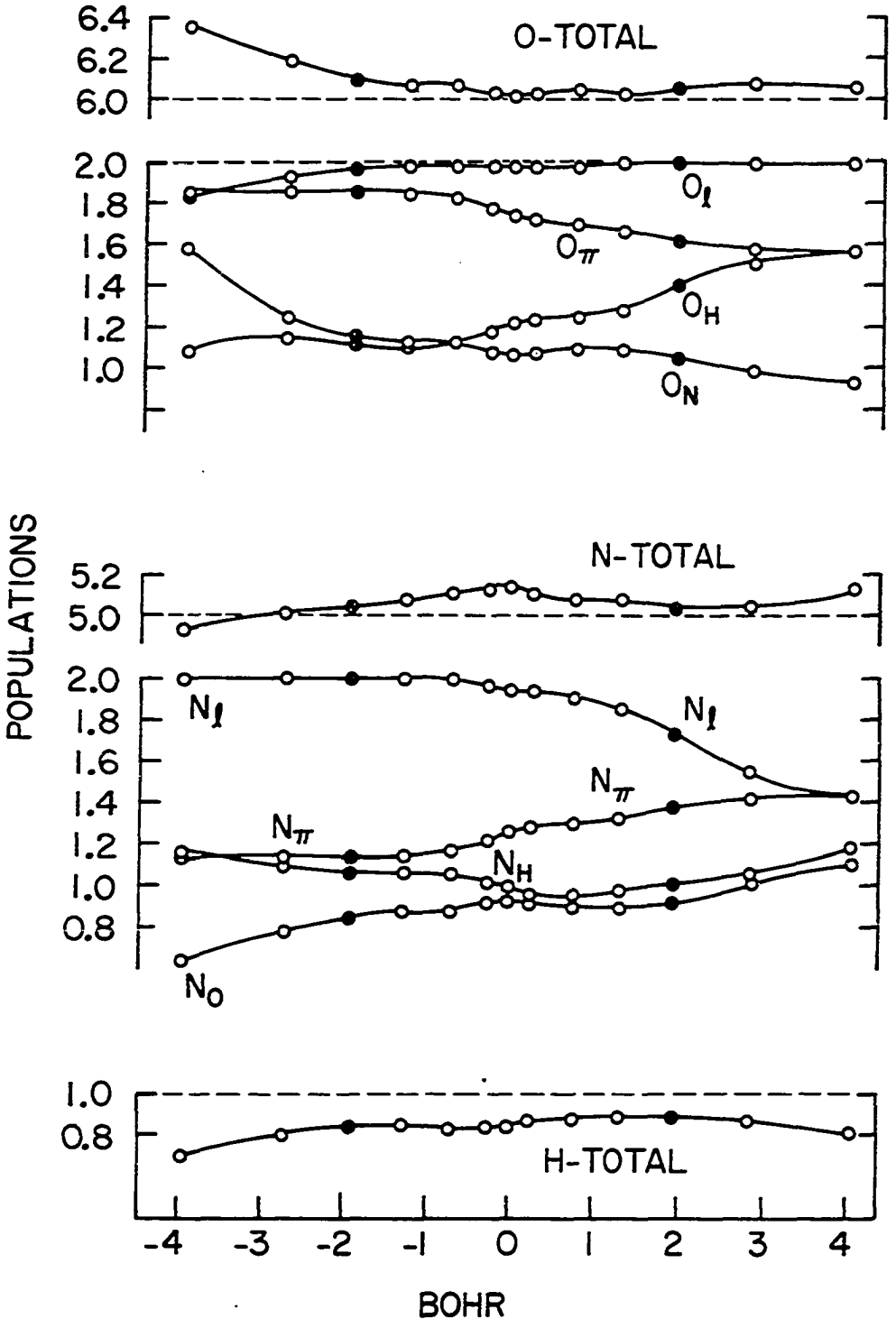

Figure 13. Occupation numbers of the DLRO's for the triplet state

C. Discussion of the N-O Bond

An examination of Figures 7 and 8 yields the overwhelming impression of how little those four orbitals which establish the N-O bond (N_σ, O_σ, $N\pi$ and $O\pi$) actually change as the H moves from left to right and how little difference there is between the singlet and the triplet. The only noticeable difference is observed for the N_π orbitals which show a small contribution on the O atom for the singlet but not for the triplet. Since Figures 12 and 13 show that the pi orbitals have considerably higher occupations in the triplet than in the singlet (because the π^* orbital is occupied in the triplet), the implication seems to be that the compactness of DLRO's increases with increasing occupation.

The remarkable constancy of the N-O bond orbitals in the singlet and triplet closely corresponds to chemical thinking. The population curves of O_σ and N_σ (labeled O_N and N_O in Figures 12 and 13) are also very similar for the singlet and triplet. The sum of the populations in these two orbitals forming the sigma bond remains about 2 across the entire range of the reaction in both states, but, whereas it is about evenly distributed between N_σ and O_σ for H being on the N side, the O_σ population is about twice that of the N_σ when hydrogen is on the O side. This is true for both states.

The sum of the O_π and N_π populations is about 2 in the singlet and about 3 in the triplet. Again this charge is nearly evenly distributed when H is on the N side but greatly shifted towards the O when H is

on the O side.

The bond orders between the N_σ and O_σ orbitals describe the N-O sigma bond. They are consistently strong, between .9 and .95, for both singlet and triplet. The bond orders between O_π and N_π are much weaker for the triplet than the singlet because of the presence of antibonding orbitals for the former. For the singlets they have a value around .88 throughout, even though there is a fair charge shift towards oxygen as the hydrogen moves on the O side of the molecule. For the triplets the value varies from .34 for the HON conformation to a value of .46 for the ONH conformation.

D. The Hydrogen DLRO

Among the orbitals plotted in Figures 9 and 10, the localized H orbital clearly shows the simplest behavior and it looks amost identical for both states. From Figure 12 we furthermore see that there is a charge transfer from H to the heavy atoms which is generally somewhat stronger when H is on the O side and is more pronounced for the linear conformations. Only for the stable singlet equilibrium does the H have a charge of unity.

E. The DLRO's O_L, O_H, N_L, N_H in the Triplet State

1. Orbital shapes

For the discussion of the remaining four orbitals let us consider the triplet state first. When the H atom is on the oxygen side, O_H

is that oxygen orbital which bonds into hydrogen, whereas N_H has nonbonding character. By contrast, when the H atom is on the nitrogen side, then N_H binds into hydrogen and O_H is a nonbonding orbital. If we follow O_H, say, when the hydrogen moves from left to right, that is, from the linear HON conformation to the linear ONH conformation, then we see that the orbital O_H starts out (in the linear HON conformation) pointing along the N-O bond axis. As the H atom swings around, so does the O_H orbital until it points perpendicular to the N-O bond, at which time it has almost pure p_x character. From there on it maintains this shape even when the H proceeds to the center of the molecule and subsequently to the N side. The exact converse behavior is observed for the N_H orbital which points along the bond axis for the linear ONH conformation and turns into a p_x orbital as the H swings around the N. When the H atom is in the center, both O_H and N_H are p_x-type orbitals and parallel to each other. Neither one can point inward to the hydrogen because both have to remain orthogonal to the orbitals O_σ and N_σ. This inability of either one to point to the H DLRO undoubtedly decreases the bonding effect and thereby accounts for the energy barrier.

The orbitals O_L and N_L are nonbonding and are polarized s orbitals nearly everywhere except at one linear conformation in each case. We saw that in the linear conformation HON, O_H has sigma character and N_H has pi character. Consequently O_L must become a p_x orbital while N_L can maintain its polarized sigma character. From

the figure it is apparent that the change from the p_x character to the polarized s character must occur for a conformation rather close to the linear one at which point the orbitals O_L, O_H, and O_N must form approximate trigonal sp^2 hybrids. As indicated in Figure 11, for the linear ONH conformation the converse is true. O_H is seen to have π_x character, hence O_L remains a polarized s orbital here, whereas N_H is a sigma orbital leading to the H, so that N_L has π_x character.

2. Populations

At the linear conformation HON, the two orbitals which are p_x-like, namely the N_H and O_L, are degenerate with the two py-like orbitals, namely N_π and O_π respectively and, indeed, the corresponding occupation numbers do coincide for each pair, as seen in Figure 11. Similarly and for the same reasons, at the linear conformation ONH, the occupation numbers of the O_H and O_π are degenerate and their populations coincide, as do those of N_L and N_π.

Furthermore when the H atom bonds with O then O_H has a population close to 1 and N_L a population close to 2, whereas when H bonds into N, N_H has a population close to 1 and O_L a population close to 2.

In the triplet state the population of the N atom always stays close to 5, although when the H atom is on the N side, its loss of charge increases the N population somewhat. When the H is on the O side the H loses somewhat more population, which leads to a corresponding increase in the O population. There is no significant transfer of charge from the O to the N where H is bonded to O. This is so

because orbitals O_{π} and O_L together carry close to 4 electrons whereas the orbitals N_{π} and N_H together carry about 2 electrons. This must be related to the fact that, in the SCF approximation, the triplet state has singly occupied orbitals which permit a substantial polarization towards oxygen to avoid an excessive population buildup on nitrogen. The resulting smallness of charge transfer over the whole range of the reaction path may explain why the stable and metastable quilibrium conformations are not too different in energy.

3. Bond order

The DLRO bond order matrices (Tables 82 to 94) confirm the directional character of these orbitals and suggest where the principal bonding effects occur. A strong bond order, around 0.9, connects O_H with H when the H is bonded to the O and a bond order of similar size connects N_H to H when H is on the N side. When the H atom is in the middle, both N_H and O_H have a bond order of about .65 with the hydrogen DLRO. Each of these two orbitals has a bond order close to zero when the hydrogen is on the other side of the molecule.

The orbitals O_L and N_L generally have quite small bond orders with the other orbitals except for the linear geometries, because of the discussed degeneracy. For the linear HON conformation the bond order between N_H and O_L is equal to that between N_{π} and O_{π}, and for the linear ONH conformation the bond order between O_H and N_L is equal to that between O_{π} and N_{π}.

F. The DLRO's O_L, O_H, N_L, N_H in the Singlet State

A cursory examination of Figures 9 and 10 shows that the singlet DLRO's are in general quite similar to those of the triplet. Not surprisingly the orbital populations, however, are quite different from those of the triplet, notably for the orbitals N_H, N_L, O_H and O_L.

When hydrogen is bonded into nitrogen, then N_H has an occupation number close to 1 and N_L a population close to 2, whereas the O_H and O_L populations both are 2. When H is bonded to O then the O_H population is close to 1 whereas O_L, N_L, and N_H all have populations about 2. Thus the orbitals N_H and O_H change in a complementary manner from lone pairs to bonding orbitals. This change occurs fairly rapidly as the H moves across the barrier.

In accordance with the Lewis structure there is a strong charge transfer from O to N when H is bonded to O. This is due essentially to the change from lone pair to bonding orbital and vice-versa in O_H and N_H. This charge transfer is somewhat compensated by a counter-moving charge transfer in the N-O bonding orbitals N_σ, N_π, O_σ and O_π, which, however, is not nearly strong enough to avoid a heavy accumulation of electrons on N, in contrast to the situation for the triplet.

The smallest amount of charge transfer between the 3 atoms is observed near the stable equilibrium. The strong charge transfer near the metastable equilibrium explains why its energy is so much higher for the singlet state. This is in contrast to the triplet state for which we found only little charge transfer and a much smaller energy

difference between the two equilibrium conformations.

The bond order pattern for the orbitals N_H and O_H, N_L and O_L is quite similar to that in the triplet state. It reflects the fact that the N_H bond breaks when the O_π bond forms and vice-versa, with two weak partial bonds existing at the middle position. The orbitals N_L and O_L also have very weak bond orders.

G. The Natural Reaction Orbitals (NRO's)

The natural reaction orbital contour plots are shown in Figures 14 to 15 for the singlet and 16 to 17 for the triplet. As is often the case for a molecule without a lot of symmetry, the NO's, like the canonical SCF orbitals, acquire a very complex appearance.

Looking at Figures 14 and 16, which show the orbitals ϕ_1, ϕ_2, ϕ_3, ϕ_4, ϕ_5, we can see that the orbital ϕ_1 is principally the N-O sigma bond. The three lone pairs and the hydrogen bond combine to form the remaining four NO's in these Figures.

ϕ_6 and ϕ_7, shown in Figures 15 and 17, are antibonding orbitals in the N-O and in the N-H (or O-H) bonds. ϕ_8 and ϕ_9 are the bonding and antibonding π orbitals.

Since the SCF approximation is dominant for all geometries, the populations of all NRO's remains fairly constant throughout. For the singlet, the NRO's ϕ_1 ϕ_2 ϕ_3 ϕ_4 ϕ_5 and ϕ_8 all have populations close to 2, whereas the antibonding orbitals ϕ_6 ϕ_7 ϕ_9 have very small populations. For the triplet, the NRO's ϕ_1 ϕ_2 ϕ_3 ϕ_4 ϕ_8 are always

Figure 14a. Contours of sigma NRO's for the singlet state for geometries A to M

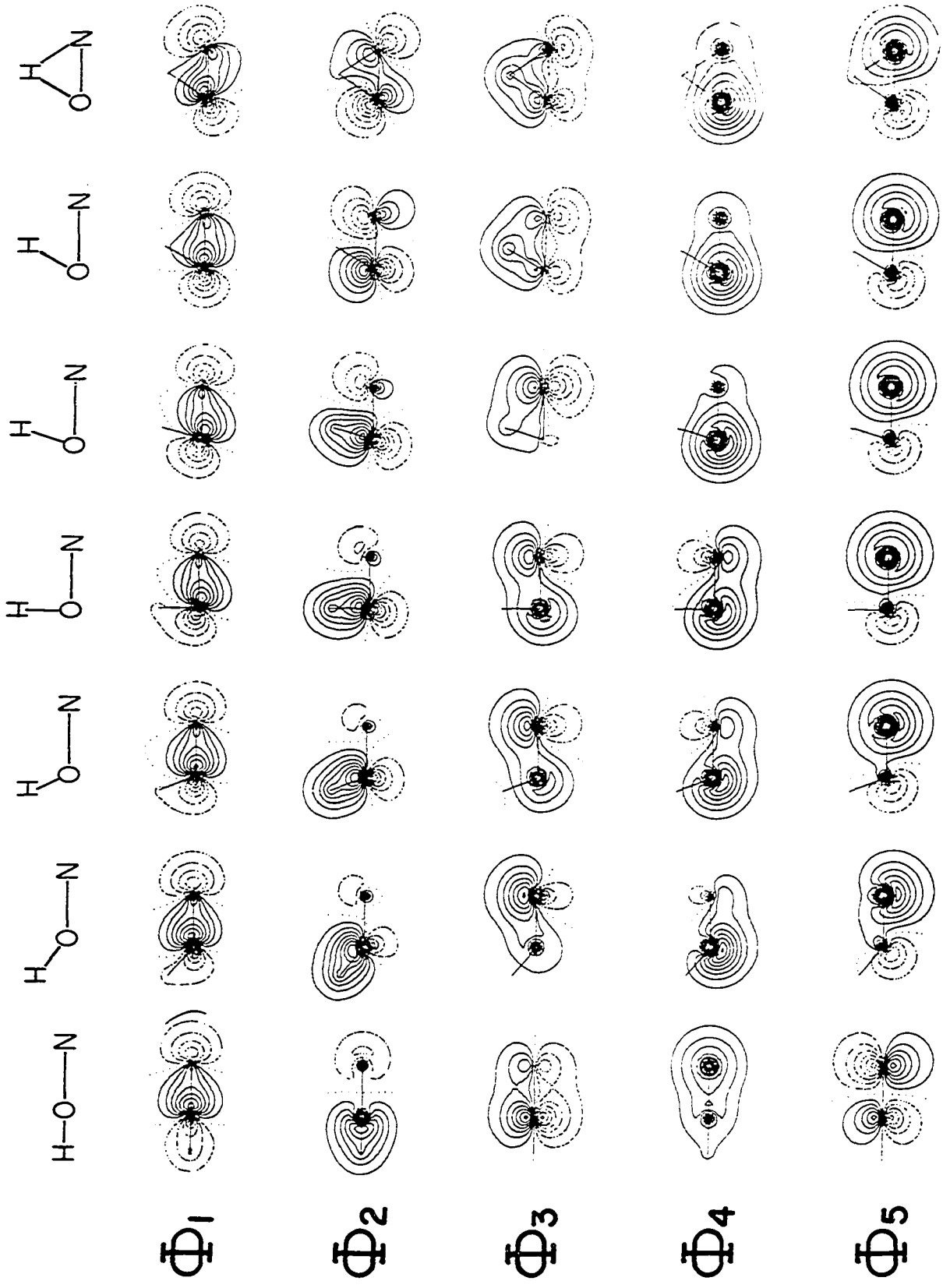
H
N
O
ϕ_1
ϕ_2
ϕ_3
ϕ_4
ϕ_5

Figure 14b. Contours of sigma NRO's for the singlet state for geometries M to L

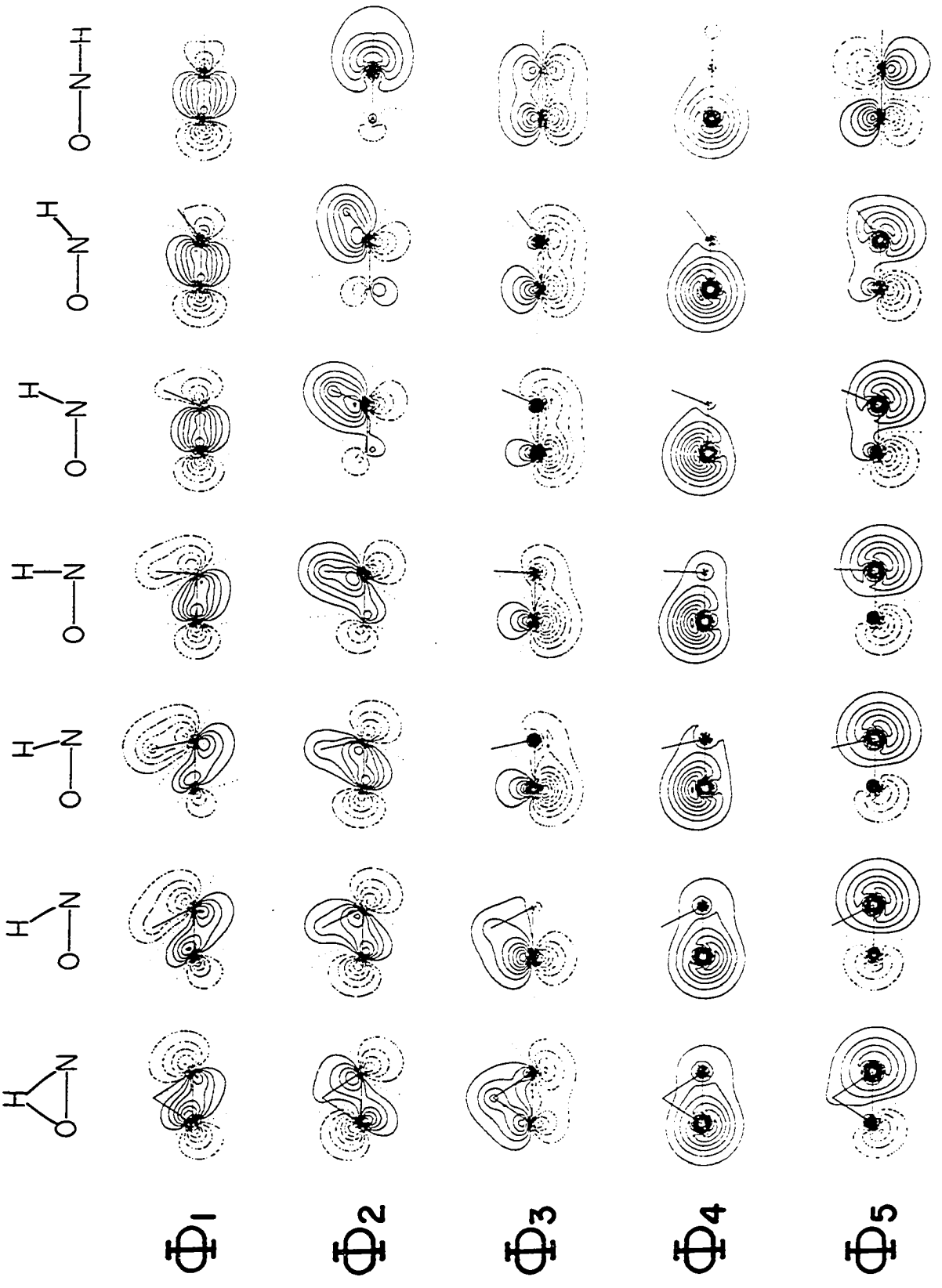
φ1
φ2
φ3
φ4
φ5

Figure 15a. Contours of sigma and pi NRO's for the singlet state for geometries A to M

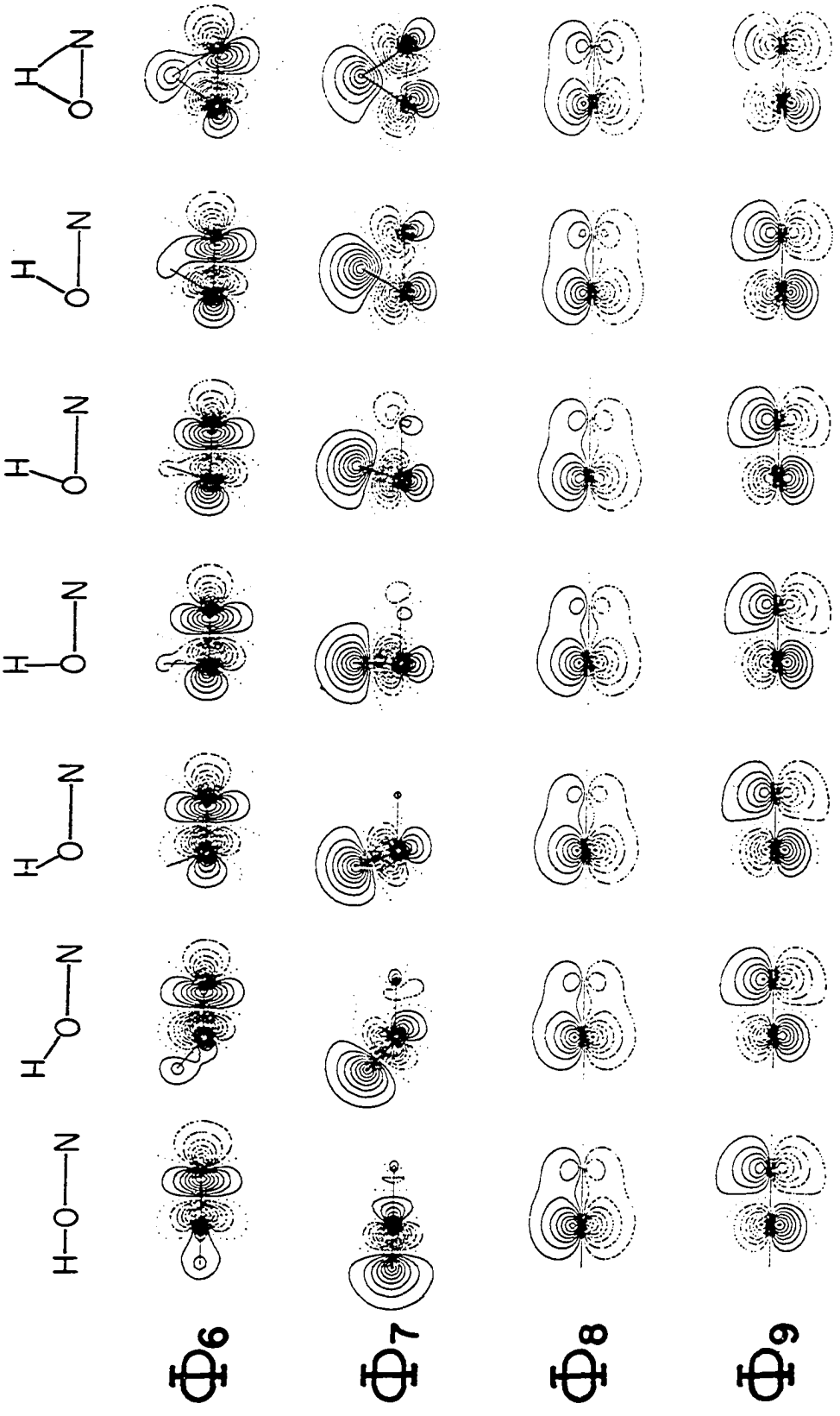
H
N
O
H
N
O
H
N
O
H
N
O
H
N
O
H
N
O
H
N
O
H
N
O
H
Φ_6
Φ_7
Φ_8
Φ_9

Figure 15b. Contours of sigma and pi NRO's for the singlet state for geometries M to L

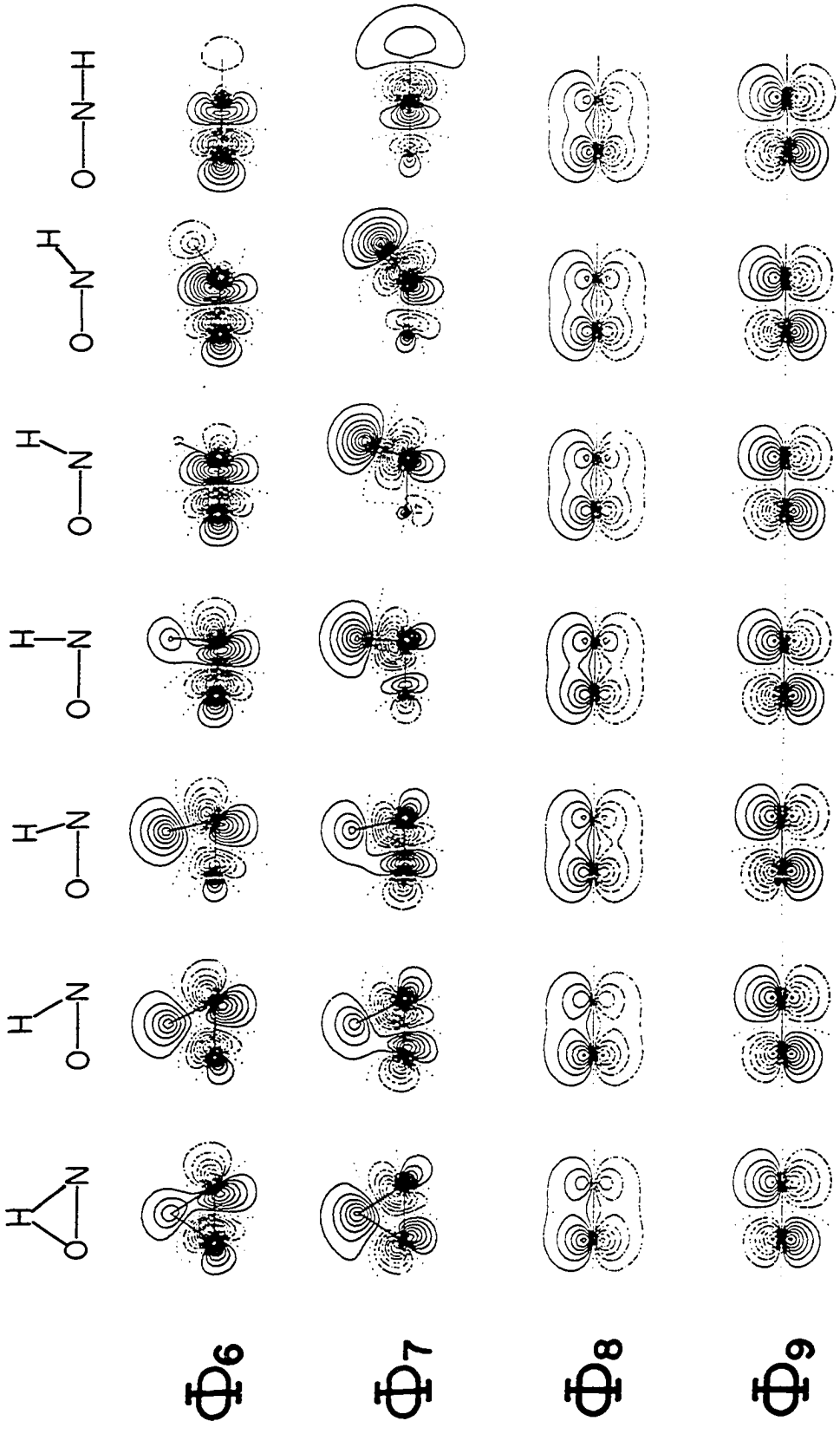
H
N
O
Φ6
Φ7
Φ8
Φ9

Figure 16a. Contours of sigma NRO's for the triplet state for geometries A to M

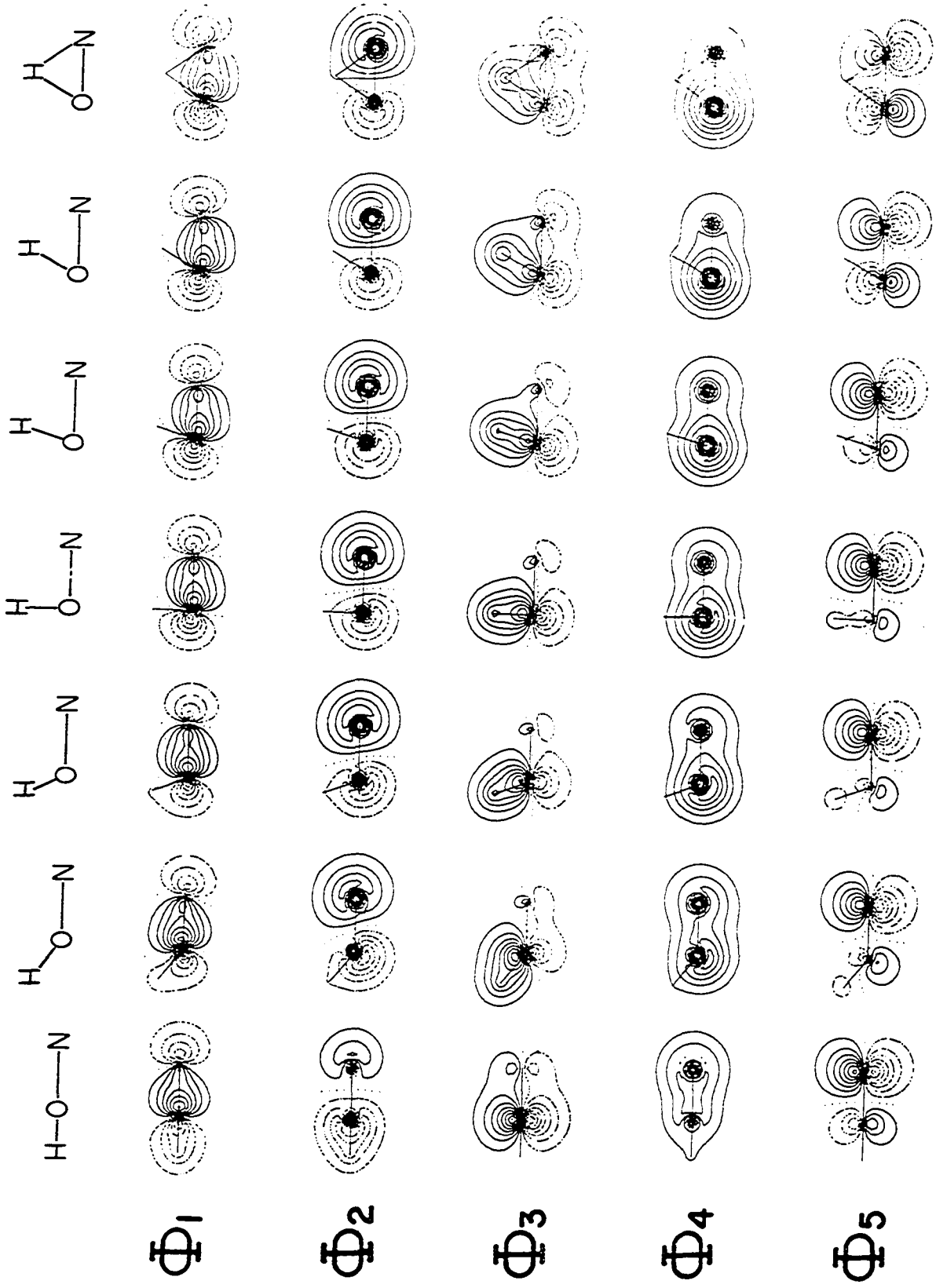
H
N
O
Φ_1
Φ_2
Φ_3
Φ_4
Φ_5

Figure 16b. Contours of sigma NRO's for the triplet state for geometries M to L

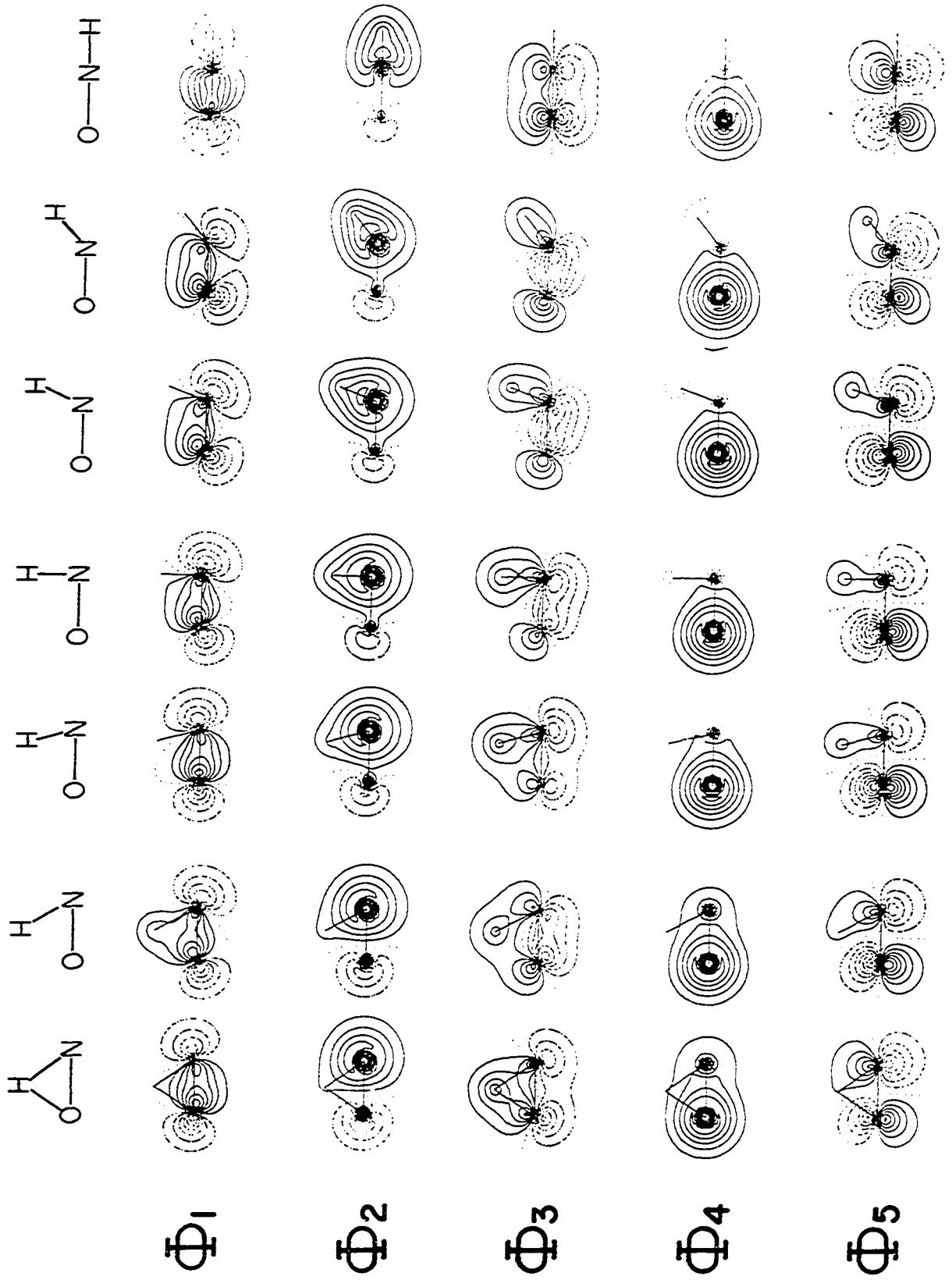
H
N
O
Φ_1
Φ_2
Φ_3
Φ_4
Φ_5

Figure 17a. Contours of sigma and pi NRO's for the triplet state for geometries A to M

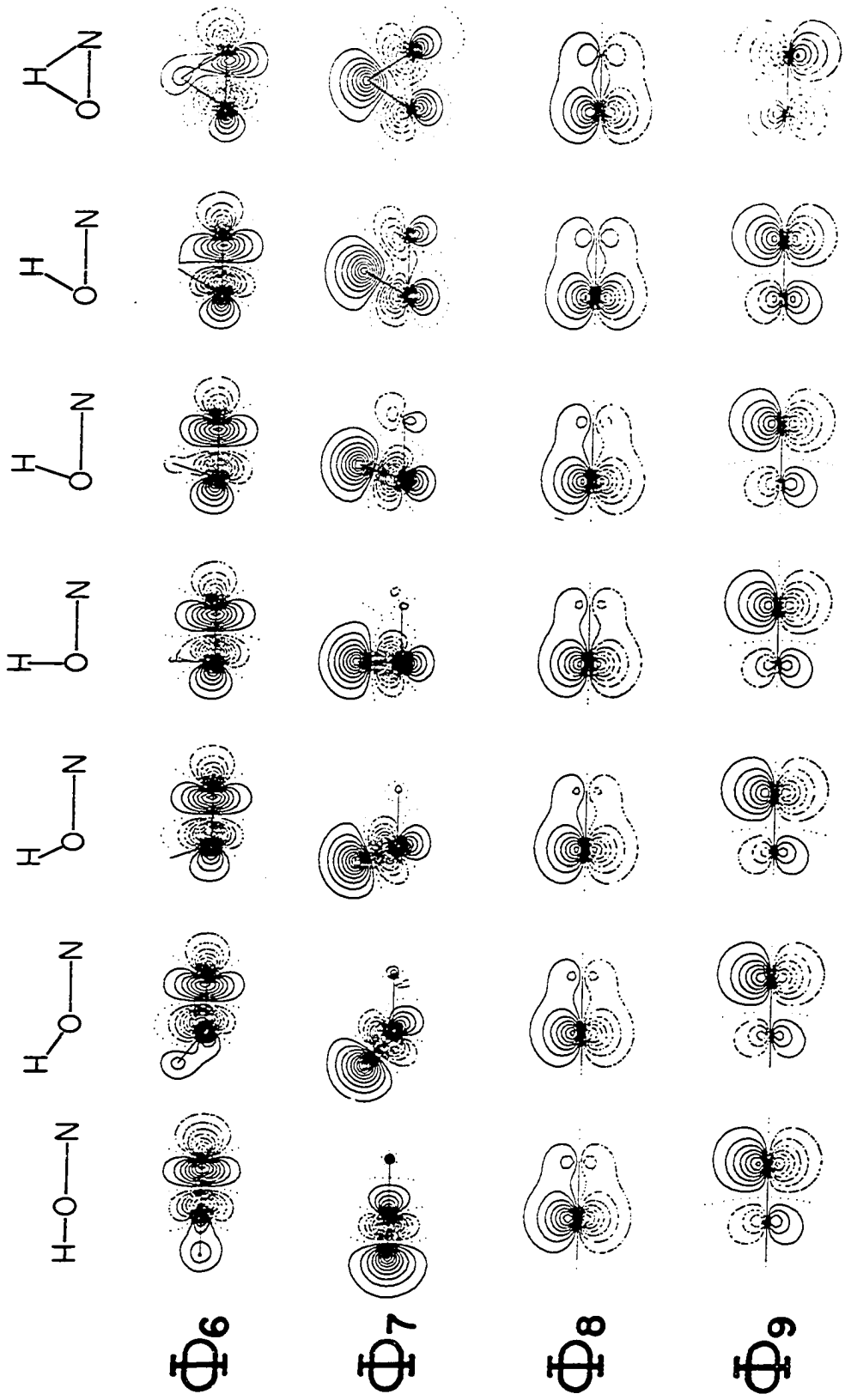
H
N
O
Φ6
Φ7
Φ8
Φ9

Figure 17b. Contours of sigma and pi NRO's for the triplet state for geometries M to L

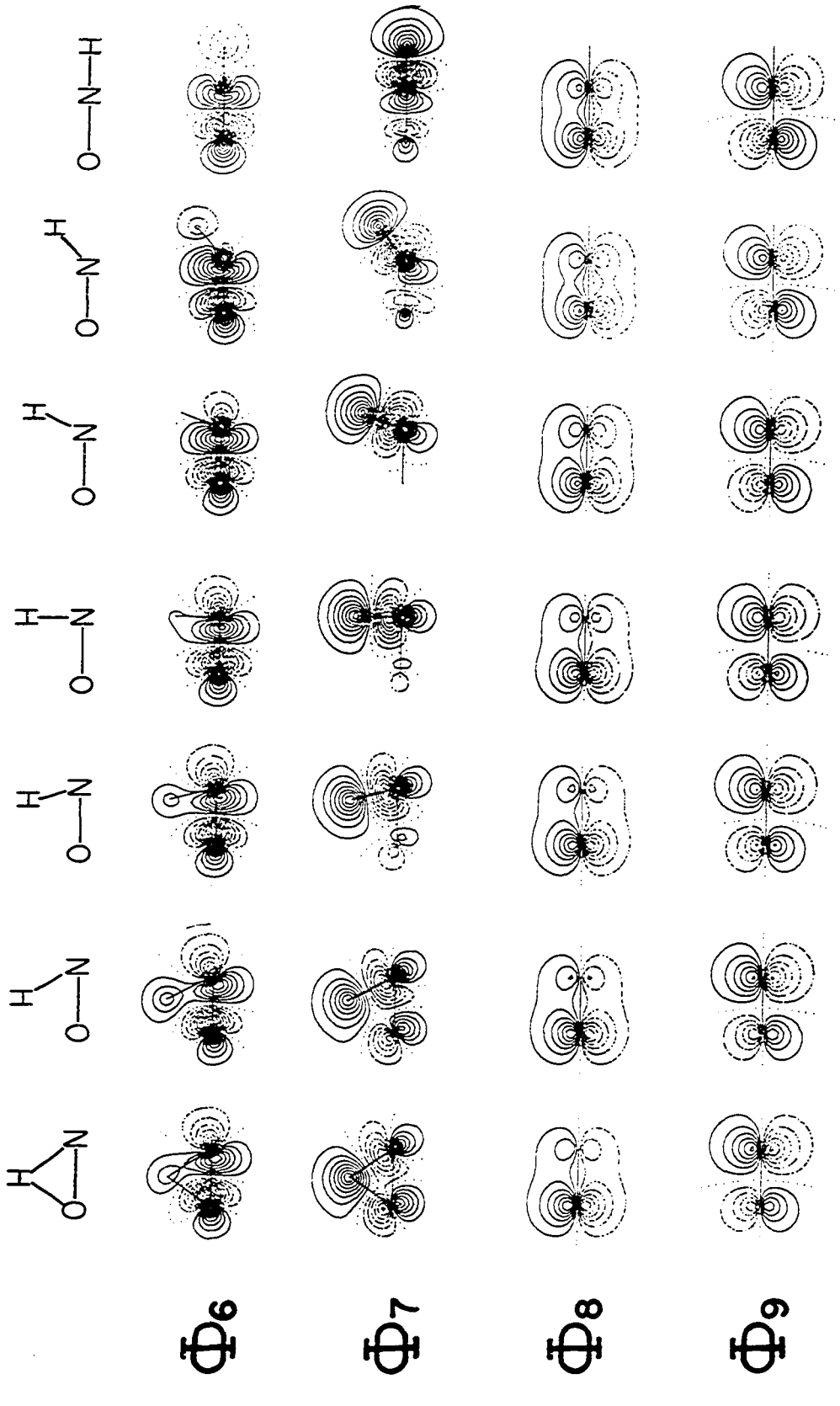
H
N
O
Φ_6
Φ_7
Φ_8
Φ_9

close to doubly-occupied whereas orbitals ϕ_5 and ϕ_9 are singly-occupied and orbitals ϕ_6, ϕ_7 have very small occupancies. For the linear conformations the orbitals ϕ_5 and ϕ_9 become π_x^* and π_y^*, respectively.

A distinguishing feature of the triplet is that the orbital ϕ_5 maintains throughout the entire isomerization a character very similar to the π_x^* character which it assumes at the two linear endpoints. This is undoubtedly so because, among all sigma orbitals it is distinguished by its occupation number of unity.

While the NO's proved extremely effective for the numerical process described in Chapter II, they appear to be less helpful for the interpretation of the isomerization.

VI. LITERATURE CITED

J. J. Ahumada, J. V. Michael, and D. T. Osborne, J. Chem. Phys. 57, 3736 (1972).

C. W. Allen, Astrophysical Quantities, 2nd ed. (Athlone Press, London, 1963).

E. Anders, in Proceedings of the 1971 Symposium on Molecules in the Galactic Environment, edited by M. A. Gordon, (Wiley, New York, 1973), p. 429.

R. R. Baldwin, A. Gethin, J. Plainstowe, and R. W. Walker, J. Chem. Soc., Faraday Trans. I 71, 1265 (1975).

J. L. Bancroft, J. M. Hollas, and D. A. Ramsay, Can. J. Phys. 40, 322 (1962).

R. D. Bardo and K. Ruedenberg, J. Chem. Phys. 59, 5956 (1973).

R. D. Bardo and K. Ruedenberg, J. Chem. Phys. 60, 918 (1974).

V. Ya. Bespalov, L. A. Kartsova, V. I. Baranovskii, and B. V. Ioffe, Dokl. Akad. Nauk SSSR 200, 99 (1971). (Chemical Abstracts, 1972, 76, No. 3248.)

H. W. Brown and G. C. Pimentel, J. Chem. Phys. 29, 883 (1958).

R. D. Brown and G. R. Williams, Chem. Phys. 3, 19 (1974).

A. B. Callear and R. W. Carr, J. Chem. Soc., Faraday Trans. II 71, 1063 (1975).

A. B. Callear and P. M. Wood, Trans. Faraday Soc. 67, 3399 (1971).

A. B. Callear and P. M. Wood, J. Chem. Soc., Faraday Trans. II 68, 302 (1972).

J. K. Cashion and J. C. Polanyi, J. Chem. Phys. 30, 317 (1959).

L. M. Cheung, Ph.D. thesis, Iowa State University (1975) (unpublished).

D. P. Chong, F. G. Herring, and D. McWilliams, J. Electron. Spectrosc. Relat. Phenom. 7, 445 (1975).

M. J. Y. Clement and D. A. Ramsay, Can. J. Phys. 39, 205 (1961).

P. A. Clough, B. A. Thrush, D. A. Ramsay, and J. G. Stamper, Chem. Phys. Letters 23, 155 (1973).

M. A. A. Clyne and B. A. Thrush, Trans. Faraday Soc. 57, 1305 (1961).

M. A. A. Clyne and B. A. Thrush, Disc. Faraday Soc. 33, 139 (1962).

F. A. Cotton and G. Wilkinson, Advanced Inorganic Chemistry (Interscience Publishers, New York, 1966).

F. W. Dalby, Can. J. Phys. 36, 1336 (1958).

R. Ditchfield, J. Del Bene, and J. A. Pople, J. Amer. Chem. Soc. 94, 703 (1972a).

R. Ditchfield, J. Del Bene, and J. A. Pople, J. Amer. Chem. Soc. 94, 4806 (1972b).

C. Edmiston and K. Ruedenberg, Rev. Mod. Phys. 35, 457 (1963).

Y. Ellinger and J. Serre, Int. J. Quantum Chem. Symp. 7, 217 (1973).

N. Fourikis, M. W. Sinclair, R. D. Brown, J. G. Crofts and P. D. Godfrey, Astrophys. J. 194, 41 (1974).

G. A. Gallup, Inorg. Chem. 14, 563 (1975).

M. S. Gordon and J. A. Pople, J. Chem. Phys. 49, 4643 (1968).

G. Haeflinger, Chem. Ber. 103, 3370 (1970).

P. C. Hariharan and J. A. Pople, Theor. Chim. Acta (Berlin), 28, 213 (1973).

P. Harteck, Ber. B. 66, 423 (1933).

D. B. Hartley and B. A. Thrush, Proc. Roy. Soc. (London) A297, 520 (1967).

K. B. Harvey and H. W. Brown, J. Chim. Phys. 56, 745 (1959).

L. J. Hayes, F. P. Billingsley, and C. Trindle, J. Org. Chem. 37, 3924 (1972).

G. Herzberg, Electronic Spectra of Polyatomic Molecules (Van Nostrand, New York, 1966).

T. Hikida, J. A. Eyre, and L. M. Dorfman, J. Chem. Phys. 54, 3422 (1971).

E. Hirschlaff and R. G. W. Norrish, J. Chem. Soc., 1580, (1936).

R. Hoffman, R. Gleiter, and F. B. Mallory, J. Amer. Chem. Soc. 92, 1460 (1970).

M. N. Hughes, Quart. Rev. (London) 22, 1 (1968).

D. Husain and R. G. W. Norrish, Proc. Roy. Soc. (London) A273, 145 (1963).

T. Ibaraki, I. Kusunoki, and K. Kodera, Chem. Letters 1973, 317.

T. Ishiwata, H. Akimoto, and I. Tanaka, Chem. Phys. Letters 21, 322 (1973).

T. Ishiwata, H. Akimoto, and I. Tanaka, Chem. Phys. Letters 27, 260 (1974).

M. E. Jacox and D. E. Milligan, J. Molec. Spectrosc. 48, 536 (1973).

J. W. C. Johns and A. R. W. McKellar, J. Chem. Phys. 66, 1217 (1977).

F. C. Kohout and F. W. Lampe, J. Amer. Chem. Soc. 87, 5795 (1965).

F. C. Kohout and F. W. Lampe, J. Chem. Phys. 46, 4075 (1967).

H. W. Kroto and D. P. Santry, J. Chem. Phys. 47, 792 (1967).

R. M. Lambert, J. Chem. Soc. Chem. Commun. 823 (1966).

P. A. Leighton, Photochemistry of Air Pollution (Academic Press, New York, 1961), p. 103.

P. Millie and G. Berthier, Colloq. Int. Cent. Nat. Rech. Sci. 191, 31 (1970).

D. E. Milligan, M. E. Jacox, S. W. Charles, and G. C. Pimentel, J. Chem. Phys. 37, 2302 (1962).

K. Oka, D. L. Singleton, and R. J. Cvetanovic', J. Chem. Phys. 66, 713 (1977).

J. F. Ogilvie, Spectrochim. Acta 23A, 737 (1967).

J. F. Ogilvie, Nature 243, 210 (1973).

J. Peslak, D. S. Klett, and C. W. David, J. Amer. Chem. Soc. 93, 5001 (1971).

C. H. Purkis and H. W. Thompson, Trans. Faraday Soc. 32, 1466 (1936).

R. C. Raffenetti, J. Chem. Phys. 58, 4452 (1973a).

R. C. Raffenetti, Chem. Phys. Letters 20, 335 (1973b).

R. C. Raffenetti, J. Chem. Phys. 59, 5936 (1973c).

R. C. Raffenetti and K. Ruedenberg, J. Chem. Phys. 59, 5978 (1973).

K. Ramaswamy and K. Ganesan, Acta Chim. (Budapest), 81, 71 (1974).

G. W. Robinson and M. McCarty, J. Chem. Phys. 28, 350 (1958).

K. Ruedenberg, R. C. Raffenetti, and R. D. Bardo, in Energy, Structure and Reactivity, Proceedings of the 1972 Boulder Conference on Theoretical Chemistry (Wiley, New York, 1973).

S. Saito and K. Takagi, J. Molec. Spectrosc. 44, 81 (1972a).

S. Saito and K. Takagi, Astrophys. J. 175, L47 (1972b).

S. Saito and K. Takagi, J. Molec. Spectrosc. 47, 99 (1973).

W. I. Salmon, in Advances in Quantum Chemistry, Volume 8, edited by P. O. Lowdin (Academic Press, New York, 1974), p. 8.

W. I. Salmon and K. Ruedenberg, J. Chem. Phys. 57, 2776 (1972).

W. I. Salmon, K. Ruedenberg, and L. M. Cheung, J. Chem. Phys. 57, 2787 (1972).

A. W. Salotto and L. Burnelle, Chem. Phys. Letters 3, 80 (1969).

A. W. Salotto and L. Burnelle, J. Chem. Phys. 52, 2936 (1970).

F. Seel and C. Bliefert, Z. Anorg. Allg. Chem. 406, 277 (1974).

M. Shanshal, Z. Naturforsch B25, 1063 (1970).

H. F. Shurvell, Can. Spectrosc. 16, 71 (1971).

R. Simonaitis, J. Phys. Chem. 67, 2227 (1963).

H. M. Smallwood, J. Amer. Chem. Soc. 51, 1985 (1929).

K. R. Sundberg, Ph.D. thesis, Iowa State University (1975) (unpublished).

H. A. Taylor and C. Tanford, J. Chem. Phys. 12, 47 (1944).

M. S. Vardya, Mon. Notic. Roy. Astron. Soc. 134, 347 (1966).

G. R. Williams, Chem. Phys. Letters 30, 495 (1975).

J. E. Williams and J. N. Murrell, J. Amer. Chem. Soc. 93, 7149 (1971).

A. A. Wu, S. D. Peyerimhoff and R. J. Buenker, Chem. Phys. Letters 35, 316 (1975).

I. S. Zaslonko, S. M. Kogarko, E. V. Mozzhukhin, Yu. P. Petrov, and A. A. Borisov, Kinet. Katal. 11, 296 (1970). (Chemical Abstracts, 1971, 73, No. 34601.)

VII. ACKNOWLEDGMENTS

The author is indebted to Professor Klaus Ruedenberg for his suggestion and guidance of this project. She wishes to thank certain former members of the Iowa State Theoretical Chemistry Group, Drs. Raffenetti, Sundberg, Cheung and Layton, for providing programs, helpful discussions, and/or encouragement. The current members of the Group, Steve Elbert, Dave Feller, and Mike Schmidt, also deserve thanks for their programs, discussions, and their artistic expertise as applied to the preparation of many of the Figures. Dr. Elbert's programming skill was responsible for making the FORS calculations possible this year. The author is grateful too for the encouragement supplied by some very good friends (some of whom also happen to be relatives or in-laws). She especially wishes to thank her once and future roommate, Duane Dombek, for his patience and devotion.

VIII. APPENDIX A: THE QUANTITATIVE BASIS ORBITALS (QBO'S)

The present investigation is based on the use of 20 quantitative basis orbitals. These were determined according to the procedure described in Section IVA. They are presented here in Tables 95 to 107; there is one table for each of the 13 geometries, points A through L.

Each Table lists the expansion coefficients of the twenty orbitals in terms of even-tempered Gaussian primitives on the three centers. The orbital exponents are obtained from the given values of α and β as $\zeta_1 = \alpha\beta$, $\zeta_2 = \alpha\beta^2$, etc.

Table 95. ETCGAO bases for HNO geometry A

Table 95a. ETCGAO basis for nitrogen

alpha(s)=0.160740 beta(s)=4.053414

prim.	s	s'	s''
1	-0.110298	1.117714	-1.063650
2	0.255233	-0.132855	2.062612
3	0.624560	-0.205695	-1.158641
4	0.262622	-0.047121	0.002731
5	0.052674	-0.009295	-0.033469
6	0.013357	-0.002055	0.000405

alpha(p)=0.054681 beta(p)=3.909314

prim.	p	p'
1	0.526664	1.064463
2	0.489019	-0.843212
3	0.182477	-0.206600
4	0.035580	-0.052589

Table 95b. ETCGAO basis for oxygen

alpha(s)=0.162417 beta(s)=4.189743

prim.	s	s'	s''
1	-0.077632	1.050672	-1.105377
2	0.168831	-0.020112	2.112314
3	0.639246	-0.220838	-1.352316
4	0.305701	-0.060885	0.228809
5	0.059921	-0.011472	0.026786
6	0.014566	-0.002532	0.015430

alpha(p)=0.040175 beta(p)=4.174823

prim.	p	p'
1	0.358978	1.083962
2	0.578146	-0.638232
3	0.271234	-0.242693
4	0.060429	-0.059192

Table 95c. ETCGAO basis for hydrogen

alpha(s) =0.038566 beta(s) =4.945683

prim.	s	s'
1	0.815600	-0.959863
2	0.233125	1.076755
3	0.043395	0.204708
4	0.007601	0.036564

Table 96. ETCGAO bases for HNO geometry B

Table 96a. ETCGAO basis for nitrogen

alpha(s)=0.099430 beta(s)=4.337184

prim.	s	s'	s''
1	0.233016	-1.218285	-2.236369
2	0.118864	-0.016135	3.980511
3	0.454723	0.676961	-1.931909
4	0.252768	0.284796	-0.020113
5	0.048894	0.054733	-0.038881
6	0.011355	0.012240	0.001245

alpha(p)=0.060494 beta(p)=3.834671

prim.	p	p'
1	0.498991	-1.288687
2	0.452145	1.038599
3	0.166184	0.199240
4	0.033150	0.064175

Table 96b. ETCGAO basis for oxygen

alpha(s)=0.167476 beta(s)=4.191637

prim.	s	s'	s''
1	0.185806	-1.343106	-2.311038
2	0.144297	0.152076	4.366583
3	0.483678	0.643827	-2.454045
4	0.234462	0.246458	0.174557
5	0.045739	0.047515	-0.006559
6	0.011135	0.011196	0.013174

alpha(p)=0.043018 beta(p)=4.126741

prim.	p	p'
1	0.279574	1.264088
2	0.568579	-0.762694
3	0.262444	-0.257375
4	0.058473	-0.063877

Table 96c. ETCGAO basis for hydrogen

alpha(s)=0.041027 beta(s)=4.462895

prim.	s	s'
1	0.570424	-1.854172
2	0.385347	1.610418
3	0.079047	0.247237
4	0.017562	0.064222

Table 97. ETCGAO bases for HNO geometry C

Table 97a. ETCGAO basis for nitrogen

alpha(s)=0.102529 beta(s)=4.262252

prim.	s	s'	s''
1	0.272116	-1.223215	-2.280254
2	0.109812	0.000560	4.079336
3	0.431578	0.677039	-2.007213
4	0.249722	0.299493	0.001550
5	0.049838	0.059000	-0.035518
6	0.011967	0.013711	0.002749

alpha(p)=0.053700 beta(p)=3.875668

prim.	p	p'
1	0.457616	1.286737
2	0.478801	-0.986912
3	0.181964	-0.215445
4	0.037287	-0.063901

Table 97b. ETCGAO basis for oxygen

alpha(s)=0.161150 beta(s)=4.197721

prim.	s	s'	s''
1	0.228786	-1.314761	-2.149151
2	0.132469	0.121692	3.742186
3	0.461874	0.660267	-1.492744
4	0.233327	0.262496	-0.276610
5	0.045755	0.050812	-0.099704
6	0.011158	0.012005	-0.015575

alpha(p)=0.047705 beta(p)=4.055814

prim.	p	p'
1	0.303720	1.291386
2	0.558354	-0.840887
3	0.249338	-0.220739
4	0.055792	-0.062263

Table 97c. ETCGAO basis for hydrogen

alpha(s)=0.029214 beta(s)=4.604949

prim.	s	s'
1	0.415826	-1.802241
2	0.517620	1.404144
3	0.100931	0.330380
4	0.021650	0.065600

Table 98. ETCGAO bases for HNO geometry D

Table 98a. ETCGAO basis for nitrogen

alpha(s)=0.105784 beta(s)=4.202926

prim.	s	s'	s''
1	0.290960	-1.231126	-2.317837
2	0.104337	0.015015	4.170140
3	0.419777	0.674291	-2.085343
4	0.248533	0.307151	0.026903
5	0.050753	0.061656	-0.032783
6	0.012516	0.014759	0.004489

alpha(p)=0.048835 beta(p)=3.908781

prim.	p	p'
1	0.427801	1.284018
2	0.496111	-0.947849
3	0.194669	-0.227020
4	0.040684	-0.063503

Table 98b. ETCGAO basis for oxygen

alpha(s)=0.156379 beta(s)=4.201922

prim.	s	s'	s''
1	0.255284	-1.292041	-2.217976
2	0.125563	0.095757	3.930210
3	0.446889	0.670987	-1.751937
4	0.233303	0.274156	-0.145308
5	0.045963	0.053279	-0.079115
6	0.011226	0.012610	-0.008165

alpha(p)=0.052066 beta(p)=3.998878

prim.	p	p'
1	0.329952	1.308349
2	0.545928	-0.900503
3	0.236728	-0.196708
4	0.053104	-0.062089

Table 98c. ETCGAO basis for hydrogen

alpha(s) = 0.022670 beta(s) = 4.711186

prim.	s	s'
1	0.364266	1.749404
2	0.548682	-1.269056
3	0.122393	-0.388869
4	0.022961	-0.067590

Table 99. ETCGAO bases for HNO geometry E

Table 99a. ETCGAO basis for nitrogen

alpha(s)=0.109204 beta(s)=4.158589

prim.	s	s'	s''
1	0.295058	-1.243440	-2.346747
2	0.101821	0.031113	4.249316
3	0.416883	0.669806	-2.162349
4	0.248408	0.308700	0.053565
5	0.051482	0.062730	-0.030450
6	0.012947	0.015340	0.006269

alpha(p)=0.045496 beta(p)=3.933803

prim.	p	p'
1	0.411588	1.278521
2	0.504663	-0.918758
3	0.202396	-0.237895
4	0.043003	-0.063731

Table 99b. ETCGAO basis for oxygen

alpha(s)=0.153039 beta(s)=4.204234

prim.	s	s'	s''
1	0.269066	-1.276258	-2.253334
2	0.121653	0.076360	4.025722
3	0.438174	0.676737	-1.888250
4	0.234265	0.281827	-0.075491
5	0.046333	0.054950	-0.065463
6	0.011330	0.013021	-0.003853

alpha(p)=0.055925 beta(p)=3.955373

prim.	p	p'
1	0.361301	1.307090
2	0.528350	-0.925442
3	0.225062	-0.198987
4	0.050300	-0.064845

Table 99c. ETCGAO basis for hydrogen

alpha(s)=0.019172 beta(s)=4.778954

prim.	s	s'
1	0.377302	1.717429
2	0.535542	-1.222054
3	0.124185	-0.415447
4	0.023172	-0.066482

Table 100. ETCGAO bases for HNO geometry F

Table 100a. ETCGAO basis for nitrogen

alpha(s)=0.112796 beta(s)=4.128779

prim.	s	s'	s''
1	0.284466	-1.256142	-2.362072
2	0.103890	0.042416	4.288519
3	0.421706	0.666723	-2.192818
4	0.249114	0.304802	0.063042
5	0.051953	0.062352	-0.034765
6	0.013233	0.015433	0.006316

alpha(p)=0.043423 beta(p)=3.950572

prim.	p	p'
1	0.394201	1.271852
2	0.515210	-0.885833
3	0.208364	-0.252353
4	0.044869	-0.064253

Table 100b. ETCGAO basis for oxygen

alpha(s)=0.151041 beta(s)=4.204653

prim.	s	s'	s''
1	0.272415	-1.270291	-2.320996
2	0.118711	0.068371	4.275643
3	0.435988	0.676248	-2.281879
4	0.236235	0.285413	0.110420
5	0.046870	0.055742	-0.017685
6	0.011470	0.013232	0.009394

alpha(p)=0.059118 beta(p)=3.924879

prim.	p	p'
1	0.403787	1.295997
2	0.501810	-0.943220
3	0.212348	-0.209341
4	0.046992	-0.068839

Table 100c. ETCGAO basis for hydrogen

alpha(s) = 0.017670 beta(s) = 4.806544

prim.	s	s'
1	0.421214	-1.699935
2	0.508631	1.228700
3	0.107538	0.418595
4	0.022740	0.069016

Table 101. ETCGAO bases for HNO geometry M

Table 101a. ETCGAO basis for nitrogen

alpha(s)=0.114660 beta(s)=4.119222

prim.	s	s'	s''
1	0.255644	-1.267225	-2.365772
2	0.108004	0.046110	4.300808
3	0.435775	0.659881	-2.203201
4	0.254006	0.296639	0.064575
5	0.052948	0.060780	-0.035708
6	0.013533	0.015065	0.006359

alpha(p)=0.042808 beta(p)=3.955827

prim.	p	p'
1	0.356363	1.289839
2	0.541240	-0.886358
3	0.215813	-0.233279
4	0.047058	-0.061518

Table 101b. ETCGAO basis for oxygen

alpha(s)=0.150529 beta(s)=4.204153

prim.	s	s'	s''
1	0.272830	-1.267750	-2.303833
2	0.118421	0.064412	4.197126
3	0.435186	0.676773	-2.148285
4	0.236866	0.286471	0.041120
5	0.047039	0.056015	-0.027305
6	0.011519	0.013302	0.005575

alpha(p)=0.060420 beta(p)=3.914412

prim.	p	p'
1	0.394572	1.296486
2	0.510524	-0.933937
3	0.210959	-0.213895
4	0.046937	-0.069502

Table 101c. ETCGAO basis for hydrogen

alpha(s) = 0.017519 beta(s) = 4.805012

prim.	s	s'
1	0.312856	1.638421
2	0.583429	-1.011431
3	0.136458	-0.528099
4	0.026382	-0.069471

Table 102. ETCGAO bases for HNO geometry G

Table 102a. ETCGAO basis for nitrogen

alpha(s)=0.116571 beta(s)=4.113192

prim.	s	s'	s''
1	0.282810	-1.270924	-2.372086
2	0.106953	0.062889	4.338882
3	0.423914	0.666714	-2.261802
4	0.245278	0.299561	0.091825
5	0.051106	0.061298	-0.034171
6	0.013088	0.015246	0.007663

alpha(p)=0.042458 beta(p)=3.958983

prim.	p	p'
1	0.349761	1.283518
2	0.543739	-0.864296
3	0.219513	-0.246428
4	0.047794	-0.061392

Table 102b. ETCGAO basis for oxygen

alpha(s)=0.150336 beta(s)=4.203179

prim.	s	s'	s''
1	0.279728	-1.264683	-2.341108
2	0.117767	0.062412	4.355355
3	0.431321	0.679377	-2.417593
4	0.235673	0.288452	0.179409
5	0.046848	0.056448	-0.002478
6	0.011481	0.013414	0.013878

alpha(p)=0.061505 beta(p)=3.907097

prim.	p	p'
1	0.406996	1.304994
2	0.500368	-0.965110
3	0.210140	-0.196484
4	0.046063	-0.068089

Table 102c. ETCGAO basis for hydrogen

alpha(s) = 0.017747 beta(s) = 4.793251

prim.	s	s'
1	0.343407	1.732951
2	0.567285	-1.237921
3	0.123285	-0.391844
4	0.024846	-0.069537

Table 103. ETCGAO bases for HNO geometry H

Table 103a. ETCGAO basis for nitrogen

alpha(s)=0.120540 beta(s)=4.111665

prim.	s	s'	s''
1	0.262276	-1.295383	-2.369850
2	0.112781	0.092860	4.377186
3	0.437572	0.659667	-2.333720
4	0.243487	0.287134	0.122798
5	0.050332	0.058360	-0.032212
6	0.012853	0.014472	0.009012

alpha(p)=0.042529 beta(p)=3.958983

prim.	p	p'
1	0.334861	1.293912
2	0.553571	-0.872203
3	0.222507	-0.233214
4	0.048567	-0.059553

Table 103b. ETCGAO basis for oxygen

alpha(s)=0.150905 beta(s)=4.199815

prim.	s	s'	s''
1	0.273280	-1.265771	-2.341528
2	0.118931	0.060705	4.349404
3	0.434181	0.678631	-2.402257
4	0.236823	0.287086	0.171977
5	0.047100	0.056246	-0.005802
6	0.011559	0.013375	0.013370

alpha(p)=0.062975 beta(p)=3.901859

prim.	p	p'
1	0.409354	1.309673
2	0.499772	-0.978384
3	0.208414	-0.188904
4	0.045218	-0.066648

Table 103c. ETCGAO basis for hydrogen

alpha(s) = 0.019426 beta(s) = 4.739418

prim.	s	s'
1	0.316008	1.766782
2	0.584820	-1.279194
3	0.130925	-0.362213
4	0.025956	-0.069773

Table 104. ETCGAO bases for HNO geometry I

Table 104a. ETCGAO basis for nitrogen

alpha(s)=0.124714 beta(s)=4.124183

prim.	s	s'	s''
1	0.230010	-1.324055	-2.360040
2	0.123393	0.128113	4.417421
3	0.457215	0.649287	-2.433389
4	0.241222	0.269854	0.170765
5	0.049143	0.054172	-0.027532
6	0.012416	0.013280	0.011364

alpha(p)=0.043643 beta(p)=3.950572

prim.	p	p'
1	0.342443	1.296802
2	0.550202	-0.886383
3	0.218875	-0.227535
4	0.047513	-0.059765

Table 104b. ETCGAO basis for oxygen

alpha(s)=0.152762 beta(s)=4.194564

prim.	s	s'	s''
1	0.262375	-1.272655	-2.339561
2	0.121272	0.066174	4.342064
3	0.439976	0.676007	-2.384321
4	0.237578	0.283023	0.162011
5	0.047223	0.055466	-0.010742
6	0.011606	0.013198	0.012358

alpha(p)=0.063459 beta(p)=3.909113

prim.	p	p'
1	0.411910	1.307636
2	0.499134	-0.978484
3	0.207164	-0.190617
4	0.044395	-0.064838

Table 104c. ETCGAO basis for hydrogen

alpha(s) = 0.023173 beta(s) = 4.646404

prim.	s	s'
1	0.343067	1.805604
2	0.566897	-1.363648
3	0.121659	-0.328213
4	0.025339	-0.068134

Table 105. ETCGAO bases for HNO geometry J

Table 105a. ETCGAO basis for nitrogen

alpha(s)=0.129104 beta(s)=4.150876

prim.	s	s'	s''
1	0.183294	-1.355437	-2.342249
2	0.140899	0.166819	4.458786
3	0.482640	0.634525	-2.563633
4	0.238310	0.247723	0.239772
5	0.047562	0.048891	-0.020148
6	0.011797	0.011740	0.014238

alpha(p)=0.045881 beta(p)=3.933803

prim.	p	p'
1	0.370313	1.291338
2	0.534802	-0.903082
3	0.208914	-0.231524
4	0.044794	-0.061130

Table 105b. ETCGAO basis for oxygen

alpha(s)=0.155955 beta(s)=4.187433

prim.	s	s'	s''
1	0.245428	-1.284846	-2.335113
2	0.125427	0.077595	4.331768
3	0.449116	0.671482	-2.361332
4	0.238132	0.276069	0.148856
5	0.047254	0.054086	-0.018048
6	0.011631	0.012874	0.010872

alpha(p)=0.062934 beta(p)=3.928928

prim.	p	p'
1	0.414549	1.299045
2	0.498434	-0.965673
3	0.206544	-0.200975
4	0.043602	-0.063297

Table 105c. ETCGAO basis for hydrogen

alpha(s)=0.030125 beta(s)=4.516546

prim.	s	s'
1	0.430357	-1.845618
2	0.502164	1.487341
3	0.100446	0.289509
4	0.022875	0.066344

Table 106. ETCGAO bases for HNO geometry K

Table 106a. ETCGAO basis for nitrogen

alpha(s)=0.133722 beta(s)=4.192017

prim.	s	s'	s''
1	0.121460	-1.387404	-2.310306
2	0.167287	0.207333	4.473250
3	0.512402	0.614721	-2.677027
4	0.234033	0.221163	0.304128
5	0.045520	0.042785	-0.012291
6	0.010999	0.009957	0.016870

alpha(p)=0.049413 beta(p)=3.908782

prim.	p	p'
1	0.411760	1.279498
2	0.511923	-0.922260
3	0.192551	-0.241810
4	0.040784	-0.062464

Table 106b. ETCGAO basis for oxygen

alpha(s)=0.160567 beta(s)=4.178433

prim.	s	s'	s''
1	0.209159	-1.301144	-2.330194
2	0.134023	0.088219	4.319794
3	0.467004	0.663256	-2.336251
4	0.240871	0.263965	0.139887
5	0.047653	0.051732	-0.032873
6	0.011746	0.012290	0.008976

alpha(p)=0.061424 beta(p)=3.961496

prim.	p	p'
1	0.416878	1.283846
2	0.497612	-0.939246
3	0.207062	-0.220081
4	0.042883	-0.062386

Table 106c. ETCGAO basis for hydrogen

alpha(s) =0.042679 beta(s) =4.353045

prim.	s	s'
1	0.581100	-1.866364
2	0.374025	1.612105
3	0.077715	0.261049
4	0.018129	0.068772

Table 107. ETCGAO bases for HNO geometry L

Table 107a. ETCGAO basis for nitrogen

alpha(s)=0.138391 beta(s)=4.129283

prim.	s	s'	s''
1	-0.083634	1.087436	-1.058239
2	0.207031	-0.082689	1.986064
3	0.631732	-0.215446	-1.013975
4	0.285541	-0.055742	-0.058139
5	0.056725	-0.010774	-0.048091
6	0.014049	-0.002393	-0.004162

alpha(p)=0.042086 beta(p)=3.978640

prim.	p	p'
1	0.432187	1.078772
2	0.551989	-0.729623
3	0.215199	-0.241054
4	0.046631	-0.057464

Table 107b. ETCGAO basis for oxygen

alpha(s)=0.191409 beta(s)=4.086165

prim.	s	s'	s''
1	-0.100730	-1.082843	-0.859758
2	0.213267	0.071185	1.438420
3	0.633257	0.214906	-0.206493
4	0.283181	0.053762	-0.565643
5	0.056458	0.010435	-0.131197
6	0.014240	0.002336	-0.035048

alpha(p)=0.064347 beta(p)=3.942282

prim.	p	p'
1	0.481864	1.079506
2	0.510725	-0.799281
3	0.211354	-0.209755
4	0.043037	-0.056901

Table 107c. ETCGAO basis for hydrogen

alpha(s) =0.039254 beta(s) =4.952483

prim.	s	s'
1	0.759984	-1.002232
2	0.294132	1.057957
3	0.054412	0.205741
4	0.009470	0.035279

IX. APPENDIX B: COMPUTER PROGRAMS

A. Existing Programs

For the execution of the present investigation a number of computer programs were essential which were developed over a number of years by various members of the Iowa State University theoretical chemistry group.

The determination of the QBO's in terms of even-tempered Gaussian primitives required orbital exponent optimizations and orbital contractions. The former were carried out with the MINPOP package, discussed below. This program was also used for the geometry optimization. The molecule-optimized orbital contractions were obtained with the help of a program developed by Dr. Richard Bardo (Bardo and Ruedenberg (1974), and improved by Dr. Cheung (1975).

All integrals between the QBO's were calculated with the BIGGMOLI integral package developed by Dr. Richard Raffenetti (1973a, b). Furthermore the BIGGMOLI SCF program by Dr. Raffenetti (1973c) was used for closed and open shell SCF calculations, with the exception of the nonlinear triplet states, for which the separated-pair independent particle MCSCF program by Dr. Kenneth Sundberg (1975) was employed.

The general MCSCF calculations were carried out with the help of a program originally prepared by Dr. Lap Cheung (1975) and subsequently improved by Dr. Stephen Elbert, who was also responsible for the configuration interaction program. The MCSCF program makes extensive

use of the programs for calculating representation matrices of the symmetric group for Serber-type spin eigenfunctions originally developed by Dr. W. I. Salmon (1974) and further improved by Dr. Lap Cheung (1975).

The orbital localization, based on the Edmiston-Ruedenberg (1963) procedure is essentially due to Dr. Raffenetti with some modification by Dr. Sundberg. The orbital contours were drawn with a program developed over a number of years in the Iowa State theoretical chemistry group, the main contributors being Drs. L. Salmon, R. Raffenetti, K. Sundberg, L. Cheung, and M. Dombek.

B. New Programs

For certain applications a new version of the BIGGMOLI SCF program, called SUPERMOLI, was prepared, since it allowed for considerably greater storage capabilities. For the CI calculations a configuration generating program was developed which automatically generates all configurations for the full reaction space for the singlet and triplet states. For the orbital analysis the construction of the DLRO's was programmed as described in Section IIIE.

For the orbital exponent optimization as well as the geometry optimization the program MINPOP was developed which finds the minimum of a nonlinear function of two variables. The basic procedure consists of determining a quadratic approximation from a number of known points. In general this means the determination of 6 constants from $N \geq 6$

arbitrary points. If $N > 6$, this is accomplished by a least-mean-squares procedure. From the quadratic approximation the minimum is predicted. The function is then calculated at this minimum point and constitutes an additional function value for the determination of the next improved quadratic approximation.

Every time such a quadratic approximation is determined, contours of this approximation can be plotted with the input points indicated on the plot. This permits a visual monitoring of the reasonableness of the program's decisions.

This basic idea is embedded in a decision-making process involving various tests and precautionary conditions. For example, a routine called BRACKET, flowcharted in Figure 20, sees to it that the minimum is always adequately surrounded by sample points. Subroutine THROW on the other hand will discard points which have outlived their usefulness.

The program can be initiated in various ways, depending on the information initially available, as shown in the OPENING section flowchart in Figure 19. Termination occurs either when the minimum satisfies certain termination criteria (shown in the TEST section flowchart, Figure 22) or when a designated number of points have been calculated.

Flowcharts of the entire program and of its subsections are shown in Figures 18 to 22, with the exception of MINPLOT, the subroutine which determines the quadratic approximation. This subroutine had been

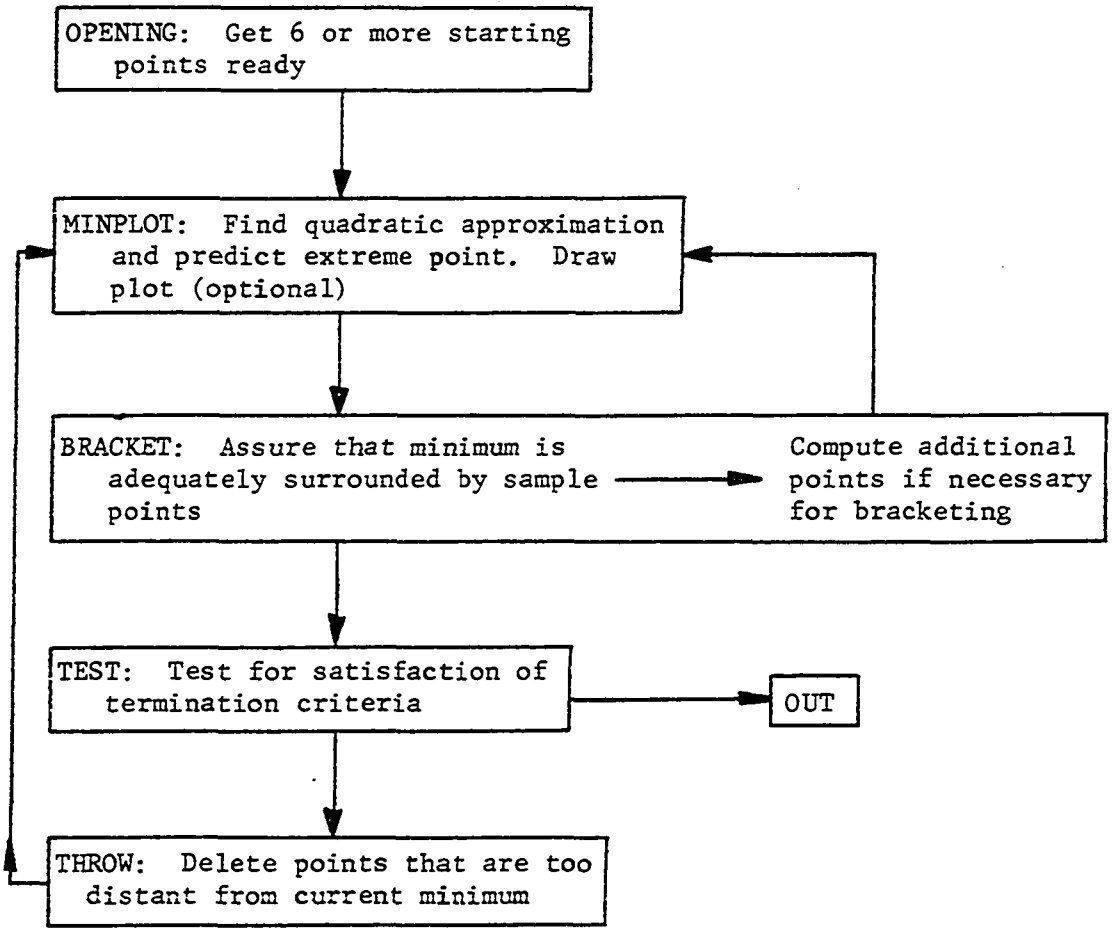

Figure 18. Overall procedure for MINPOP

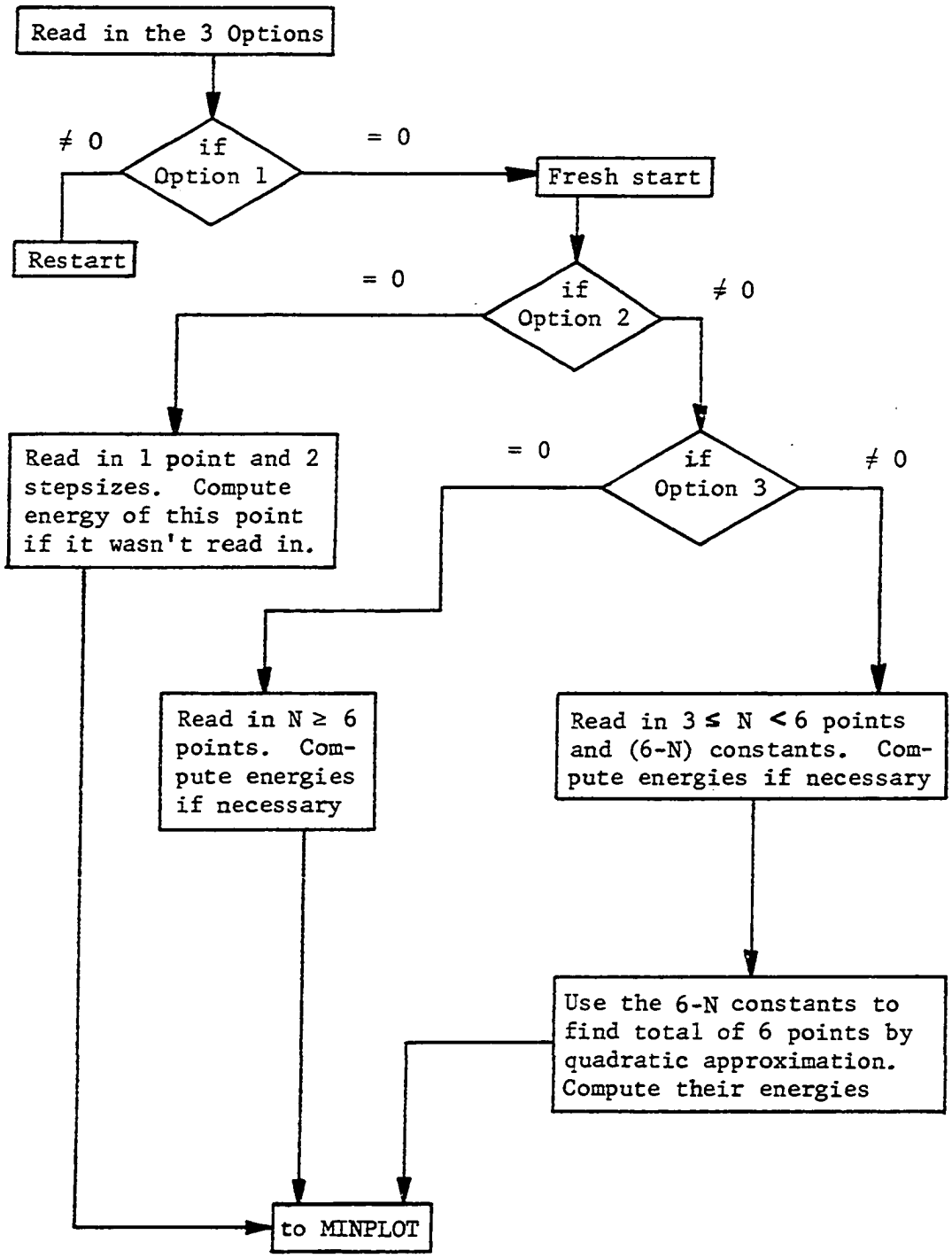

Figure 19. Flowchart for OPENING section of MINPOP

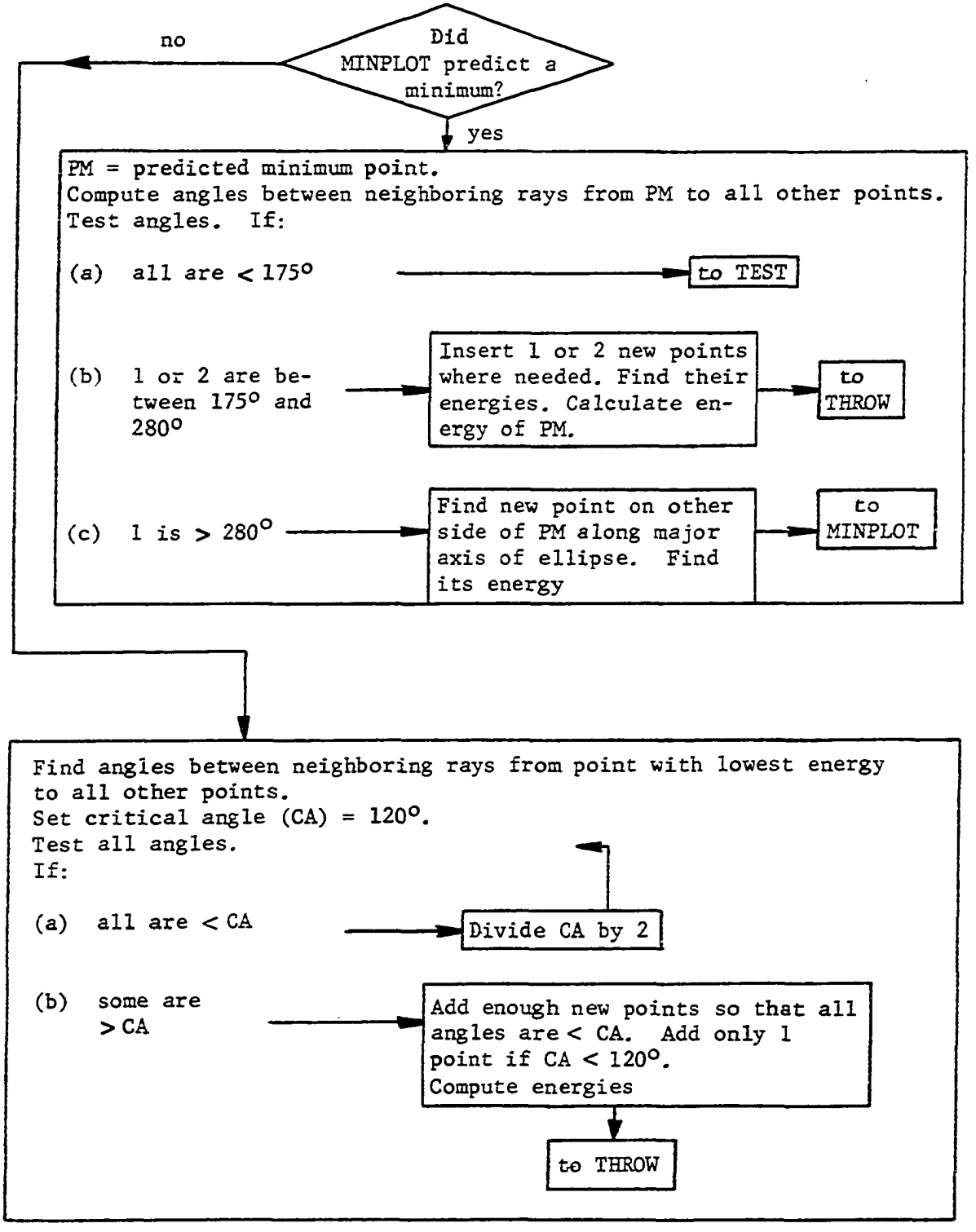

Figure 20. Flowchart for BRACKET section of MINPOP

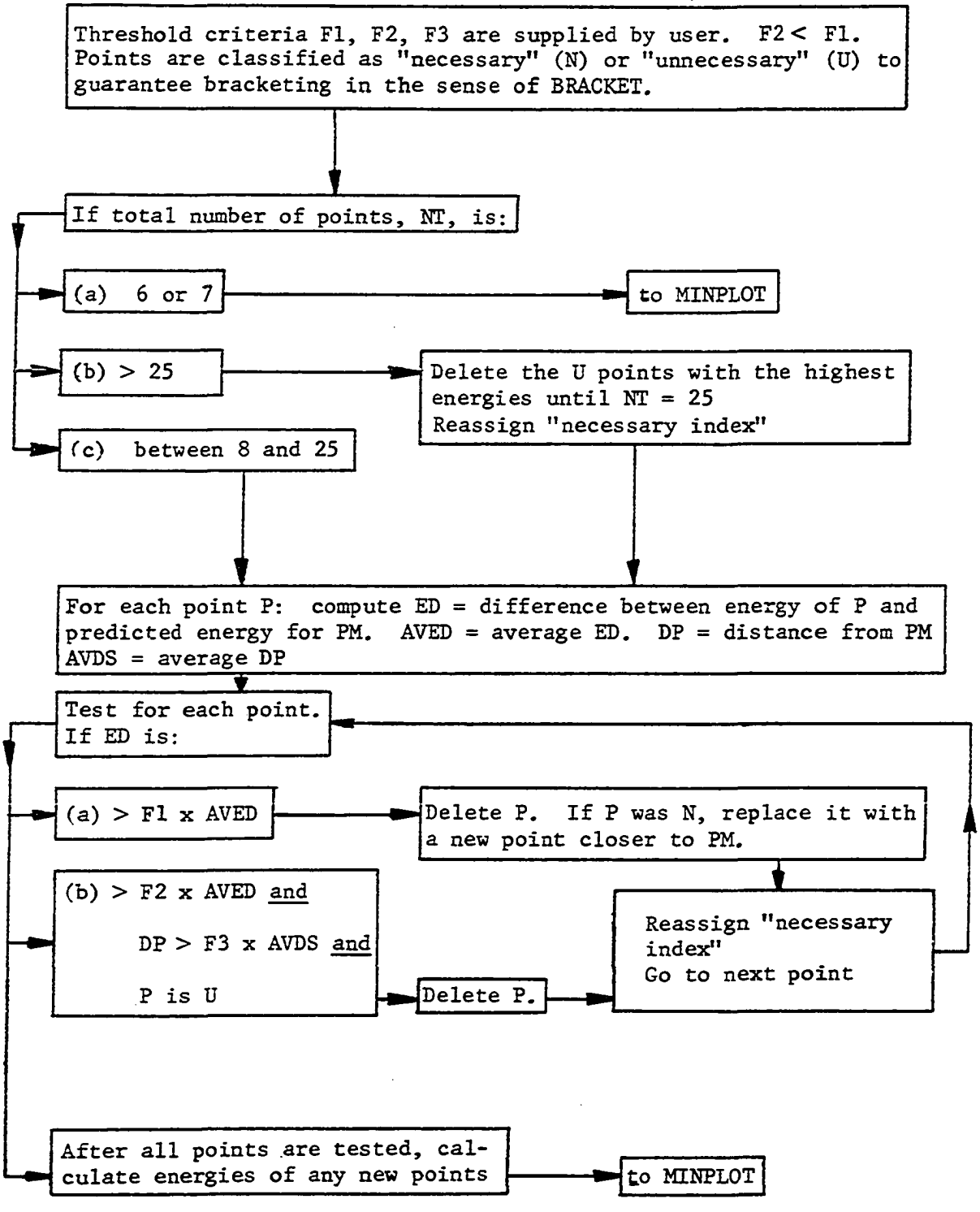

Figure 21. Flowchart for THROW section of MINPOP

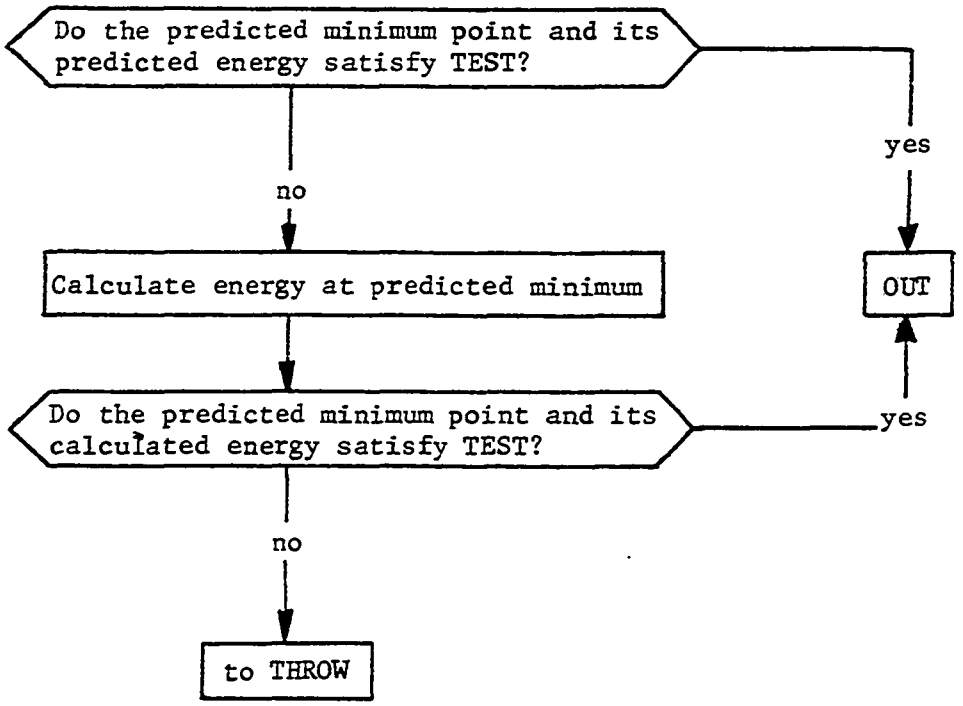

TEST: demands that the following three conditions be met:

(1) The predicted minimum point is close enough (within a distance criterion) to some previously calculated point P.

(2) The predicted or calculated energy at the minimum point is close enough (within function criterion) to the energy value at P.

(3) The energy value at P is close enough to the lowest function value.

Figure 22. Flowchart for TEST section of MINPOP

previously written by Dr. Lap Cheung (1975) and David Feller. For the optimizations done for the present investigation, the MINPOP program was combined with the BIGGMOLI routines (Raffenetti, 1973a, b, c) to calculate SCF energies as the function values.